STUDIES ON THE PROPERTIES OF AGGREGATING CASEIN SYSTEMS

A thesis submitted to the University of Glasgow for the degree of Doctor of Philosophy in the Faculty of Science

By

ELSPETH PATERSON

NOVEMBER
1980

HANNAH RESEARCH INSTITUTE
AYR

ProQuest LLC.
789 East Eisenhower Parkway
P.O. Box 1346
Ann Arbor, MI 48106 – 1346

I would like to thank Dr D.G. Dalgleish for his advice and guidance throughout the duration of this project.

I am also grateful to Professor J.A.F. Rook for the use of facilities at the Hannah Research Institute.

I would also like to thank Mrs Ellis Barbour for typing this work.

CONTENTS

LIST OF FIGURES

Chapter 4

LIST OF TABLES

SUMMARY

The growth in weight average molecular weight in aggregating casein systems was observed using light scattering. The kinetics of the aggregation of both α_{s1}-casein and β-casein in the presence of Ca^{2+} were determined by linking a stopped flow apparatus to the light detection system. The effect of temperature on both of these reactions was also investigated. Two stages were identified in the reaction.

Precipitate fractions of casein were determined for the combinations of Ca^{2+} and casein used in kinetic experiments under the same conditions.

On the basis of results from these experiments a mechanism for the Ca^{2+} induced aggregation of α_{s1}-casein was proposed. The first stage of the reaction was described as a series of multimerization equilibria which are dependent upon the average charge on the α_{s1}-casein molecule. This equilibrium produces an octamer which is sufficiently large to precipitate from solution upon further aggregation. The rate constant for this second stage association of the reaction has been found to be dependent on the charge and also the concentration of precipitable material. The equilibrium stage of the aggregation reaction is more temperature dependent than the precipitation process.

Although many similarities were observed between the β-casein and the α_{s1}-casein aggregation, there were differences, mainly ascribable to self-aggregation of β-casein in the absence of Ca^{2+}. The effect of temperature on the reaction kinetics of β-casein was also investigated and in common with α_{s1}-casein aggregation the first stage is more temperature dependent than the second. Higher fractions of β-casein are precipitable than for the same Ca^{2+} and α_{s1}-casein concentration at their respective reaction temperatures. The nature of the precipitable aggregate of β-casein was not defined.

1.

1.1 Definition of Casein

Milk contains an exceptional nutritive combination of minerals and protein. This nourishment in liquid form distinguishes it for feeding the young of all mammals. Although about 86.7% of bovine milk is in fact water, the remainder is composed on average of fat 4%, protein 3.5%, lactose 4.8% and minerals 0.7% (1).

The milk fats are distributed throughout the fluid in small microscopic globules enveloped in a very thin membrane and held in suspension. There are two classes of protein in milk, namely caseins, which comprise approximately 80% of total milk protein, and serum proteins. Casein exists mainly as large colloidal spheres known as micelles to which the opacity of milk can be attributed.

Cheese, which is a preparation of protein precipitated from milk, was known to the Greeks and Romans before the Christian era, and it is from the Latin noun 'caseus', meaning cheese, that the word casein is derived. The modern definition of the caseins is that group of milk phosphoproteins precipitable by acidification of milk to pH4.6 at 20^{o}C. Serum proteins, among which are α-lactalbumin and the lactoglobulins, do not normally precipitate at pH4.6, but will do so after salt additions. After removal of the fat and casein from milk the resulting liquid is known as whey, hence the alternative name 'whey proteins' given to the serum proteins present in whey which are largely soluble at the isoelectric point of casein (2,3,4).

Calcium, potassium, sodium and magnesium in conjunction with chloride, phosphate and citrate are the main inorganic constituents of milk. Phosphorus in various phosphate forms, either associates with calcium and protein to form the casein micelle complex or remains

in the milk serum (5). Similarly divided between the casein micelles and the aqueous environment are citrate ions. Together with trace elements such as copper and iodine these substances dissolved in water form the ionic medium in which casein micelles are suspended. Sulphur in milk is largely present as part of the amino acids methionine and cysteine.

1.2 The Casein Fractions

In 1830 Braconnot (6) first recorded a method of separating casein from whey protein by acid precipitation. Not until 1918 was there an indication of the heterogenity of bovine casein, when Osbourne and Wakeman (7) isolated an alcohol soluble protein which contained only 0.1% phosphorus compared to unfractionated casein which contained 0.85% phosphorus. In 1929 Linderstrøm-Lang (8) further demonstrated casein heterogenity by isolating a component rich in phosphorus which could be precipitated by calcium ions and another component with a much lower phosphorus content which was stable to calcium ions.

Electrophoretic methods employed by Mellander (9), 1939, revealed three fractions which were designated α, β and γ according to mobility at pH7.6, α being the most mobile. These same fractions were isolated by Hipp et al. (10) in 1952 utilizing solubility differences in urea solutions. At pH4.6 both α- and β-casein are soluble in 6.6M urea but α-casein is insoluble when the urea concentration is lowered to 4.6M while β-casein will precipitate only if the urea level is reduced below 3.3M.

Nearly fifty years after a calcium soluble protein had been identified, Waugh and von Hippel (11) purified this fraction which they called κ-casein, and noted its ability to stabilize the other fractions

against precipitation by calcium ions. Previously κ-casein had been part of the α-casein fraction obtained by urea fractionation (10). The definition of κ-casein is that fraction of whole α-casein which is soluble in 0.4M $CaCl_2$ at pH7 and 0 to 4°C (12). Two κ-casein polymorphs, A and B are observed as separate zones in alkaline urea-gel electrophoresis after disulphide bonds are reduced (13,14,15).

The α_s fraction, that part of α-casein which is sensitive to precipitation by calcium ions, comprises approximately 50% of whole casein (16). Annan and Manson (17) using column chromatography at pH4 followed by starch gel electrophoresis at pH9.2 demonstrated the presence of seven distinct components namely α_{so}-, α_{s1}-, α_{s2}-, α_{s3}-, α_{s4}-, α_{s5}- and α_{s6}-casein in order of decreasing mobility. By far the most abundant of these proteins is α_{s1}-casein which has the same peptide chain as α_{s0} but a lower phosphate content. The other α_s-caseins are all formed from another distinct amino acid backbone and are referred to as the α_{s2}-caseins.

The sequence of α_{s2}-casein has recently been established and has features similar to α_{s1}-casein (18-20). Both are insoluble in the presence of calcium and have a high content of phosphate groups (between 10 and 13 for α_{s2}-casein). Increasing the degree of phosphorylation on other possible sites leads to formation of α_{s3}-, α_{s4}- and α_{s6}-casein. Due to the presence of two cysteinyl residues, formation of disulphide bridges is possible in the α_{s2}-casein group. The α_{s5}-casein band disappeared after reduction with 2-mercaptoethanol to be replaced by the α_{s6}-casein band and an apparent increase in the amounts of α_{s2}, α_{s3}, and α_{s4}-casein (17). Hoagland et al. (21) also found that α_{s3} and α_{s4}-casein were produced by reduction of the α_{s5}-casein complex.

A sequence of three genetic variants of α_{s1}-casein designated

A, B and C were reported (22-24). A fourth variant, α_{s1}-casein D was later detected (25). Similarly, β-casein was found to have a series of variants termed A^1, A^2, A^3, B, C, D and B_Z (26,27). These differed from each other by only one or two amino acid changes and varient C also had one less phosphate group attached (28,29).

Isolation of γ-casein had been achieved by taking advantage of its solubility in 50% ethanol suggesting that γ-casein was identical to the alcohol soluble protein of Osborne and Wakeman (7,30). The γ-fraction of whole casein is soluble in 3.3M urea but insoluble in 1.7M urea at pH4.7 upon addition of 1.6M ammonium sulphate and has been shown to be heterogeneous by ion-exchange chromatography (10,31). Determination of the amino acid content of γ-casein fractions revealed similarities to sections of β-casein (32,33).

Four γ-casein types are identified, γ, R, S and TS, all having amino acid sequences identical to parts of β-casein or its genetic polymorphs. Residues 29 to 209 of β-casein were found to be identical to the sequence of γ-casein (34,35). Other γ-casein sequences were found corresponding to the variations observed in β-casein polymorphs. The minor γ-caseins TS-A^2 and S-caseins correspond to residues 106 and 209 of β-casein A^2 and β-casein B respectively. Similarly the C-terminal end of β-casein has the γ-casein B sequence which has arginine at position 122 whereas R-casein has the β-casein and γ-casein A^2 sequence but is smaller than the temperature sensitive TS-A^2 by two amino acid residues.

1.3 α_s-casein

1.3.1 Sequence and properties of α_{s1}- and α_{s0}-casein

The α_s-caseins, in addition to being insoluble in 4.6M urea

at pH4.6 are precipitated by 0.4M $CaCl_2$ at pH7 and 0.4°C (36). The French research group of Ribadeau-Dumas (19,20) determined the sequence of the 199 amino acids which form the primary structure of α_{s1}-casein shown in Fig. 1.1.

One additional phosphate on Ser-41 is the only difference between α_{s1}- and α_{s0}-casein (37). According to the n.m.r. studies of Ho et al. (38) the phosphate moieties are present as monoesters, formed by condensing with the alcohol function of serine residues. In total, α_{s1}-casein has eight phosphoserines, four of these being grouped together in a "phosphate cluster" composed of SerP-Ile-SerP-SerP-SerP at residues 64-68 (19). Some specificity of the phosphorylating enzyme is suggested by the observation that anionic groups of either another phosphoserine or a glutamate residue are located at the n + 2 position where n is the position of the phosphoserine in question (39).

This structure has a molecular weight of 23615 (20) which agrees well with sedimentation and light scattering studies (40,41). Acidic residues are concentrated in the regions 132 to 199 and especially also 43 to 89 where seven of the eight phosphoserines and twelve side chain carboxylate groups are located. The net charge at pH6.6, (as in natural milk) reported by Schmidt to be -22.8, is largely accounted for by this section leaving a net negative charge of only one or two on the rest of the molecule (40).

Proline residues limit structural coiling possibilities due to the steric restrictions they impose . Seventeen proline residues, comprising 8.5% of α_{s1}-casein are evenly distributed along the protein chain indicating that α_{s1}-casein is likely to be an unordered coiled structure with little α-helix or β-structure (19,42).

Apart from two regions, 43-89 and 114 to 131, the remainder of the chain is predominantly hydrophobic. According to the findings

```
  1  H.Arg-Pro-Lys-His-Pro-Ile-Lys-His-Gln-
 10  Gly-Leu-Pro-Gln- Glu-Val-Leu-Asn-Glu-Asn-
 20  Leu-Leu-Arg-Phe-Phe-Val-Ala -Pro-Phe-Pro-
 30  Gln-Val-Phe-Gly-Lys-Glu-Lys-Val-Asn-Glu-
 40  Leu-Ser-Lys-Asp-Ile-Gly-Ser-Glu-Ser-Thr-
                               P       P
 50  Glu-Asp-Gln-Ala-Met-Glu-Asp-Ile-Lys-Gln-
 60  Met-Glu-Ala-Glu-Ser-Ile-Ser-Ser-Ser-Glu-
                     P       P   P   P
 70  Glu-Ile-Val-Pro-Asn-Ser-Val-Glu-Gln-Lys-
                           P
 80  His-Ile-Gln-Lys-Glu-Asp-Val-Pro-Ser-Glu-
 90  Arg-Tyr-Leu-Gly-Tyr-Leu-Glu-Gln-Leu-Leu-
100  Arg-Leu-Lys-Lys-Tyr-Lys-Val-Pro-Gln-Leu-
110  Glu-Ile-Val-Pro-Asn-Ser-Ala-Glu-Glu-Arg-
                           P
120  Leu-His-Ser-Met-Lys-Glu-Gly-Ile-His-Ala-
130  Gln-Gln-Lys-Glu-Pro-Met-Ile-Gly-Val-Asn-
140  Gln-Glu-Leu-Ala-Tyr-Phe-Tyr-Pro-Glu-Leu-
150  Phe-Arg-Gln-Phe-Tyr-Gln-Leu-Asp-Ala-Tyr-
160  Pro-Ser-Gly-Ala-Trp-Tyr-Tyr-Val-Pro-Leu-
170  Gly-Thr-Gln-Tyr-Thr-Asp-Ala-Pro-Ser-Phe-
180  Ser-Asp-Ile-Pro-Asn-Pro-Ile-Gly-Ser-Glu-
190  Asn-Ser- Glu -Lys-Thr-Thr-Met-Pro-Leu-Trp.OH
```

Fig. 1.1

Amino acid sequence of α_{s1}-casein B. Residues 14 to 26 are deleted in α_{s1}-casein A. Ala-53 is replaced by Thr-P in α_{s1}-casein D. Glu-192 is replaced by Gly in α_{s1}-casein C. (19,20)

of Bigelow (43) from studies on one hundred and fifty proteins, average hydrophobicity considered as a function of molecular weight may vary between values of 440 and 2020. On Bigelow's scale α_{s1}-casein has a value of 1170 and therefore is classed as a hydrophobic protein.

Polymerization of α_{s1}-casein, in the absence of Ca^{2+} is strongly dependent upon concentration, ionic strength, temperature and pH (40). Swaisgood and Timasheff collected sedimentation velocity data over the alkaline pH range for various ionic strengths. Octamer units were present at pH8 and 0.15M NaCl, with dimer as the main kinetic unit, whereas monomer and dimer were the main molecular forms at pH8 and 0.01M NaCl. Similarly increasing the pH to 9 lowers the weight-average molecular weight, indicating that monomer and dimer are the predominant species. These results suggested that dissociation of oligomers is driven by electrostatic repulsion as the protein becomes more charged (at higher pH values) and screening decreases (at lower ionic strengths) (44).

Previously Ho and Waugh (45) had obtained similar results with the α_s-casein complex which contained α_{s1}- and the other α_s-caseins. Solutions of 0.5 to 2% α_s-casein became turbid and a gelatinous precipitate formed between pH5.6 and 6.4 when I was 0.4. However, when the ionic strength (I) was 0.05 no precipitate formed until the pH was between 5.3 and 3.5. Direct proportionality between the α_s-casein stability and e^I was indicated by considering the α_s-casein particles to be impenetrable charged spheres according to the electrostatic theories of Scatchard and coworkers (46,47). At higher ionic strengths colloidal stability was reduced and precipitation occurred at lower H^+ concentrations.

Increased association of the α_{s1}-C variant compared to the α_{s1}-B variant has also been ascribed to the slightly reduced net charge

on α_{s1}-C as a result of a minor amino acid change (48). No gross conformational change was indicated by optical rotatory dispersion studies as the monomer aggregated to form trimers or tetramers (49). Temperature effects on aggregation are not substantial in comparison to the effects of ionic strength, although increasing the temperature produces greater weight average molecular weights indicating that association is endothermic (50). A positive entropy of association suggests that the aggregating units are held together by hydrophobic bonds.

Increasing the concentration of α_{s1}-casein also results in larger molecular weights, the monomer undergoing a number of association steps up to about hexamer.

1.3.2 Binding of Ca^{2+} to α_{s1}-casein and precipitation

As a result of its overall negative charge, α_{s1}-casein will bind Ca^{2+} and other cations (45,51). The binding constants decrease in the order $Mg^{2+} > Ca^{2+} > Ba^{2+} > Sr^{2+}$ for the divalent cations which interact more strongly than monovalent ions. Phosphate groups have been indicated by i.r. measurements to be strong calcium binding sites as spectral shifts typical of such interactions were observed at very low ratios of calcium ions to casein phosphorus atoms (52). Calcium binding may also occur at other anionic sites such as the carboxylate group on aspartic and glutamic acid residues (45,53).

Addition of calcium ions to α_{s1}-casein results in precipitation of the protein. Noble and Waugh (54) studied the solubility of the calcium/α_s-caseinate system as a function of added calcium. This is shown in Fig. 1.2.

Clearly there is a critical calcium concentration for a given α_s-casein concentration, below which precipitation will not occur.

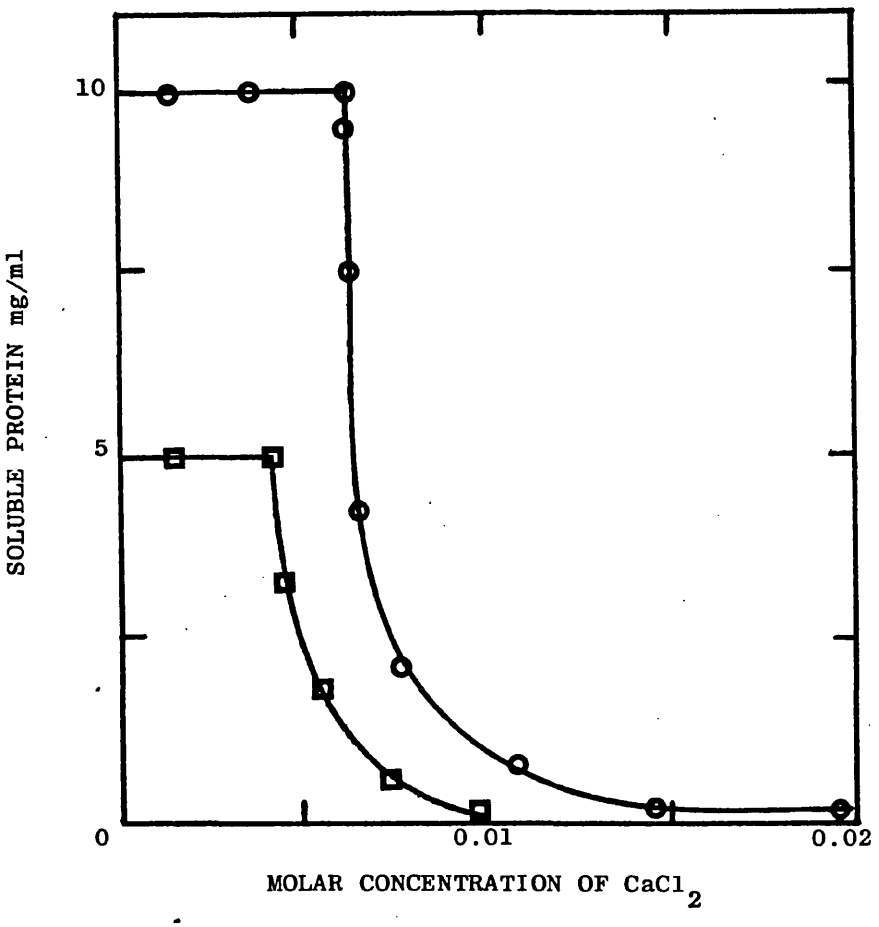

Fig. 1.2 Solubility of calcium α_s-caseinate as a function of added $CaCl_2$ for two solutions, both in 0.07M KCl and 0.01M imidazole-HCl buffer (pH7) at 37°C. ○, 10 mg/ml α_s-caseinate; □, 5 mg/ml α_s-caseinate.

Higher casein concentrations require a higher calcium concentration to precipitate the protein. Noble and Waugh argue that without calcium binding to α_s-casein the precipitation point on the solubility curve would be independent of protein concentration.

The amount of calcium bound to each α_s-casein molecule prior to precipitation was estimated from the quantity of calcium added before the rapid decrease in solubility. The additional calcium required to precipitate the protein was also noted. By fitting these data to a solubility product of the form

$$K = \left[\alpha\text{-}Ca_m\right] \left[Ca\right]^n \qquad (1.1)$$

where K is the solubility product, m is the number of calcium ions bound and n is the number of additional calcium ions required to precipitate the protein, values of m = 7 and n = 4 showed least deviation from the experimental curves.

However, further investigation by Waugh et al. (55) revealed that the average number of calcium ions bound per mole of protein, $\bar{\nu}_{Ca}$, increased non linearly with calcium ion concentration. Dickson and Perkins (53) confirmed this relationship with the free calcium ion concentration and, using the radioisotope ^{47}Ca, determined from an extrapolated Scatchard plot that an average 8.5 moles of calcium will bind to each α_{s1}-casein molecule at precipitation. After dephosphorylation this figure is reduced to 1.2 moles of Ca^{2+}. Bingham et al. (56) using a molecular weight of 23,600 for α_{s1}-casein found that 7 moles of calcium ions were bound prior to precipitation in 0.07M KCl at 37°C, three further calcium ions per monomer being required to precipitate the protein. Only 2 moles of calcium were bound during precipitation of dephosphorylated α_{s1}-casein under the same conditions, with no evidence of significant binding prior to the precipitation process. Despite this, free calcium ion concentrations required for

precipitation were not lower than those for native α_{s1}-casein.

Waugh et al. (55) suggested that α_{s1}-casein precipitates when the charge on the protein is reduced to a given level. Removal of phosphate groups reduces the net negative charge on the protein but not the calcium ion concentration at which flocculation will occur. These observations lend support to the proposal that calcium binds more strongly to phosphate than to the other groups.

Replacement of calcium chloride by about five times its precipitating concentration in KCl failed to produce a casein precipitate (56). However, increasing the ionic strength in the presence of calcium ions decreased calcium binding to α_s-casein (55). Slattery (57) adjusted these calcium binding values calculated using a molecular weight of 27,300 (55) to provide results based on the α_{s1}-casein molecular weight of 23,615. He assumed that the net charge on the molecule and hence the electrostatic repulsion were reduced by calcium binding, and that conformational changes will then occur to bring the charged groups closer together. The effect of binding at one site would affect the extent of binding at other sites through electrostatic interactions. The electrostatic models considered revealed the dominance of the acidic peptide section of α_{s1}-casein containing the phosphoserine cluster.

Dalgleish and Parker (58) studied the effect of ionic strength, pH and temperature on calcium binding. They used a less detailed method of analysing the calcium binding to α_{s1}-casein which incorporated a substitution effect after each calcium binding event. The calcium ion concentration required to initiate precipitation is known as the critical calcium concentration, Ca^{2+}_c. According to results from Dalgleish and Parker and those of Slattery recalculated by this simplified procedure, the critical calcium concentration increases when

ionic strength is increased. However, the amount of bound calcium required to initiate precipitation was actually reduced from 7.5 moles at 50mM NaCl to 3.7 moles at 200mM NaCl. In fact a linear relationship between the average number of Ca^{2+} bound per mole of protein at the point of precipitation, $\overline{\nu}_c$, and the concentration of NaCl was determined.

As calcium ions bind to the protein, protons are displaced (55). Decreasing pH from 7.5 to about 6 results in a decrease in the average number of bound calcium ions required to initiate precipitation from 7.6 to 4.6 (58). The protons are clearly titrating acidic residues and reducing the net negative charge on the monomer. As hydrogen ion concentration decreases the extent of ionization of acidic residues will increase and more calcium ions must be bound to reduce the charge and precipitate the protein.

Adding calcium to α_{s1}-casein at pH7 causes a conformational change which is necessary to allow aggregation of protein and subsequent precipitation (59). Between pH5 and 6 this conformational change is not observed by fluorescence spectroscopy prior to precipitation suggesting that in this pH range, the protein molecule has adopted the conformation required for precipitation. Neutralization of the protein charges by Ca^{2+} or H^+ may reduce repulsion within the molecule and result in a contraction, which could transfer the tryptophan residue to a more hydrophobic environment, meanwhile exposing other calcium binding sites. Further neutralization of these sites leads to flocculation.

Reaction of α_{s1}-casein with calcium has been shown to be exothermic up to the calcium concentration of micellisation at which point endothermic hydrophobic bond formation becomes the main thermal process (60). Simple site binding of calcium does not appear to be

important in the thermal process.

The average number of bound calcium ions necessary for precipitation of α_{s1}-casein varied only slightly with temperature. Marginally less bound calcium is required at higher temperatures, the critical binding $\bar{\nu}_c$, being about 7.5 moles per mole of protein over a temperature range of 4°C to 40°C.

Calcium binding to α_{s1}-casein increases as the temperature is raised. Thus the free calcium concentration required to produce a given level of binding is much lower at higher temperatures (58).

Precipitates of the calcium α_s-caseinate system were found to be less solvated as the average number of site bound calcium ions increased, i.e. with low salt concentrations and higher pH values (55).

1.4 β-casein

1.4.1 Sequence and properties of β-casein

Many similarities between α_{s1}-casein and β-casein are evident. Both are precipitated from milk serum at pH4.6 and 20°C. Although β-casein is also soluble in 6.6M urea it will precipitate from 3.3M urea solutions at pH4.6 (12). Analysis of the peptide sequence of bovine β-casein has been completed and is given in Fig. 1.3 (61).

This sequence gives a molecular weight of 23982 for β-casein A^2. The region in α_{s1}-casein from residue 62 to 70 which contains four phosphoseryl groups is similar to the region of β-casein from residue 13 to 21. There is a total of five phosphoserines in β-casein the only other being at position 35.

Adding to the concentration of negative charge within the first 21 residues are seven glutamate residues, five of which have pKa's associated with their carboxylic acid groups of approximately

```
  1 H-Arg-Glu-Leu-Glu-Glu-Leu-Asn-Val-Pro-
 10 Gly-Glu-Ile-Val-Glu-Ser-Leu-Ser-Ser-Ser-
                          P       P   P   P
 20 Glu-Glu-Ser-Ile-Thr-Arg-Ile-Asn-Lys-Lys-
 30 Ile-Glu-Lys-Phe-Gln-Ser-Glu-Glu-Gln-Gln-
                           P
 40 Gln-Thr-Glu-Asp-Glu-Leu-Gln-Asp-Lys-Ile-
 50 His-Pro-Phe-Ala-Gln-Thr-Gln-Ser-Leu-Val-
 60 Tyr-Pro-Phe-Pro-Gly-Pro-Ile-Pro-Asn-Ser-
 70 Leu-Pro-Gln-Asn-Ile-Pro-Pro-Leu-Thr-Gln-
 80 Thr-Pro-Val-Val-Val-Pro-Pro-Phe-Leu-Gln-
 90 Pro-Glu-Val-Met-Gly-Val-Ser-Lys-Val-Lys-
100 Glu-Ala-Met-Ala-Pro-Lys-His-Lys-Glu-Met-
110 Pro-Phe-Pro-Lys-Tyr-Pro-Val-Gln-Pro-Phe-
120 Thr-Glu-Ser-Gln-Ser-Leu-Thr-Leu-Thr-Asp-
130 Val-Glu-Asn-Leu-His-Leu-Pro-Pro-Leu-Leu-
140 Leu-Gln-Ser-Trp-Met-His-Gln-Pro-His-Gln-
150 Pro-Leu-Pro-Pro-Thr-Val-Met-Phe-Pro-Pro-
160 Gln-Ser-Val-Leu-Ser-Leu-Ser-Gln-Ser-Lys-
170 Val-Leu-Pro-Val-Pro-Glu-Lys-Ala-Val-Pro-
180 Tyr-Pro-Gln-Arg-Asp-Met-Pro-Ile-Gln-Ala-
190 Phe-Leu-Leu-Tyr-Gln-Gln-Pro-Val-Leu-Gly-
200 Pro-Val-Arg-Gly-Pro-Phe-Pro-Ile-Ile-Val.OH
```

Fig. 1.3

Primary structure of β-casein A^2. Pro-67 is replaced by His in β-casein A^1. His-106 is replaced by Gln in β-casein A^3. β-casein B and C are the same as β-casein A^1 except that Ser-122 is replaced by Arg in β-casein B and Glu 37 is replaced by Lys in β-casein C which has no posphate group on Ser-35. (61)

4.9 indicating that they will be largely dissociated (16). This section contributes a net charge of -12, the total for the whole chain being estimated to be -13 at pH6.6 (62). Hence the rest of the chain contributes a net negative charge of only one. Acidic and basic residues, besides being sparse over the region of residues 22 to 209, are evenly balanced and their distribution forms no pattern.

Overall, β-casein has an average hydrophobicity of 1330 cal. per residue, which classes it among the most hydrophobic proteins on Bigelow's scale (61,43). Excluding the highly charged head of the molecule the average hydrophobicity value rises to 1500 for residues 108 to 209 (16). Many properties of β-casein are likely to be a direct result of the contrasting character of the 'head' and 'tail' of the protein chain.

Due to the large proportion of proline residues, 16.7%, in β-casein, α-helix formation will be severely limited. As no more than two of these 35 sterically hindered residues are adjacently positioned the possibility of poly-L-proline $\underline{\overline{II}}$ structure suggested by optical rotatory dispersion investigations is precluded (63).

Payens and van Markwijk (64) investigated the aggregation properties of β-casein using viscometric and ultracentrifugation techniques. A strongly temperature dependent association had previously been noted (65,66). At 13.5^{o}C the degree of polymerization of β-casein is greater than 22, cooling to 4^{o}C being required to ensure that only monomer is present at protein concentrations of about 15 mg/ml (64). Such increased association with higher temperatures is typical of hydrophobic bond formation. Viscosity measurements were observed to decrease with increasing temperature indicating that the intrinsic viscosities of β-casein polymers are lower than that of the monomer. This suggests some folding or coiling of polymers as the molecular weight increases, although this could be explained by a decrease in

hydration (67).

Removal of the isoleucine and valine residues at the C-terminal end of β-casein drastically reduces its ability to associate at 8.5°C (68). This effect has been confirmed, and attributed to loss of these hydrophobic residues upsetting the balance between hydrophobic forces favouring aggregation and electrostatic forces opposing it (69). Increasing the net negative charge of β-casein by acetylation of lysine residues caused a reduction in the sedimentation coefficient indicating that the tendency to aggregate had diminished (70).

Apparent weight average molecular weights increased to a limiting size of approximately 540,000 at 8.5°C as concentration increased to 20 mg/ml of protein (64). The size of polymers produced is also thought to be dependent upon the concentration as well as the temperature (71).

Differences in the physical properties of β-casein variants are observed, notably the increased tendency of β-casein C to associate compared to β-A and β-B (72). Swaisgood (16) has calculated that β-casein C will have the smallest net charge of the three at -8.3. It is therefore apparent that the exceptional associative properties of β-casein are a function of the electrostatic repulsions as well as the hydrophobic attractions.

1.4.2 Binding of Ca^{2+} to β-casein and precipitation

Like α_{s1}-casein, β-casein will bind cations although the binding capacity is much lower (53). At pH6.6, the pH of normal milk, the charge on the β-casein molecule is -13. The value becomes -30 at pH11.5 and rises to +13 at pH values below 3, as the extent of protonation of acidic residues varies (73). The presence of calcium ions

lowers the pH of a given solution as hydrogen ions are released from binding sites. Precipitation occurs at lower pH values in the presence of calcium eg. pH4.9 reduces to pH4.3. Binding of Ca^{2+} to β-casein is also reduced as the pH is lowered (53).

As expected, the amount of Ca^{2+} bound increases with free Ca^{2+} concentration (55). As for α_{s1}-casein there is a critical free calcium concentration below which a given β-casein concentration will not form a precipitate. The extent of calcium binding which initiates precipitation of the complex is lower than that of α_s-casein. This observation has been substantiated by subsequent calculations of $\bar{\nu}_C$ for both (58,74).

The smaller net charge on β-casein is essentially all accounted for by a short acidic peptide at the N-terminal end identified by Peterson (27). This contains all five organic phosphate groups, five carboxylate groups and two arginine groups, giving rise to a region of high charge density. As the local charge density on a fixed site increases the fraction of this charge balanced by the counter-ions assembling around is thought to increase. Thus the dependence of calcium binding on ionic strength is thought to be greater than if the charge were evenly distributed over the molecule (55).

Slattery and Waugh (75) have examined models of charge binding to β-casein which emphasize the electrostatic interactions between binding sites in the acidic peptide due to the density of charge groups. The observed decrease in pH as calcium ions are bound is compared to that calculated from the binding constants for the ions present with corrections for the density of the charge groups in the acidic peptide. Proton releases are greater than predicted by calcium binding calculations, indicating the role played by amino acid groups such as histidine which binds protons but not calcium. Increasing the

ionic strength reduces the number of protons bound thereby altering the net charge on the protein.

This result agrees well with the observation of reduced calcium binding at lower pH values (53). Utilizing the simplified binding theory which envisages an initial binding constant, K^*, for the first Ca^{2+} bound to β-casein and a substitution parameter, N, which accounts for changes in the calcium binding constants as a result, the effect of ionic strength and temperature on calcium binding was obtained (74).

Increasing ionic strength decreases the binding of Ca^{2+} to β-casein. Although the initial binding constants were similar for α_{s1}- and β-casein, reflecting perhaps the presence of the acidic peptide in each, subsequent binding of Ca^{2+} to β-casein was lower than for α_{s1}-casein.

A calcium chloride concentration of 0.007M at pH6.6 will precipitate 10 mg/ml β-casein at 37°C. The temperature required for precipitation of this protein solution is much higher than would be necessary for α_{s1}-casein. Temperature has a considerable effect on the calcium-initiated association of β-casein. The free calcium ion concentration required to precipitate β-casein is very high at 20°C but is dramatically reduced as the temperature is raised to 40°C (74).

The level of bound calcium which initiates precipitation is lower at higher temperatures, and certainly lower than that of α_{s1}-casein at an equivalent temperature. Again the lower charge on β-casein might be thought to account for this but calculation of the charge on the caseins at the precipitation point shows that the charge on β-casein is close to zero, becoming more negative as the temperature increases whereas α_{s1}-casein has a charge of about -7.5 in the 20°C to 40°C range. The charge is not considered as important a factor in the precipitation of β-casein as for α_{s1}-casein. The temperature

dependence of the precipitation is typical of situations where hydrophobic interactions determine the solubility of the protein (76).

1.5 κ-casein

κ-casein is defined as that fraction of whole α-casein soluble in 0.4M $CaCl_2$ at pH7 and 0 to 4°C (12). Whole α-casein is soluble in 6.6M urea but insoluble in 4.6M urea. As the third most abundant milk protein, κ-casein accounts for about 10% of total milk protein. The only milk protein capable of stabilising α_s-casein against precipitation by 0.02M $CaCl_2$ is κ-casein.

The primary sequence of both genetic variants of κ-casein has been established and are as depicted in Fig. 1.4 (77). The absence of a region of anionic character provided by serine phosphates can perhaps account for the reduced binding of Ca^{2+} exhibited by κ-casein (53). There is in fact only one serine phosphate at position 149.

Variations in the molecular weights of κ-casein are attributable to the presence of up to 5 carbohydrate units, attached to serine and threonine OH groups. These are thought to be tri-saccharides, each of which would increase the molecular weight of κ-casein by 657 (78,79). When free of carbohydrate, this glycoprotein has a molecular weight close to 18,900 (29). Intermolecular disulphide bonds are another feature of κ-casein, formed by linking two cysteine sulphydryl groups. Large homopolymers are formed having molecular weights above 150,000 (80).

The C-terminal end of this 169 amino-acid chain contains 53 residues without any cationic groups and if considered in isolation from the remainder, would have a charge of -11. One third of this section of κ-casein is composed of seryl and threonyl residues, some of which have the sugars attached. Hill and Wake (81) have suggested that this

1 H-Pyr-Glu-Gln-Asn-Gln-Glu-Gln-Pro-Ile-

10 Arg-Cys-Glu-Lys-Asp-Glu-Arg-Phe-Phe-Ser-

20 Asp-Lys-Ile-Ala-Lys-Tyr-Ile-Pro-Ile-Gln-

30 Tyr-Val-Leu-Ser-Arg-Tyr-Pro-Ser-Tyr-Gly-

40 Leu-Asn-Tyr-Tyr-Gln-Gln-Lys-Pro-Val-Ala-

50 Leu-Ile-Asn-Asn-Gln-Phe-Leu-Pro-Tyr-Pro-

60 Tyr-Tyr-Ala-Lys-Pro-Ala-Ala-Val-Arg-Ser-

70 Pro-Ala-Gln-Ile-Leu-Gln-Trp-Gln-Val-Leu-

80 Ser-Asp-Thr-Val-Pro-Ala-Lys-Ser-Cys-Gln-

90 Ala-Gln-Pro-Thr-Thr-Met-Ala-Arg-His-Pro-

100 His-Pro-His-Leu-Ser-Phe-Met-Ala-Ile-Pro-
R

110 Pro-Lys-Lys-Asn-Gln-Asp-Lys-Thr-Glu-Ile-

120 Pro-Thr-Ile-Asn-Thr-Ile-Ala-Ser-Gly-Glu-

130 Pro-Thr-Ser-Thr-Pro-Thr- Ile -Glu-Ala-Val-

140 Glu-Ser-Thr-Val-Ala-Thr-Leu-Glu- Ala -Ser-
P

150 Pro-Glu-Val-Ile-Glu-Ser-Pro-Pro-Glu-Ile-

160 Asn-Thr-Val-Gln-Val-Thr-Ser-Thr-Ala-Val-OH

Fig. 1.4

The amino acid sequence of κ-casein B. In κ-casein A Ile 136 is The and Ala 148 is Asp. Rennin sensitive bond is between Phe 105 and Met 106.

portion will be hydrophilic since its hydrophobicity on Bigelow's scale is 860, which is low, and the numerous hydroxyl groups will be able to hydrogen bond with water molecules.

This C-terminal section is included in the macropeptide which results from cleavage of a sensitive bond between a phenylalanine residue and a methionine residue at positions 105 and 106 respectively. Chymosin (rennin), an enzyme found in the lining of calf stomach, will cleave this bond to produce the macropeptide and the segment corresponding to the first 105 residues of κ-casein which is known as para-κ-casein. In comparison, para-κ-casein is more hydrophobic in character, having a value of 1300 on Bigelow's scale.

Overall, κ-casein is between α_{s1}- and β-casein in its hydrophobicity value of 1224 but an open chain structure is likely due to charge repulsion, resulting in a high degree of solvation of both polar and non polar residues. A large number of proline residues, 19, are distributed at intervals along the length of the κ-casein chain thereby limiting structural coiling possibilities as demonstrated by Herskovits (82).

Despite the overall net charge of -3.3 at pH6.6 the distribution is such that the macropeptide of κ-casein B has a negative charge of -7.8 while the para-κ-casein section has a positive charge of 4.5. Basic residues such as arginine and lysine predominate in para-κ-casein which explains the charge distribution. Hill and Wake (81) suggested that the ability of κ-casein to stabilize the other caseins in micelles was a result of its amphiphilic nature. The hydrophobic para-κ-casein carrying a small positive charge would interact with the hydrophobic sections of α_{s1}- or β-casein which had small negative charges, while the hydrophilic macropeptide remained in an aqueous environment. Prevention of precipitation of α_{s1}- and β-casein by calcium ions could be effected in this manner, the

protective κ-casein holding the protein suspended.

Obviously attack by rennin (chymosin), removes the hydrophilic section rendering the casein/para-κ-casein complex insoluble, resulting in aggregates of the protein being displaced from solution. This process is fundamental in the preparation of cheeses.

The solubility of κ-casein in alcohol can also be understood in terms of the number of hydroxyl groups in the macropeptide.

1.6 Casein micelles

In milk, most of the protein is not free in solution, but, together with calcium and phosphate it aggregates to form colloidal particles known as casein micelles. Precise structural details of casein micelles are not known but many hypotheses exist as to their form (83-88). The primary structures of the three major proteins and their individual properties will be important in determining their contribution to micelle formation and stability.

Non uniformity of size is characteristic of casein micelles in untreated milks. Size distributions are broad ranging from 40nm in diameter to 300nm (83). Electronmicrograph displays of casein micelles show them to be approximately spherical with uneven surfaces and number average diameter of around 140nm (89).

Inelastic light scattering studies determined that 95% of micelles by weight have a diameter between 80 and 440nm, the most abundant size being about 160nm diameter (90). Techniques used to fix micelles in preparation of electron micrographs were thought to cause shrinkage of the micelles (89). Counting techniques may also contribute to the smaller average particle sizes determined by electron-microscopy while light scattering values will be influenced to a greater extent by small numbers of very large particles. Thus some discrepancies

between micelle sizes in the literature are attributable to the method of determination used.

It has also been suggested that micelles have a water rich shell which contributes to micelle stability (91,92). Such a water layer would not be visible in electronmicrographs but would contribute significantly to the radius of gyration detected by light scattering. Although only 1% of this layer would be protein it could produce a radius increase of 10nm. The micelles would have "hairs" protruding from the surface into the surrounding liquid. These hairs would be hydrophilic protein chains (93). However, it has been shown that size distributions determined by light scattering and electronmicroscopy can be adjusted to give the same results if the limitations of each technique in determining very small and very large particles is estimated (92). In this case there is no necessity to postulate any water rich coat.

Many research groups have advocated the presence of submicelles, which appear in the electronmicrographs of Farrell (94) and Shimmin and Hill (83). Such subunits reported to be about 10nm in diameter were proposed as the building blocks for larger micelles. More recent studies of Schmidt et al. (95) have substantiated this proposal.

Obviously weight and size of particles are not directly comparable since densities may vary. For the casein micelle system Dewan et al. (96) measured sedimentation coefficients of micelle fractions. They concluded that casein micelles behaved as homogeneous spheres of constant density since the sedimentation coefficient varied with molecular weight raised to the power of two thirds; a result typical of such systems. The model of a micelle as being a collection of spherical subunits leads intrinsically to regions of variable density with essentially only solvent in the interstices (97). Since

the submicelle radii are approximately 0.05 of most micelles, the concept of micelle homogenity is not completely invalidated. However elastic and quasi-elastic light scattering studies do suggest that particles with low molecular weights may be less compact than those of higher molecular weight (98).

Electronmicrographs are the main source of evidence supporting a subunit structure for micelles. Holt (98) has reinterpreted this visible evidence to be the result of variations in hydrophobicity. The extent to which various regions of the micelle will stain is explained to be dependent on the hydrophobic measure of a given region, and hence the resemblence to a spherical subunit structure visibly displayed. A gel or sponge like structure with local density fluctuations is preferred by this author.

The concept of 'hairy micelles' is intermediate between the subunit model and gels. Protein chains would necessarily also extrude from the surface of subunits, somewhat reconciling the subunit model and gel formation.

Problems exist in correlating micelle size with quantity of protein present and molecular weight. Since the volume of a sphere is proportional to the radius cubed one might assume a similar relationship between micelle molecular weight and particle radius (92).

The degree of hydration of casein micelles increases as calcium ion concentration decreases (55). Another investigation corroborates this finding and notes that no protein is released from the micelle as calcium is lost implying that the size of the micelle must increase with solvation and voluminosity (99). The micellar framework therefore seems able to swell or shrink as the calcium content changes.

Besides the influence of calcium ions on the water content of

casein micelles, lowering the temperature increases the voluminosity (100). However β-casein dissociates from the micelle as the temperature drops and the increase in voluminosity from 4 at 25°C to 4.7 at 5°C is associated with a release of micellar β-casein (101). Rose (102) reported an increase of β-casein in milk serum from 34% of serum protein at 35°C to 47% at 4°C. The ability of β-casein to associate with increasing temperature is due to the hydrophobic associations of this protein (103). Besides β-casein, which has an extremely hydrophobic tail, κ-casein will also diffuse out of the micelle and to a much lesser extent α_{s1}-casein (104,105).

Overall the average quantities of the three major caseins are α_s-caseins, 50%; β-casein, 40%, and κ-casein, 10%. Extensive analysis of bovine milks has disclosed a stoichiometric relationship between the caseins of 4 $\alpha_{s1,0}$:4β:1α_{s2}:1.5K (106). Previously Rose (85) tendered a ratio of 3α_{s1}:2β:1K-casein in his model of casein micelles. This model proposes that β-casein monomers will self associate. This is known to be an endothermic process. Subsequent attachment of α_{s1}-casein monomers and finally κ-casein leads to polymer formation with incorporation of calcium phosphate into the network as a stabilizing agent.

Payens (107) proposed a similar interaction model which emphasized hydrophobic bonding, and the role of calcium ions in conjunction with phosphate or carboxylic acid groups in holding the aggregates together. Similarly Waugh and his coworkers (108) favour a process whereby addition of calcium ions causes aggregation of α_{s1}- and β-caseins. Having reached limiting dimensions these aggregates, in the absence of κ-casein would then precipitate. Interaction between primarily α_{s1}-casein and κ-casein is thought to create a complex layer around the core which prevents precipitation (76).

High concentrations of κ-casein on the surface are necessarily an element of this coat-core model. The polymer size may then be dictated by the quantity of κ-casein available. Several studies have concluded that small casein micelles contain higher relative amounts of κ-casein than larger micelles (108-110). Detection of the carbohydrate moieties of κ-casein with periodic acid-silver methanamine led Kudo et al. (111) to several discoveries. Small micelles (diameter <100nm) under the electron microscope had silver deposited throughout, while in larger micelles it was located in surface layers only. Since κ-casein is the only micellar glycoprotein, the glycosylated form is indicated by this method. Variation in the degree of glycosylation of κ-casein has been reported and is apparently less in large micelles which led Slattery (112) to propose that assembly of micelles precedes glycosylation in the bioassembly of natural bovine micelles. However, the presence of small amounts of glycosylated κ-casein throughout the micelle suggests that glycosylating enzymes are in contact with κ-casein during micelle assembly (111).

Micelle size might also be affected by the degree of glycosylation of κ-casein which is expected to be greater at the surface. Provision of this mechanism for limiting growth of micelles by the formation of a richly glycosylated κ-casein skin dispels critics of the coat-core model who predicted that precipitation or complete dissolution would be expected, not micelle formation. Rose et al. (113) did however confirm increases in proportions of κ-casein with decreasing micelle size using chromatographic techniques where variations in the carbohydrate component of κ-caseins would not affect the result. Whether κ-casein has a role stabilizing aggregates through formation of a shell holding other components is as yet unproven.

The ability of κ-casein to stabilize the α_{s1}- and β-caseins

against precipitation by calcium ions was emphasized in a reversed role proposed by Parry and Carroll (84). Having determined no concentration of κ-casein on the micelle surface Parry suggested κ-casein as a nucleation site around which the calcium insoluble caseins would gather. All three components would, under these circumstances, occupy surface positions in similar proportions to their natural occurrence in milk, but be non-uniformly distributed through the micelle. Colloidal calcium phosphate is included in the structure of this model as its importance in determining micelle stability has been noted (102,114-116). Proteolysis of all three major casein components by an insoluble papain polymer in their naturally occurring proportions suggested that preferential localisation of κ-casein on the micelle surface was unlikely (117).

A parallel network structure proposed by Garnier and Ribadeau-Dumas (86) gives κ-casein trimers a key position at the nodes of radially orientated α_{s1}- and β-casein chains forming a Y junction. This forms an open porous network with a uniform distribution of all three components throughout in an average repeat unit of $2\alpha_{s1}$-:2β-:1κ-casein monomers. Solvent water can be held in the framework cavities (2.5 g/g of protein) which would make penetration of the micelle by large molecular weight molecules such as carboxypeptidase A (MW = 36,000) easy. The tendency of κ-casein to form trimers and larger aggregates lend support to this model (118,120).

At high ionic strengths spherical polymers of variable composition form from mixtures of bovine caseins (76). The maximum radius of these particles was 10nm. Slattery and Evard (121) suggested that these particles are comparable to sub-micelles. However, like the micelle itself the exact nature of sub-micelles is open to debate. Ideas evolved to describe the structure of micelles may be appropriate in describing sub-micelle formation.

Morr (87) has proposed a subunit model which has calcium phosphate linkages between small spherical subunits of about 30nm. These subunits are formed by aggregation of α_{s1}- and β-casein monomers in the presence of calcium into a core with a κ-casein coat surrounding it as proposed by Waugh for the whole micelle.

Formation of micelles from submicelles is supported by Pepper (122) who found that first cycle casein (whole casein separated by high speed centrifugation and freed of calcium at pH6.85) consists of unit complexes of associated α-, β- and κ-caseins of approximately 10nm which if used as the building block for micelles should have a uniform composition of these caseins. Other experiments dissociating micelles also resulted in units of 10nm diameter (123,124).

Opposing a stoichiometric relationship between the caseins is the correlation between micelle size and κ-casein content (113). In the model of Slattery and Evard (121) there is a statistical population of the caseins in each submicelle of approximately thirty monomer caseins. Several κ-casein monomers then interact and remain together on the surface of a submicelle of α_{s1}- and β-casein. That part of the surface of the submicelle covered by κ-casein is hydrophilic, the rest of the surface being composed of the more hydrophobic proteins with calcium ions bound. This amphiphilic submicelle then orientates itself to minimize energy levels by having the hydrophilic surface areas projected outwards and the hydrophobic surfaces towards the centre of the micelle. No interaction between hydrophilic and hydrophobic surfaces is likely, the extent of κ-casein on the surface therefore limiting micelle growth.

Higher concentrations of κ-casein would then reduce the average micelle size as higher proportions of the submicelle surface would be hydrophilic, as demonstrated for a combination of α_s- and κ-caseins in

equilibrium (125). The average size of natural micelles is also reduced when the percentage of κ-casein is increased (126). Calculations of micelle size distributions based on this model of casein micelles formed from submicelles of variable composition, with an overall stoichiometry of $2\alpha_s$:2β:1κ-casein reproduced a number of experimental patterns (127).

Solutions of caseins which are free of colloidal calcium phosphate have highly increased viscosities indicating the role which it plays in maintaining structure (115). Artificially prepared casein micelles have been found to increase in size with colloidal calcium phosphate content (128). The ratio of casein to colloidal phosphate in milk micelles is around 10 which would indicate extensive binding of casein by colloidal calcium phosphate preventing its changing to the crystalline hydroxyapatite form.

The nature of the phosphate links are unknown. Besides links of Ca^{2+} to serine phosphate and HPO_4^{2-} linked to these calcium ions or those associated with carboxyl groups ^{31}P n.m.r. studies have suggested the existence of casein-NH_3^+-PO_3^{3-}-Ca^{2+} links (129). The high incidence of lysine and arginine residues in all three proteins: α_{s1}-casein has 18, β-casein has 11 and κ-casein has 14; makes this type of bond formation viable (130).

Electronmicrographs of artificial casein micelles synthesized from various salt/protein combinations endorsed the suggestion that a citrate apatite was present (114,131). Milk salt determinations in conjunction with Lyster's (132) conclusions that micellar phosphate is primarily hydroxyapatite have led Holt (133) to consider a complex such as $\left(Ca_5OH(PO_4)_3\right)_5 \left(CaMg_2(Cit)_2\right) (CaHPO_4)_2$ to form salt bridges between the proteins. X-ray diffraction did not detect any crystalline forms of hydroxyapatite despite its predicted insolubility from the solubility product.

Previously Lin et al (134) suggested a size determining micellar framework composed of predominantly α_s-casein and colloidal phosphate. Controlled removal of subcritical quantities of calcium ions from micelles released quantities of β- and κ-casein without disturbing a framework of predominantly α_s-casein. Soluble caseins from the surrounding serum can also be incorporated into the micelle, without increasing the radius thereof, by small additions of calcium ions. Two types of calcium linkages may be inferred (135). Weaker calcium ion linkages may hold soluble caseins to a micellar framework where Ca^{2+} is held more strongly.

As mentioned previously, β-casein will readily dissociate from micelles on cooling (102). Up to 60% may be released without noticeable change in the hydrodynamic radius as the calcium ion activity is reduced leaving only 40% of the structural role which Payens (107) envisaged for β-casein (134).

The total calcium content of skim milk is estimated to be 30mM but calcium ion content of the milk serum is only about 2.9mM (136-138). Over 60% of calcium ions in skim milk are associated with micelles either as colloidal calcium forming a frame with phosphate and citrate or bound to casein.

1.7 Aggregation of Proteins

1.7.1 Equilibrium

Many proteins form aggregates which have specific biological functions. Biopolymers such as collagen, myosin and haemoglobin are a few of the numerous associated proteins whose function depends upon the protein's state of aggregation and its stability. Water is the solvent in biological systems and the ionic and other species dissolved in it

may greatly influence protein aggregation.

For an association reaction to occur spontaneously the free energy change, ΔG, must be negative. Since

$$\Delta G = \Delta H - T\Delta S \qquad (1.2)$$

where ΔH and ΔS are the changes in enthalpy and entropy respectively at reaction temperature T, such a process is either exothermic or has a positive entropy change. Bloomfield (139) suggests that the latter of these two possibilities pertains to the aggregation of proteins. Normally the entropy of a given system would be reduced when two or more molecules combine, but solvent water molecules, thought to form ordered clusters around non polar groups would be free to adopt a more random arrangement if these non-polar groups associated. The entropy of the system would therefore be increased. Increased self-association of β-casein with rising temperature can be attributed to this effect (64). Calcium induced aggregation of α_{s1}-casein becomes endothermic when the $[Ca^{2+}]$ is sufficiently large to induce precipitation, indicating that the association process is driven by the entropic effect of desolvation (60).

Protein conformation may be either unordered structure or more ordered helical and intramolecularly bonded structures. Certain conformations may be stabilized by the exothermic nature of hydrogen bond formation or bonds between sulphydryl groups. Dipole interactions, such as the specific ion pairing PO_4^--Ca^{2+}-PO_4^- which may occur in caseins involve considerable enthalpic as well as entropic factors contributing to the stability of the aggregates.

Ionic strength and pH also affect the extent of protein aggregation, perhaps by producing conformations which differ in their ability to associate. For example, in the pH range 5 to 6 α_{s1}-casein adopts a conformation necessary for precipitation (59).

Studies on the aggregation of caseins have not to date been considered in terms of an equilibrium between monomer and polymer caseins such as Steiner (140) used to analyse insulin tetramerization. Intermediate species such as dimer and trimer are considered to exist as part of a series of equilibria, and association constants. The equilibrium constant for dimer formation K_2 is defined by

$$K_2 = \left[M_2\right] / \left[M_1\right]^2 \qquad (1.3)$$

where $\left[M_x\right]$ is the molar concentration of the species which has degree of association x. Similarly

$$K_3 = \left[M_3\right] / \left[M_1\right]\left[M_2\right] \qquad (1.4)$$

or $$K_3' = \left[M_3\right] / \left[M_1\right]^3 = K_2K_3$$

The weight average molecular weight of a polymer in solution is given by

$$\overline{M}_w = \sum^x n_x m_x^2 \; / \; \sum^x n_x m_x \qquad (1.5)$$

where m is the monomer molecular weight and n_x is the number of moles of species x. Steiner combined these two relationships and, by assuming that pentamer was the most aggregated form of insulin, defined the molecular weight as

$$\overline{Mw} = \frac{\left[M_1\right] m^2 + 4\left[M_2\right]m^2 + 9\left[M_3\right]m^2 + 16\left[M_4\right]m^2 + 25\left[M_5\right]m^2}{m\left(\left[M_1\right]+\left[M_2\right]+\left[M_3\right]+\left[M_4\right]+\left[M_5\right]\right)} \qquad (1.6)$$

Equilibrium constants can then be related to $\overline{Mw}$ by

$$\overline{Mw} = 1/c\left(\left[M_1\right] m^2 + 4K_2\left[M_1\right]^2 m^2 + 9K_3K_2\left[M_1\right]^3 m^2 + 16\,K_2K_3K_4\left[M_1\right]^4 m^2 + 25\,K_2K_3K_4K_5\left[M_1\right]^5 m^2\right) \qquad (1.7)$$

with c as the total weight concentration of all species. Manipulation of these equations allows K_2, K_3, K_4 and K_5 to be graphically determined.

In general, association products of insulin monomers were favoured by increased ionic strengths and less acidic pH values. Both conditions will decrease the positive charge associated with the protein.

The heat of dissociation was found to be linearly dependent upon the square of the charge on the monomer. Dissociation is favoured by higher temperatures and the heat of dimerization was found to be of the order of 62.7kJ/mol at pH2.65 in 0.05M KCl.

Increasing ionic strengths and reducing the pH between 7 and the isoeletric point at pH4.6 will decrease the net negative charge of both α_{s1} and β-casein. Aggregation is again favoured by this reduced monomer charge (58,74).

Verwey and Overbeek (141) developed a theory for calculating interaction energies using a uniformly charged sphere as the subunit model. The electrostatic work V_o, required to bring two such subunits together can be estimated by calculating the surface potential ψ^o on each sphere

$$\psi^o = \frac{4 \pi a^2 \sigma}{D} \left(1/a_1 - \frac{K}{(1+Ka_2)} \right) \qquad (1.8)$$

where a_2 is the sum of the radii of two interacting charged spheres i.e. monomer and chloride ion in the case of insulin; K is the Debye-Hückel constant depending on the interacting valencies and σ is the surface charge density. If ψ^o is assumed to be constant and independent of interparticle distance then

$$V_o = 0.39 \; D \; a \; (\psi^o)^2 \qquad (1.9)$$

Alternatively the electrostatic part of the chemical potential derived from Debye-Hückel theory can be calculated as

$$\mu_1^{\varepsilon} = \frac{N^o \varepsilon^2 Z^2}{2D} \left(1/a_1 - \frac{K}{(1+Ka_2)} \right) \qquad (1.10)$$

giving a free energy $\Delta\mu_{\varepsilon}$ for electrostatic interaction of

$$\Delta\mu_{\varepsilon} = \mu_2^{\varepsilon} - 2 \mu_1^{\varepsilon} \qquad (1.11)$$

which is related to the net charge per subunit Z (140). Discrepancies between interaction energies calculated by the above method and the

empirical results for insulin association were traced to the approximation of spherical geometry.

Casein polymerization in the presence of Ca^{2+} produces very large polymers which eventually precipitate. Indefinite multimerization processes of this nature were considered by Tang et al. (142) in terms of the equilibria involved. Four distinct types of association were hypothesized and the self association of β-lactoglobulin was compared to these models.

In the first of these models all molar association constants are assumed to be equal.

$$k_{12} = k_{23} = k_{34} \ldots\ldots \text{ where } k_{ij} = \frac{[M_j]}{[M_{j-1}][M_1]} \qquad (1.12)$$

Some indefinite associations of alcohols have lower dimerization constants and therefore do not fit this simple model (143). In this case $k_{12} \neq k_{23} = k_{34}$ ..... A third association model is described by the equation

$$nM_1 \rightleftharpoons qM_2 + hM_4 + jM_6 + \ldots\ldots \qquad (1.13)$$

where all species containing odd numbers of subunits are absent beyond monomer. Here dimerization is followed by association to form larger aggregates with other preaggregated forms. All molar association constants are once again assumed to be equal. i.e. $k_{12} = k_{24} = k_{46} = k_{26}$. If the dimerization constant k_{12} was less than the others, a fourth type of association arises.

Equilibrium constants K_1, K_2, K_3 etc. can be defined in terms of concentrations (mg/ml). For example $K_2 = k_2/M_1$ where M_1 is the monomer molecular weight. The concentration of dimer would then be $C_2 = 2 K_2 C_1^2$.

From their studies on insulin, Pekar and Frank (144) found

that association constants for all association steps were equal. Insulin polymerization is a stacking process with an essentially constant increment of free energy accompanying each addition. Although Lewis and Adams (145) first characterized association of β-lactoglobulin A as being of the same type, later results were better interpreted as the third type of association (142).

There is a possibility that the indefinite associations which both α_{s1} and β-casein are subject to, could be analysed according to these considerations.

1.7.2 Kinetics

Besides the equilibrium properties of association reactions some consideration has also been given to the dynamics of these interactions. Koren and Hammes (146) have studied the dimerization of insulin, β-lactoglobulin and α-chymotrypsin. These reactions were induced by the method of temperature jump and monitored by changes in pH associated with aggregation.

The rate constant for insulin dimerization was determined to be 1.14×10^8 $M^{-1}S^{-1}$ which approaches the rate of a diffusion controlled reaction. According to Amdur and Hammes (147) the rate constant for a diffusion controlled reaction is given by

$$k = \frac{4\pi N}{1000} (R_A + R_B) (D_A + D_B) f \quad 1m^{-1}S^{-1} \qquad (1.14)$$

where N is Avogadro's number, $R_A + R_B = R_{AB}$ = distance of closest approach of two species A and B where D_A and D_B are their respective diffusion coefficients and f is the factor which accounts for electrostatic interactions. This gives a maximum rate constant for a diffusion controlled reaction in solution of 5×10^9 $M^{-1}S^{-1}$, unless electrostatic and steric effects are much larger than usual.

Lower rate constants of 4.7×10^4 $M^{-1}S^{-1}$ for β-lactoglobulin and 3.7×10^3 $M^{-1}S^{-1}$ for α-chymotrypsin were determined at pH3.7 and 4.3 respectively. Under these conditions both proteins would be highly charged and repulsive interactions strong.

Smoluchowski (148) developed a mathematical theory for diffusion controlled aggregation processes where large polymers were formed i.e. unlike the associations described above, indefinite self-association is considered. The rate of collision between particles was related to the radius of the particle R, the diffusion coefficient D and the concentration of particles. D increases as the radius decreases so that the product DR is effectively constant. Naturally D is dependent upon temperature and viscosity of the medium.

If ν_x is the concentration of x-mer and ν_0 the initial concentration of monomer then the rate of reaction can be expressed as

$$\frac{d\nu_1}{dt} = -4\pi\ DR\ \nu_1\ \Sigma\ \nu_x \qquad (1.15)$$

All rate constants for reactions between monomers and monomers; aggregates and monomers, and aggregates of all kinds were assumed to be equal and given the value k_s. Adopting a second order reaction process gives

$$\frac{d\nu_1}{dt} = -2k_s\nu_1\Sigma\nu_x \text{ where } 2k_s = 4\pi DR \qquad (1.16)$$

The rate constant k_s is effectively a measure of the rate of diffusion of particles through solution at a given temperature. Smoluchowski established that

$$\Sigma\nu_x = \nu_o\ (1 + \nu_o k_s t)^{-1} \qquad (1.17)$$

and

$$\nu_x = \frac{\nu_o\ (k_s \nu_o t)^{x-1}}{(1 + k_s \nu_o t)^{x+1}} \qquad (1.18)$$

Adapting the expression for weight average molecular weights from molar to concentration terms gives

$$\overline{MW} = \frac{M_o \Sigma x^2 \nu_x}{\Sigma x \nu_x} \qquad (1.19)$$

Substituting equations 1.17 and 1.18 in this expression produces a linear dependence of $\overline{Mw}$ upon time (see Appendix 1)

$$\overline{Mw} = Mo\ (1 + 2k_s \nu_o t) \qquad (1.20)$$

Extensive aggregation of α_{s1}-casein is observed when Ca^{2+} is added. Parker and Dalgleish (149) followed the association process using light scattering methods to determine the weight average molecular weights. Reaction profiles typically exhibited a linear growth of $\overline{Mw}$ with time after an initial phase during which particle growth was less rapid. The constancy of $d\overline{Mw}/dt$ in the second phase was attributed to the diffusion controlled polymerization mechanism envisaged by von Smoluchowski. A value of $2.24 \times 10^6\ M^{-1}S^{-1}$ was obtained for k_s.

1.7.3. Aggregation of caseins as colloidal particles

Many proteins in solution are highly charged and the caseins are a prime example. Separation of casein fractions has been achieved using methods depending upon charge differences, such as electrophoresis and chromatography (17,150). This charge arises from ionization of functions such as carboxylate on amino acid residues and phosphoserines. Neutralization of this charge can be achieved by adjusting the pH of the protein solution. The protein is least soluble when neutralized and may precipitate (150). As observed for β-lactoglobulin and α-chymotrypsin, electrostatic repulsion can greatly affect the rate of association of proteins.

Collisions between solute particles are frequent due to

Brownian motion. Cohesion may or may not result. In principle cohesion occurs when the area of interface between two phases is reduced as such interfaces are high in energy. However two conditions may intervene to prevent cohesion. Firstly, if particles carry an electric charge there is repulsion between two similarly charged species. Secondly, penetration of the particle by molecules of the dispersion medium, usually water, minimize interfacial energy.

Casein micelles can be considered to be colloidal particles suspended in milk serum. The voluminosity of these micelles as previously discussed, may extensively influence their stability as the hydration of 3.7g H_2O/g protein is extremely large when compared to other globular proteins (67,151). This high degree of hydration leads to a view of a very porous structure. Cohesion between two such particles would not appreciably lower the surface area in contact with solvent molecules.

In the case of charged species such as the individual caseins, water molecules will be associated with the charge groups, held by ion-dipole or dipole-dipole interactions as well as hydrogen bonding to amino or hydroxyl groups. Besides the hydrating water molecules and loosely associated solvent water, counter ions will be required within the vicinity to effect electroneutrality. These are envisaged in a layer beyond the hydration layer of the protein and are also appropriately hydrated. This is known as the Helmholtz diffuse double layer.

Within the double layer the potential will decrease rapidly with distance from the charge and then more slowly. The thickness of the double layer is defined to be the distance over which the potential drops to $1/e = 0.37$ of its original value (152). An increase in electrolyte concentration would increase the concentration and shielding

effect of the counterions in the double layer leading to a faster decay of potential with distance from the charge surface and a corresponding decrease in the size of the double layer. Similarly the screening effect of counterions with valencies of two or even three is much greater and reduces the size of the double layer. It is expected that particles having a small double layer and smaller effective size would diffuse more rapidly through solution. Increasing temperature is expected to increase thermal agitation.

Reducing the charge on the caseins reduces the repulsive forces between them. The energy barrier preventing cohesion of the particles is reduced thereby increasing the number of collisions which will result in cohesion. The potential energy curve for two colloidal particles approaching each other is shown in Fig. 1.5 where ν_m is the energy barrier to coalescence. After crossing this energy barrier two particles have closed to a distance where the London-Van der Waals forces are greater than the electrical repulsion of the double layers (153).

Reaction between aggregating particles was described by von Smoluchowski (148) as a bimolecular reaction having a rate constant k_s i.e.

$$- \frac{d[M]}{dt} = k_s [M]^2 \qquad (1.21)$$

where M is the concentration of monomer. No barrier to reaction is envisaged by this theory except the restraints that temperature, T, and viscosity η will place upon the rate constant k_s since

$$k_s = 4kT/3\eta \qquad (1.22)$$

where k is the Boltzman constant (154). Introduction of an energy barrier requires modification of this expression by a term W which retards flocculation (153).

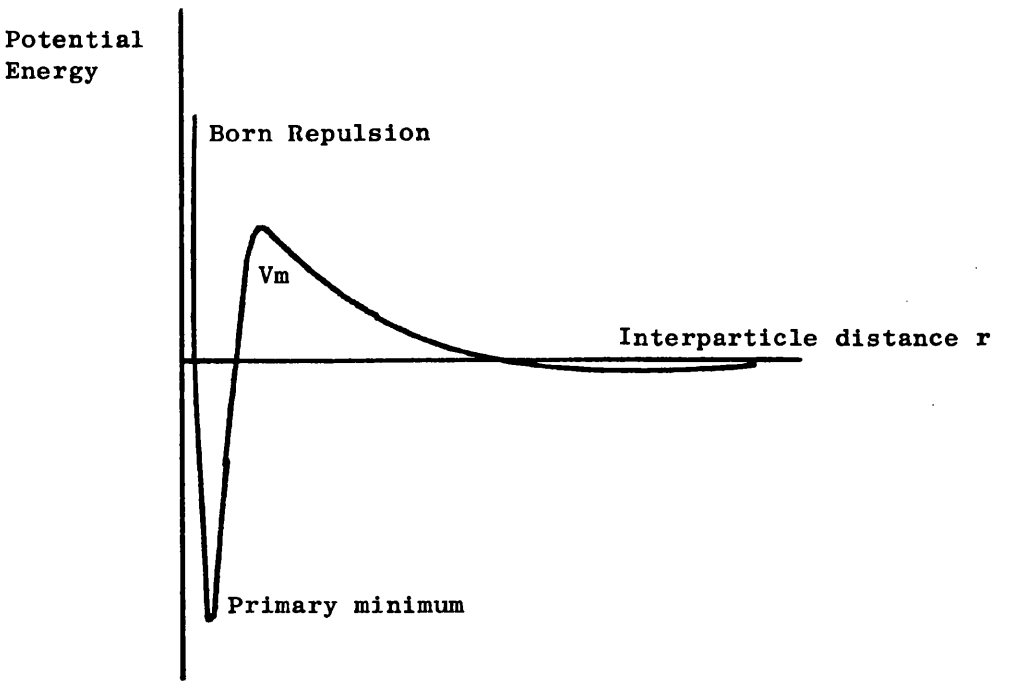

Fig. 1.5 Diagram of the total Potential Energy curve for two colloidal particles. Vm is the energy barrier retarding the coagulation of stable colloids.

$$W = 2\alpha \int_{2\alpha}^{\infty} \exp(V_t/kt)\, dr/r^2 \qquad (1.23)$$

where α is the particle radius and Vt the potential energy of a pair of micelles at interparticle surface to surface distance r.

To evaluate the potential energy term V_p, the attractive and repulsive energy contributions must be added.

$$V_p = V_A + V_R \qquad (1.24)$$

Derjaguin (155) defined the repulsive term as

$$V_R = \frac{\varepsilon \alpha \psi_o^2}{2} \ln (1 + e^{-kr}) \qquad (1.25)$$

where ε is the dielectric constant, k the Debye-Huckel parameter referring to the thickness of the double layer and ψ_o is the surface potential when the particles are at their equilibrium positions. Attraction between particles decreases enormously with increasing interparticle distance.

$$V_A = \frac{\text{const}}{r^6} \qquad (1.26)$$

The rate of reaction will obviously depend upon the size of the energy barrier ν_m. Arrhenius found that the rate of reaction was related to the activation energy E_a, which Fuchs (119) and Overbeek related to the maximum ν_m in the PE curve.

$$\ln k = \ln A - Ea/RT \qquad (1.27)$$

Horne and Dalgleish (156) combined equations (1.27) and (1.25) producing

$$\ln k = \ln A - \left(FQ^2 \ln (1 + \exp^{-kr_o}) - \frac{\text{const}}{r_o^6} \right) /RT \qquad (1.28)$$

such that the activation energy is defined in terms of Q which is the charge on a spherical particle and is related to the surface potential by

$$Q = \alpha\varepsilon (1 + \kappa\alpha) \psi_o \qquad (1.29)$$

The particle radius is also involved in the F term which is purely a convenient substitution.

$$F = \frac{1}{\alpha\varepsilon}(1 + \kappa\alpha)^2$$

From equation 1.28 it is clear that flocculation is impeded by increasing the charge on the particles. The interparticle distance corresponding to the maximum energy position is r_o and will alter slightly with changes in the charge of the spheres. The effects and implications of this variation were considered in depth by Horne and Dalgleish (156) who concluded that the height of the energy barrier or E_{max} was very close to a linear relationship with the square of the charge on a sphere i.e.

$$E_{max} = xQ^2 + y$$

as would in fact be concluded from a much simpler inverse square relationship for charge repulsion.

Spectrophotometric plots representing changes in solution turbidity showed the same features in the reaction profile of α_{s1}-casein with Ca^{2+} which had previously been observed by laser light scattering, namely a lag phase followed by a linear section (149,156). By extrapolation of the linear portion to zero absorbance the length of the lag phase was indicated. This time was called the coagulation time CT, and was shown to be a parameter which could be used to diagnose the rate of reaction. Linear relationships were obtained when ln (CT^{-1}) was plotted against Q^2. A linear relationship between the rate constant for the rate determining step in the aggregation process and Q^2 was demonstrated.

The rate of precipitation was not directly dependent upon $[Ca^{2+}]$ but rather upon the charge on the protein as a result of Ca^{2+} binding.

1.7.4 Polyfunctional aggregation

Casein aggregation can be considered as a polymerization reaction and it is possible to explain aspects of this by a polyfunctional condensation model. According to this model, the first prerequisite for a monomer to be able to react to form aggregates is that it should have two or more active sites (only one reactive site per molecule can only lead to dimer formation). If there are two reactive sites per monomer a linear polymer is formed whereas a crosslinked or branched polymer will result from aggregation of monomers with more than two reactive sites or functionalities (157).

High molecular weight polymers are produced more readily as the number of functionalities is increased. Binding of Ca^{2+} to α_{s1}-casein could create the monomer functionalities although an exact description of the functionality is not necessary (158). The average number of Ca^{2+} bound will affect the average number of functionalities, per monomer, f, created.

Any polymer system formed by monomers with $f > 2$ will have some functional groups which are unreacted. Where the number of monomers in a given particle is x, these will be $(fx-2x+2)$ free functionalities.

According to Gordon (159) the weight average molecular weight is related to the proportion of reacted functionalities, γ, by the expression

$$\overline{Mw} = M_o \left(\frac{1 + \gamma}{1-(f-1)\gamma} \right) \qquad (1.32)$$

The molecular weight will be infinite when $(f-1)\ \gamma = 1$. For a system with $f = 3$ only half the functionalities will have reacted at the gel point i.e. $\overline{Mw} \rightarrow \infty$.

If the concentration of free functionalities is initially C_o and after time t, becomes C_t then the concentration of reacted functionalities at that time is (C_o-C_t). The proportion of reacted functionalities is $(C_o-C_t)/C_o$. Substitution in Eq. 1.32 gives

$$\overline{Mw} = M_o\left(\frac{2C_o-C_t}{C_o-(f-1)(C_o-C_t)}\right) \qquad (1.33)$$

Assuming that the rate of reaction of two monomers depends only on two functionalities meeting then a second order rate equation will operate. The rate of reaction will vary with kC^2 where C is the concentration of free functionalities at a given time t and k is constant. Integrating and substituting C_o as the initial concentration of free functionalities gives

$$C_t = C_o \Big/ (1 + C_o kt) \qquad (1.34)$$

Combining equations 1.33 and 1.34 gives

$$\overline{Mw} = M_o\left(\frac{1 + 2ktC_o}{1-(f-2)\ ktC_o}\right) \qquad (1.35)$$

Thus when $(f-2)\ kC_o t = 1$ the molecular weight will tend to infinity, in other words the gel time, t gel, is $\left((f-2)kC_o\right)^{-1}$. Where dilute solutions are used precipitation will occur rather than gelation. Notice that if f = 2 precipitation should only occur at infinite time. However, the appearance of precipitate will occur in finite time.

By plotting the theoretical molecular weight as the polymerization proceeds, a reaction profile depicts a lag phase during which $\overline{Mw}$ increases only slowly with time, followed by a dramatic increase in $\overline{Mw}$ over a very short time interval. The molecular weight rapidly approaches infinity during this time as shown in Fig. 1.6.

Increasing the average number of functionalities per monomer will substantially reduce the gelation or precipitation time (see Fig. 1.6).

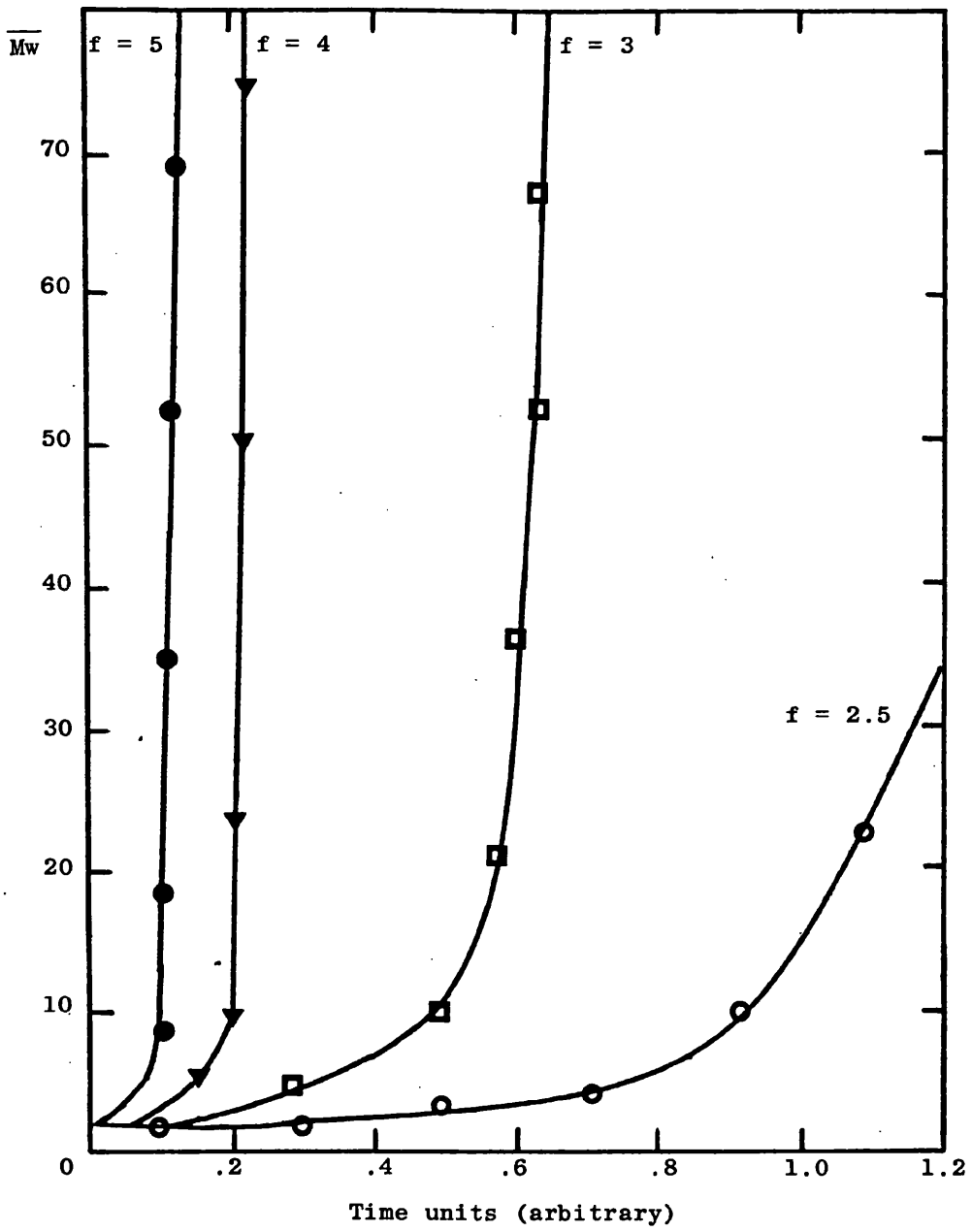

Fig. 1.6 Change in $\overline{Mw}$ with time in the polymerization of monomer units with average functionalities f. ●, f = 5; ▼, f = 4; ◘, f = 3; ○, f = 2.5.

The length of time which elapses prior to rapid growth in molecular weight can be defined as the gel time.

The lag phase, predicted by this theory, in the growth of molecular weight with time suggests that aggregation of α_{s1}-casein induced by Ca^{2+} might follow this mechanism. The length of lag phase is determined by the average number of functionalities per monomer (see Fig. 1.6) which would be a result of the average number of Ca^{2+} bound per monomer, $\bar{\nu}$. Thus the lag phase is predicted to decrease when $\left[Ca^{2+}\right]$ is increased. This is actually observed (149).

However the linear growth of $\overline{Mw}$ with time which subsequently occurs is not predicted by the polyfunctional model. Instead $\overline{Mw}$ calculated from Eq 1.35 rapidly tends to infinity after the lag phase. The time course of the reaction of Ca^{2+} with α_{s1}-casein was explained in terms of the polyfunctional model which accounts for the slower reaction in the early stages and then in terms of a Smoluchowski reaction scheme which explains the failure of the $\overline{Mw}$ to tend to infinity (149).

1.8 AIMS AND OBJECTIVES

A preliminary investigation of the kinetics of α_{s1}-casein aggregation in the presence of Ca^{2+} was carried out by Parker and Dalgleish (149). The method of light scattering and stopped flow was shown to be valid for this system. The investigation was limited to a single calcium ion concentration and to three α_{s1}-casein concentrations in a restricted range. It was proposed therefore to extend this work by investigating the kinetics of α_{s1}-casein aggregation over a wider range of reactant concentrations.

A reaction mechanism was proposed which involved polymerization of a polyfunctional monomeric system until particles are formed which are limited in their rate of reaction by the rate at which they can diffuse through solution. This polyfunctional mechanism, outlined in Section 1.7.4, does not predict the correct second stage for the reaction and in addition does not clearly define a functionality. The diffusion controlled rate constant is considerably smaller than expected for a truly diffusion limited reaction rate indicating that an activation energy is still involved in the reaction. Thus it is difficult to argue that the second stage of the reaction is truly limited by the rate of diffusion making breakdown of the polyfunctional theory on this basis unlikely.

One of the aims of this project was therefore to find a mechanism which could explain the observed reaction kinetics and other known properties of the Ca^{2+}/α_{s1}-casein reaction. Although an equilibrium between soluble and precipitable material in this reaction had been observed by other workers (54,56) and again during the study by Dalgleish and Parker, this was not adequately accounted for in the mechanism which they proposed. A further aim of this project was to

investigate the soluble/precipitable protein equilibrium involved in the reaction.

Horne and Dalgleish (156) demonstrated that the rate of aggregation of α_{s1}-casein in the presence of Ca^{2+} could be related to the charge on the protein monomer. This study investigated the effect of Ca^{2+} concentration in detail but the effect of α_{s1}-casein concentration was not so clearly defined. No mechanism was suggested to account for this observation which was derived from measurements of changes in solution turbidities. As a result the concentrations which could be investigated were limited. It was expected that this present work would allow development of an overall reaction mechanism, incorporating charge considerations along with the other effects, to successfully predict the pattern of molecular weight growth in solution which cannot easily be done directly from turbidity measurements.

No previous investigation of the effect of temperature on the association reaction of α_{s1}-casein in the presence of Ca^{2+} has been made. One objective of this project was to observe and quantify the effect of temperature on this reaction.

Another objective of the present work was to investigate the kinetics of the reaction of β-casein in the presence of Ca^{2+} as there has to date been no such elucidation of this reaction of β-casein. It was hoped that a mechanism could be proposed for this reaction. Although the effect of temperature on the self association of β-casein has been reported (69) this has not been the case for the association of β-casein in the presence of Ca^{2+}. A further objective was to study the association of β-casein in the presence of Ca^{2+} at a variety of different temperatures, with a view to including the effect of temperature along with the effect of other variables which must be encompassed in any mechanism. It will also be of interest to ascertain whether the

soluble/precipitable protein equilibrium exists for the Ca^{2+}/β-casein reaction.

The broad aim of this project was therefore to investigate those questions and problems outlined above, to clearly define the forces and mechanisms involved in the aggregation reactions of both α_{s1}- and β-casein in the presence of Ca^{2+}. Using the information on the behaviour of these two simplified systems, future work could investigate the effects of the other constituents on the aggregation reaction until the factors controlling micellisation in a natural milk system are clearly defined.

2. Materials and methods

The following chemicals, used in this work, were supplied by B.D.H. Chemicals Ltd., Poole, England: sodium chloride, calcium chloride hexahydrate, barbitone, mercaptoethanol, and tris (hydroxymethyl) methylamine.

May and Baker Ltd., Dagenham, England supplied sodium formate, formic acid, sodium hydroxide pellets, ammonium chloride, ammonia solution, methanol and concentrated hydrochloric acid.

The procion blue dye was supplied by I.C.I., Manchester, England, and the imidazole by Sigma London Ltd., Fancy Road, Poole, England.

The other chemicals, namely disodium ethylenediamine tetra-acetic acid, urea and sodium 5,5-diethyl barbiturate were supplied by Hopkin and Williams, Chadwell Heath, Essex, England.

2.1.1. Preparation of whole casein

Milk was obtained from an individual Ayrshire cow which was selected as being free from mastitis. To each 5 ℓ of milk 300 mls of a solution of 0.5M Na_2-EDTA and 1M NaOH was added. After centrifugation (MSE Mistral 6L, 2000 RPM, 4 x 1 ℓ swing-out rotor) for 30 minutes at 18°C, followed by 30 minutes at 5°C, a small section of the cream layer was scooped out allowing the skim milk to be siphoned off from below. Whole casein was precipitated from this solution by acidification with 1M HCl to pH4.7 at 25°C after an equal volume of distilled water had been added.

Filtration and draining of the casein using a Whatman 113V folded filter (H. Reeve Angel and Co. Ltd., London) yields casein in the form produced by Zittle and Custer (160). The casein was redissolved in distilled water with continuous addition of 1M NaOH to

maintain the solution at pH7. Precipitation by acidification to pH4.7 and filtration, was repeated and the casein was redissolved in a minimum volume of FFU buffer (59mM sodium formate, 0.25M formic acid, 6.6M urea, pH3.5) to a concentration of approximately 50mg/ml.

2.1.2. Column chromatography of whole casein

A wide diameter (16cm) preparative column of length 20cm was used, containing SP-C25 Sephadex (Pharmacia, Great Britain, Ltd., London) swollen in FFU buffer. The solution of whole casein (10 litres) was applied to the top of the column, followed by 2 bed volumes of FFU buffer. The column was then eluted at $5^{o}C$ with FFU buffer and the effluent collected in hourly fractions (~ 500 mls).

Spectroscopic determination at 278nm using a Cary 118C spectrophotometer were corrected by the absorbance at 320nm to give the protein concentration. This correction removed any turbidity effects since turbidity $\tau \propto \lambda^{-4}$. The true reading was corrected as (161)

$$\text{True value} = \text{value at 278nm} - (320/278)^{4} \times \text{value at 320nm} \qquad (2.1)$$

The elution profile is shown in Fig. 2.1 where the corrected optical densities are plotted. Electrophoresis (see Section 2.1.5.) of a sample from the first band, A, against samples of α_s-, β- and κ-casein reveal that this band had a high protein content and was identified as β-casein.

After all of peak A had been eluted (30 litres of elution volume collected) a salt gradient of NaCl was applied. To produce a gradient increasing from zero to ~ 0.25M, 35 litres of 0.5M NaCl in FFU buffer was continually syphoned into 35 litres of FFU buffer which was gradually being drawn on to the column.

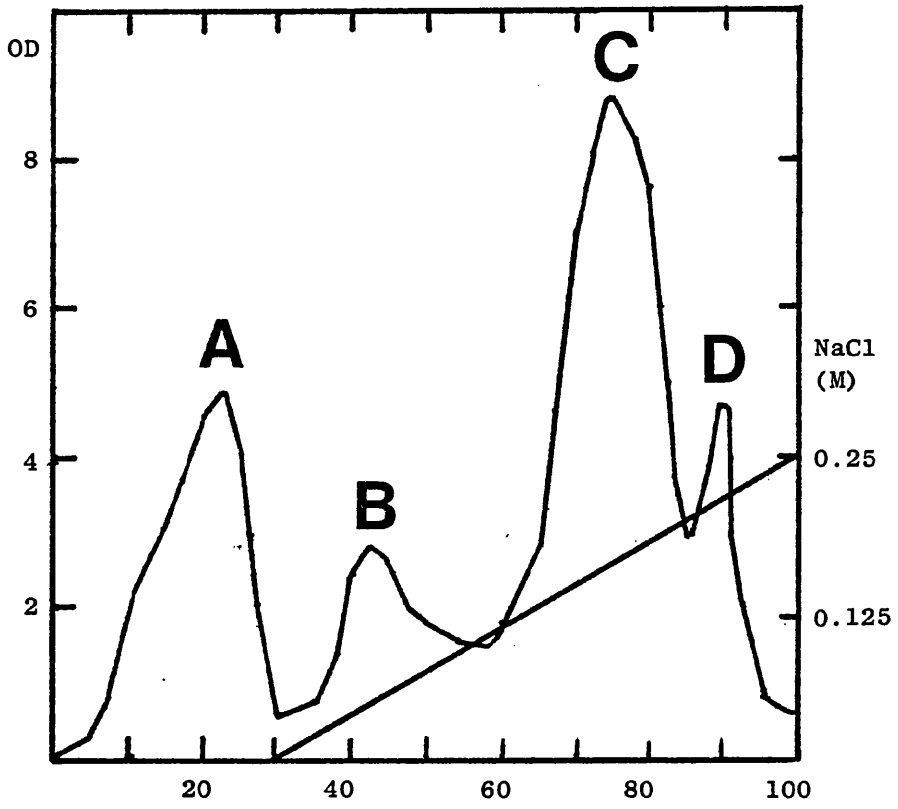

Fig. 2.1. Elution profile of whole casein on the preparative 16 x 20 cm column of sephadex SP-C25: absorbance at λ = 278mm of the eluted fractions (500 mls). The straight line shows the concentration of salt from the gradient during elution.

Three further bands with a high protein content were identified (Fig. 2.1). Peak B was shown by electrophoresis to be κ-casein. Peaks C and D were attributed to $\alpha_{s0,1}$- and α_{s2}-caseins respectively, by comparison with α_{s1}-casein on electrophoresis (see Fig. 2.2).

2.1.3. Isolation of β-casein

The first group of fractions, peak A, which had been shown by electrophoresis to be β-casein, were pooled and exhaustively dialysed against distilled water at 5°C until the protein precipitated. After removing the β-casein suspension from the dialysis tubing, the pH was adjusted to 4.7 before filtering. The precipitate was redissolved in 20mM imidazole at pH7 and this solution was then dialysed against 15 litres of this 20mM imidazole buffer at pH7. Vials containing 25 ml of this β-casein solution at a concentration of 1g in 25 ml , as determined by spectrophotometry at 278nm, were stored at -20°C until required. (1g/l β-casein at 278nm has an absorbance of 0.47 (76, 162)). The yield of β-casein from 30 litres of full cream milk was 30g.

2.1.4. Isolation of α_{s1}-casein

Fractions containing predominantly α_{s1}-casein (peak C) were examined electrophoretically. Those fractions which fell between the half heights of the peak were determined to contain only α_{s1}-casein and were pooled. The leading edge of peak C (around 65 litres of elution volume) contained α_{s0}- and α_{s1}-caseins while the trailing edge of peak C beyond 82.5 litres of collected eluant contained α_{s2}-caseins as well as the α_{s1}-casein. The pooled fractions (elution volume 68 to 82 litres) were exhaustively dialysed against distilled water at 5°C, and the pH was then raised to 4.7. After being isolated by filtration

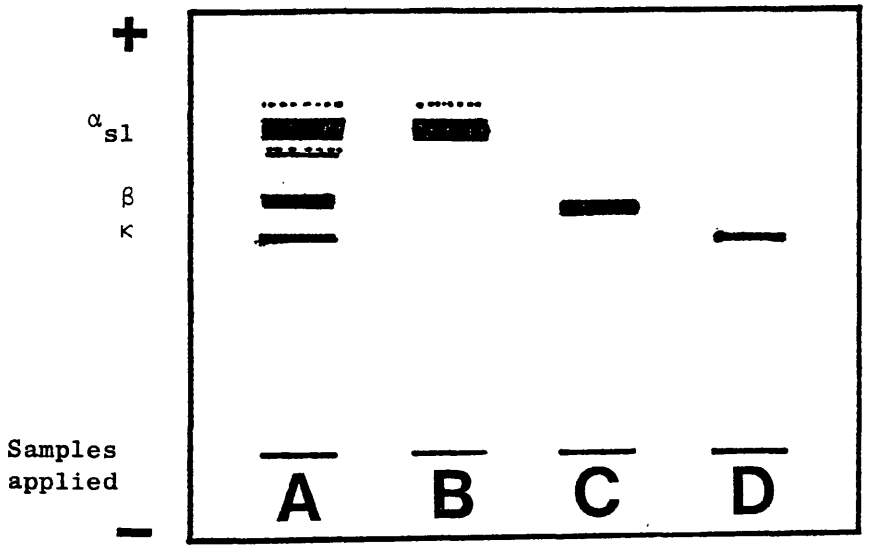

Fig. 2.2. Relative electrophoretic positions of different casein fractions. Sample A is whole casein; B, $\alpha_{s1,0}$-casein; C, β-casein, and D, κ-casein. The dotted line in sample B represents the position of α_{s0}-casein which is also present in sample A along with the α_{s2}-caseins at the position marked ==== below the α_{s1}-casein band.

the α_{s1}-casein precipitate was redissolved in 20mM imidazole at pH7. Dialysis for 24 hours against a 20mM imidazole solution was followed by adjustment of the concentration to 1g in 25 mls (α_{s1}-casein concentrations were determined spectrophotometrically at 278nm using $E^{1cm}_{1\%,278}$ = 10) (163). Vials containing 25 mls of α_{s1}-casein in this 20mM imidazole solution at pH7 were frozen and stored at -20°C until required. This separation procedure is essentially that described by Annan and Manson (17). The yield of α_{s1}-casein from 30 litres of full cream milk was 71.7g.

2.1.5. Electrophoresis on cellulose acetate ("Cellogel")

One strip of "Cellogel" (H. Reeve Angel and Co. Ltd., London) was soaked in buffer at pH8.2 for 10 minutes. This buffer consisted of tris (hydroxymethyl) methylamine, 0.3g; Na_2-EDTA, 0.12g; urea, 42g; sodium 5,5-diethyl barbiturate, 0.67g and mercaptoethanol, 200µlitres dissolved in distilled water to a volume of 100 mls.

The "Cellogel" was then placed on an electrophoresis tray which contained a similar buffer (tris (hydroxymethyl) methylamine, 0.25g; Na_2-EDTA, 0.1g; barbitone, 0.188g, and 1M HCl to reduce the pH to 8.2, made up to a volume of 500 mls in distilled water.

Each protein sample (100 µlitres) was placed on top of a few mg of solid urea in a small tube, to saturate the solution with urea. From this 5-10 µlitres of sample was extracted and spread along a 1cm length marked on the cellogel. A voltage, 240V was then applied across the strip for 45 minutes.

When the run was complete, the cellogel was removed and placed in staining solution for 10-15 minutes. The staining solution was prepared by dissolving 0.1g of procion blue dye in 98 mls of methanol and 2 mls of concentrated HCl, and filtering. Following staining, the

strip was washed with 3 changes of methanol to remove any unbound dye. before drying at room temperature.

To facilitate subsequent analysis α_{s1}- and β-casein standards were applied on parallel paths beside the samples (see Fig. 2.2).

2.2.1. Calcium ion solutions for light scattering

All calcium solutions were made up in 20mM imidazole, 50mM NaCl at pH7. A solution of approximately 20mM $CaCl_2$ was prepared from Analar grade $CaCl_2$ $6H_2O$. The exact concentration of this solution was determined by titrating against standard EDTA solutions, using an automatic titrator fitted with a calcium ion sensitive electrode (Radiometer type F2112 Ca, Radiometer, Copenhagen, Denmark) as the indicator electrode for a Radiometer PHM64 pH meter. The Na_2-EDTA was oven dried before weighing for preparation of 5mM and 1mM EDTA solutions. To each portion of calcium solution, 1ml of pH10 buffer was added before determination of Ca^{2+} concentration. (70g NH_4Cl, 568 mls ammonia in 1 litre : pH10). This ensures that complete titration of Ca^{2+} takes place.

Dilution of the standardised 20mM $CaCl_2$ solution was used to prepare solutions containing exact concentrations of Ca^{2+} in the range 13 to 18mM all in 20mM imidazole, 50mM NaCl at pH7. All of the calcium solutions were then filtered through cellulose nitrate filters (Sartorius Gmbh, Göttingen, West Germany) pore size 0.05μ to remove dust particles.

2.2.2. Casein solutions for light scattering

Vials containing 1g of protein frozen in 25 mls of 20mM imidazole were allowed to thaw. An equivalent volume (25 mls) of 20mM imidazole, 100mM NaCl at pH7 was added to the casein solution,

Casein solutions of the required concentration were then produced by diluting this solution with 20mM imidazole, 50mM NaCl buffer at pH7. All protein solutions were filtered, under pressure, through a Sartonius Membrane filter, pore size 0.05μ, before use.

Any 20mM imidazole, 50mM NaCl buffer at pH7 required for light scattering experiments was similarly filtered.

2.2.3. The flow system

Particle molecular weights can be determined by light scattering. Aggregation of caseins as a result of Ca^{2+} addition is a fast reaction at the concentrations used in this work. Following the molecular weight changes requires a stopped flow system to monitor the reaction from the point at which these reactants are mixed. The flow system used in this work was required to fit within the glass tank of a Malvern light scattering system.

The reaction of Ca^{2+} with caseins is also very sensitive to temperature and thermal regulation of the reactants and reaction system was essential. As a result of the reaction being strongly temperature dependent, an accurate measure of the reaction temperature was desirable. The flow system was designed to comply with these constraints.

Calcium and casein solutions were contained in identical syringes mounted beside each other with a horizontal bar placed across the top of both plungers (see Fig. 2.3(i)). Applying sudden pressure to this bar forces equal volumes of each solution into the small channels of the flow system (see Fig. 2.3(ii)). The solution from each syringe then divides into four narrower jets of solution as the channels of the mixer are divided and narrowed. Thorough mixing of the two reactants is ensured by this procedure.

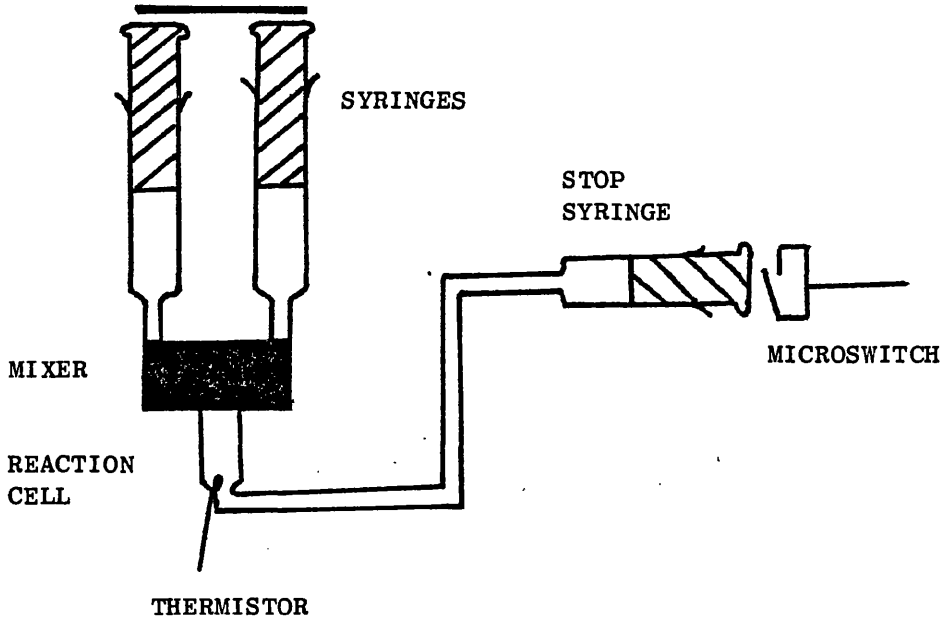

Fig. 2.3 (i). Diagram to illustrate the flow of reactants through the stopped flow system

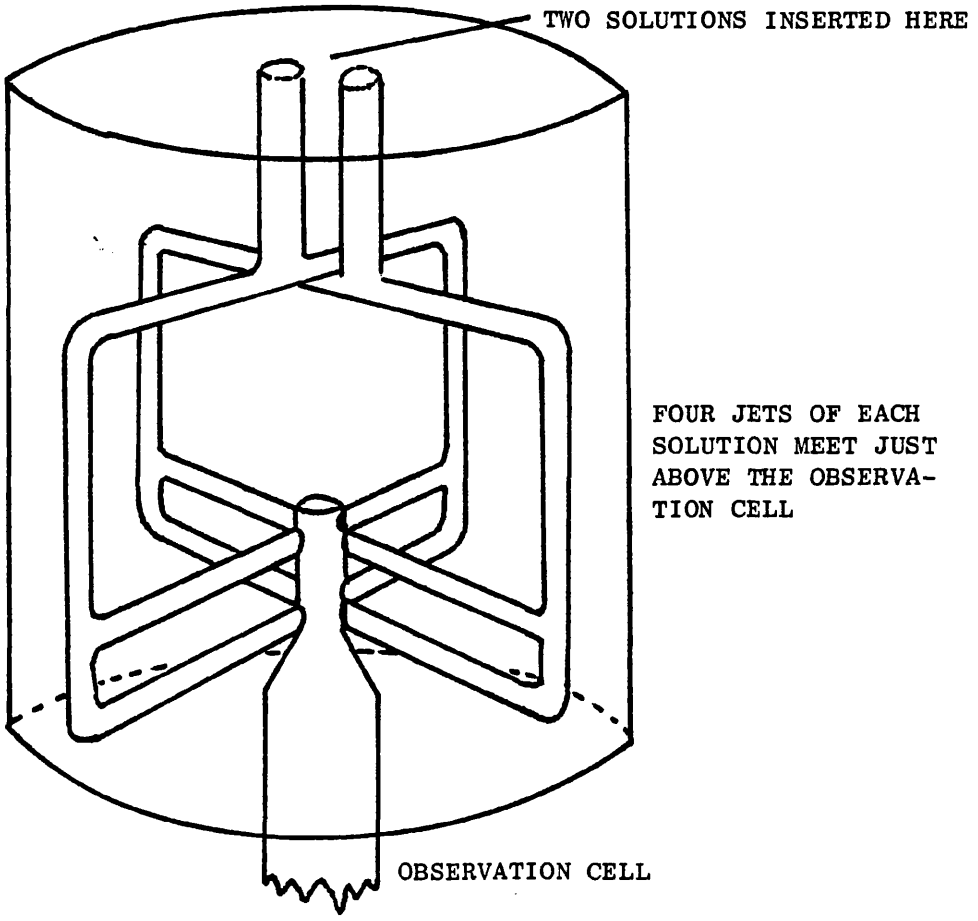

Fig. 2.3 (ii). Enlarged diagram showing the section of the flow system where the solutions are thoroughly mixed.

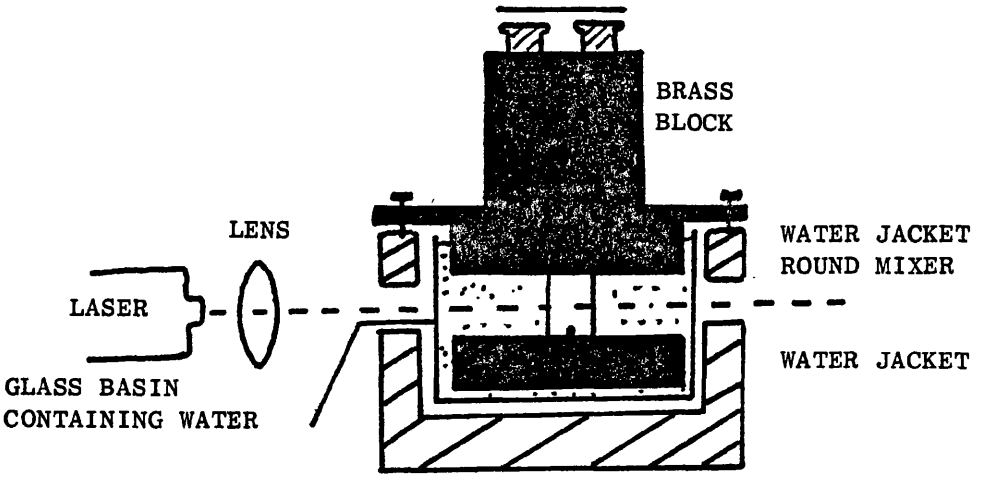

Fig. 2.3(iii) Arrangement of stopped flow system (complete with thermostatting water jackets) in the light scattering apparatus.

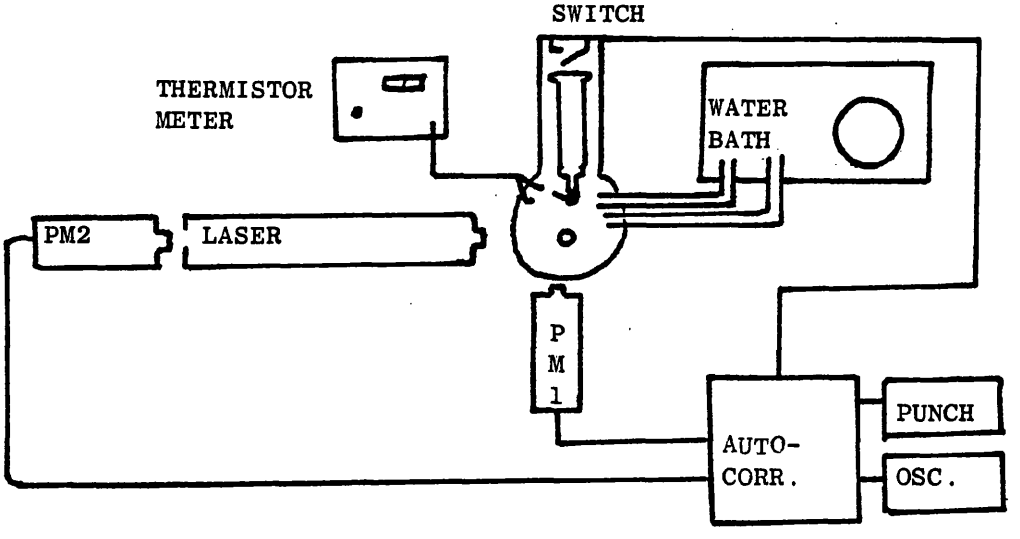

Fig. 2.3(iv) The layout and connections between the pieces of apparatus.

Immediately below the mixing chamber is the light scattering cell into which the reaction mixture is subsequently driven (see Fig. 2.3(i) and (ii)). Flow is then directed along the bottom of the flow system below the laser beam to a connecting section positioned opposite the viewing section out of line of the laser beam (see Plates 1 and 2). Exit from the flow system for the reaction mixture, via a channel in the connecting section and a small valve (see Plate 2), is into a small glass syringe (5 mls). Upon filling the plunger extends until it connects with a small microswitch which stops the flow of reagents and simultaneously initiates photon counting (see Fig. 2.3(i)). The stop syringe was emptied after each kinetic measurement (experimental run) by changing the position of the valve. The apparatus was then quickly reset for the next run. Eight to ten runs could be obtained from each pair of syringes.

Prior to connecting the syringes to the flow system they were incubated in a water bath at the required temperature for at least one hour. To maintain the solutions at this temperature a brass block which completely surrounded the syringes was fixed to the top of the flow system and water, from the same water bath, circulated through numerous channels in this block (see Fig. 2.3(iii) and Plates 3 and 4). A water jacket also surrounds the mixer above the scattering cell and the channel below the light scattering cell as shown in Fig. 2.3(iii) and Plate 2. These water jackets around the flow channels were constructed to occupy as large a volume of the glass basin as is possible without obstructing the laser beam or the viewing section.

The water held stationary in the glass basin of the Malvern system is more efficiently thermostatted by reducing its volume and filling this space with the water jackets with which it will exchange

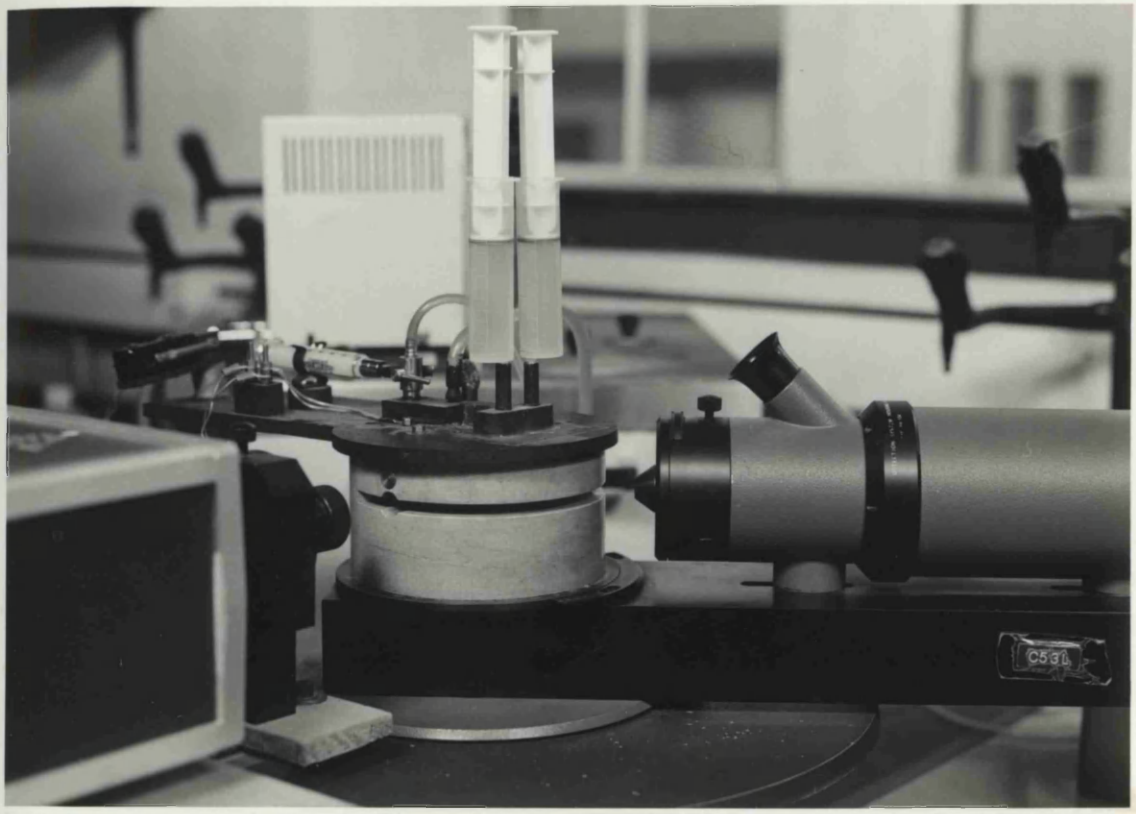

Plate 1. Stopped flow system inserted into the Malvern light scattering system

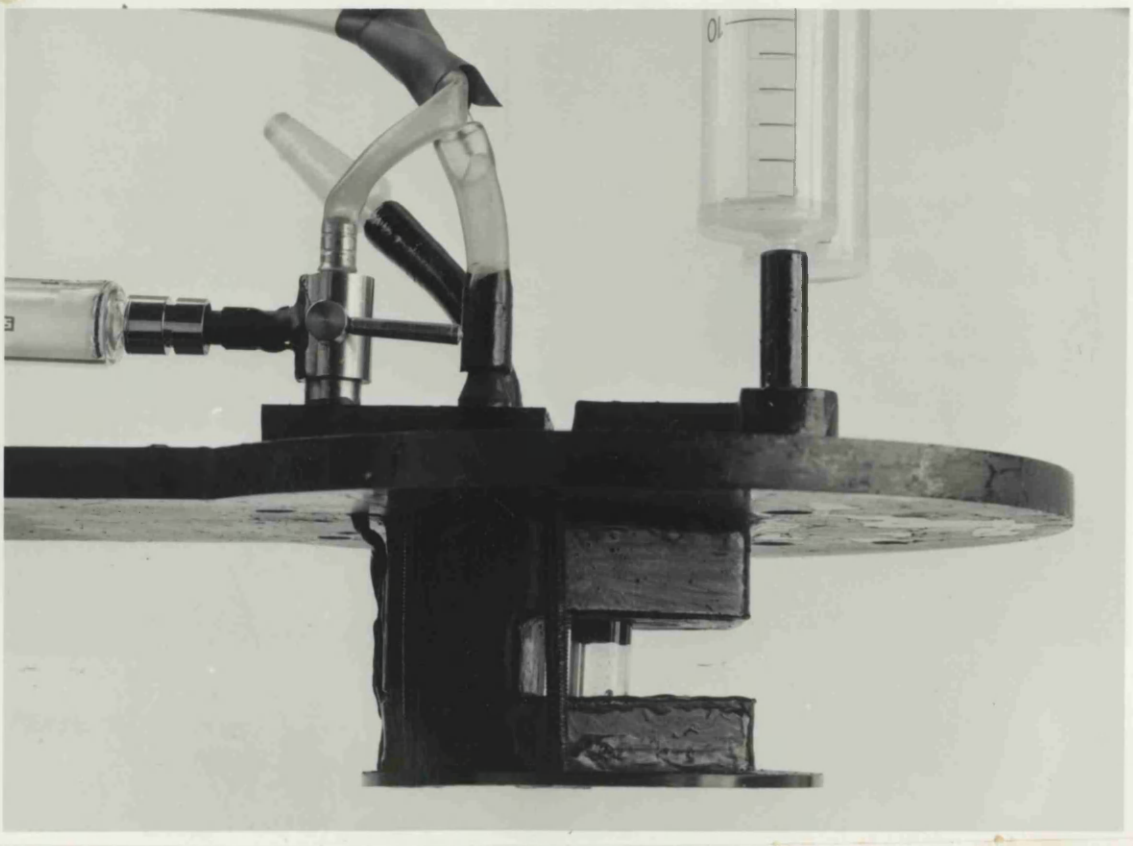

Plate 2. The stopped flow apparatus. The observation cell and water compartments above and below it are shown. This part fits within the glass basin of the light scattering system

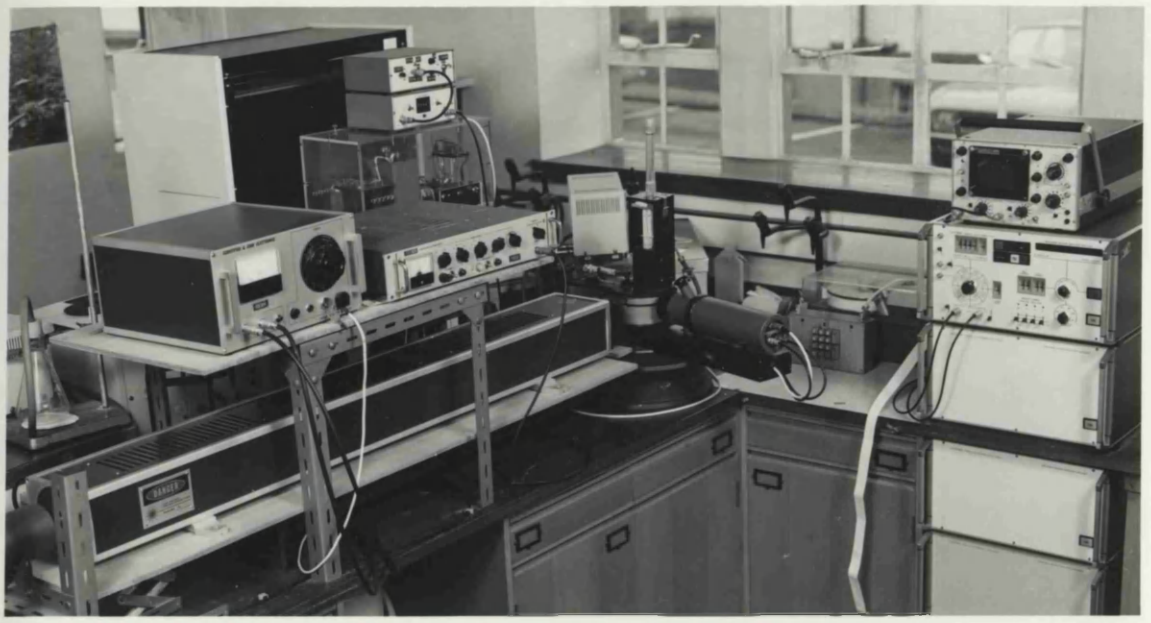

Plate 3. Overall view of the light scattering/stopped flow apparatus with the brass thermostatting block in position

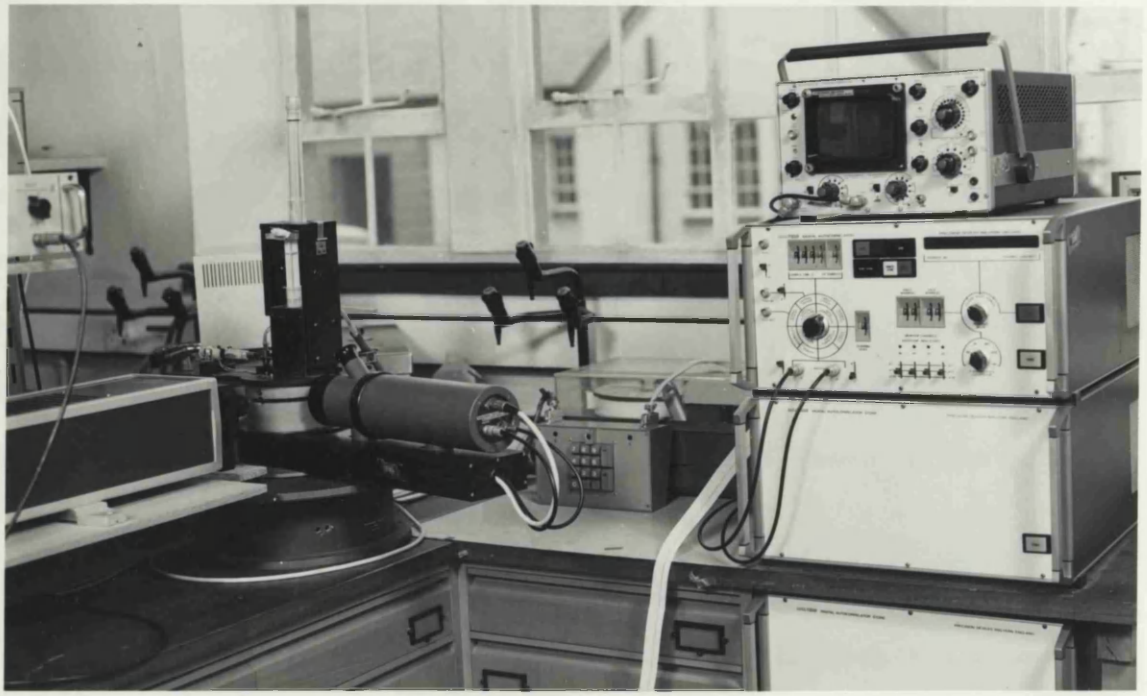

Plate 4. Closer view of the apparatus showing the tape punch beside the autocorrelator with the oscilloscope above

heat. At the bottom of the reaction cell a small thermistor was inserted (see Fig. 2.3(i) and Plate 2). This thermistor was calibrated (see Section 2.5.2) allowing the temperature of the reaction mixture to be accurately determined.

A photomultiplier situated in the horizontal plane of the laser beam, could be set to angles between 30^{o} and 130^{o} to the direction of the incident laser beam while directed at the reaction cell (see Fig. 2.3(iv) and Plates 3 and 4). Photons detected by this photomultiplier (PM1) were counted by an autocorrelator over 96 successive time intervals, when triggered by the microswitch. A second photomultiplier (PM2) situated behind the laser is also connected to the autocorrelator (see Fig. 2.3(iv)). A separate channel in the autocorrelator totals the photons detected by PM2 over the same 96 counting intervals immediately following contact between the stop syringe and the microswitch. The autocorrelator is connected to an oscilloscope on which the data are visibly displayed - a series of bright dots representing the autocorrelator channels, the distance of each dot from the baseline indicating the number of photons in a particular time interval. This information can then be transferred from the autocorrelator stores to punch tape (see Fig. 2.3(iv) and Plate 4). The overall layout of the apparatus is shown in Plate 3.

2.2.4. Equipment for measuring scattered light

A 50mW He-Ne laser (Scientifica Ltd., London) which emitted light of wavelength λ = 632.8nm was used in these experiments. The light beam was directed through a focussing lens and then through the optical unit containing the reaction cell of the flow system (see Fig. 2.3(iii) and Plate 1). Light scattered from the reaction cell was detected by the photomultiplier which was movable to angles between

30^{o} and 130^{o} to the direction of incident laser light.

A Malvern 4300 digital autocorrelator (Malvern Instruments Ltd., Malvern, England) was used in the multiscaling mode to count the photons detected by the photomultiplier. The 4th to 99th channels of the autocorrelator were used to store the numbers of photons emitted over 96 successive time intervals. To allow reactions of different rates to be followed, the channel time could be set to values between 0.001 seconds and 0.995 seconds.

The intensity of light detected by the second photomultiplier from the back of the laser is proportional to the intensity of incident light on the reaction cell. The total number of photons counted by this monitor over the same 96 time intervals during which counts from PM1 are stored is contained in channel number 2 of the autocorrelator. Channel 0 of the autocorrelator gives the sum of the photons detected over the same reaction time by PM1.

The visible display of changes in light intensity (detected by the photomultipliers) could be output in ASCII format to a Facit tape punch (Fortronic, Dunfermline, Fife) thereby providing a permanent record of each experimental run. The autocorrelator was then reset (i.e. no counts in each channel) in preparation for the next experimental run.

2.2.5. Experimental method

Two syringes of filtered 20mM imidazole/50mM NaCl, pH7 buffer were inserted into the flow system. Sufficient buffer was injected into the flow system to extend the stop syringe until it connected with the microswitch and initiated photon counting. The photomultiplier was then set to another angle before buffer solution was again injected into the flow system. The light scattered from

the buffer solution was measured at eleven different angles at 10^{o} intervals between 30^{o} and 130^{o} inclusive. The measurement of scattered light intensity always followed immediately after a fresh injection of solution to account for any effect turbulence might have on the light scattering measurement.

By the same procedure an angular variation was measured for a protein solution at a defined concentration in the absence of Ca^{2+}.

Only the total number of photons detected by the photomultiplier as emitted from the reaction cell was noted for each angle. This value, given in channel 0, divided by the number of photons detected by the monitor photomultiplier over the same counting period, given in channel 2, gave the measured scattering ratio, relatable to I/I_o for buffer and protein solutions, corrected for fluctuations in laser intensity. A correction factor of sin θ where θ is the angle of observation was then applied to these values to account for the change in volume of the illuminated sector observed at each angle (164). Subsequent subtraction of the value obtained for buffer from that of the protein solution gave the light scattered by the protein alone. Averaging the values obtained at all eleven angles provided a casein scattering value which could be used in subsequent experiments. The casein scattering was determined for each concentration of casein used.

A calcium chloride solution of desired concentration was placed in one syringe and a casein solution in the other. By simultaneously injecting equal volumes of the two solutions into the flow system the time course of the aggregation which ensues can be followed by the increased scattered light intensity.

Although the reaction cell had a volume of less than 1 cm^3, approximately 5mls of reaction mixture (2.5 mls each of Ca^{2+} and casein

solutions) was injected into the system at each experimental run to ensure that no premixed solution remained within the reaction cell from the previous run observed.

An experiment consisted of measurement of light scattering at all eleven angles for a given calcium concentration, casein concentration and temperature. Measurement at each angle was repeated 3 times and recorded on punched tape.

2.2.6. Light scattering theory

Light is scattered in all directions by a suspension of fi e particles, and this is known as the Tyndall effect. Such solutions are cloudy or turbid and the attenuation of scattered light from an illuminated solution can be expressed in the form of the Lambert-Beer law.

$$\text{Log } I/I_o = \tau \ell \qquad (2.2)$$

where I and I_o are the intensity of transmitted and incident light respectively, ℓ is the length of cell through which light passes and τ is the turbidity of the solution (165).

Solutions which are not cloudy but appear perfectly clear will also scatter light. This phenomena, called the Rayleigh effect results from polarization of molecular electronic shells by the electromagnetic light wave. Where the wavelength of light is far from any absorption band, the energy is dissipated by the electrons continuing to oscillate at the frequency of the incident light source, emitting light in all directions.

Lord Rayleigh (166) in 1899 developed the first theories on light scattering for particles which were small compared to the wavelength, λ_o, of incident light. The Rayleigh ratio R_θ is a measure of light scattering and is defined as

$$R_\theta = i_\theta \, r^2 \, I_o^{-1} \tag{2.3}$$

where i_θ is the intensity of scattered light and r is the distance of observation from the scatterer. The turbidity of a solution and the Rayleigh ratio or reduced intensity of scattered light at any angle θ are related according to

$$\tau = \frac{16\pi}{3} \, R_{\theta,u} \tag{2.4}$$

In a gas the molar mass M can be related to its concentration c, the refractive index increment (dn/dc), and the Rayleigh ratio by equation 2.5, where plane polarised light is used.

$$R_\theta = M.c. \left(\frac{dn}{dc}\right)^2 \left(\frac{2\pi^2}{Na \, \lambda_o^4} \right) \tag{2.5}$$

Clearly light scattering depends on changes in the refractive index as the gas concentration is altered. In liquids small density fluctuations occur due to Brownian motion, thereby producing changes in dn/dc in small volumes of the liquid. Adding solute to a solvent gives rise to additional fluctuations due to local variations in solute concentration. These effects can be separated to give the reduced scattering intensity of the solute, R_θ as

$$R_\theta = R_\theta \text{ (solution)} - R_\theta \text{ solvent} \tag{2.6}$$

Where solute particles are smaller than $\lambda/20$ the molecular weight can be related to R_θ (solute) by equation 2.7.

$$K(\lambda) \; . \; R_\theta^{-1} = Mw^{-1} + 2A_2c \tag{2.7}$$

where

$$K(\lambda) = \frac{2\pi^2 \, \tilde{n}_o^{\,2} \, (d\tilde{n}/dc)^2}{\lambda^4 \, Na}$$

$\tilde{n}_o$ and $\tilde{n}$ are the refractive indices of solvent and solution respectively. In an ideal solution solvent and solute do not interact greatly but with

good solvents the deviation from ideality can be expressed as a power series of the concentration of solute c, represented by the term with virial coefficient A_2 in Eq 2.7.

The molecular weight obtained is a weight average molecular weight since the polarizability and the extent to which a molecule will scatter light increases with its size. In a solution containing i components of molecular weight M_i at molar concentration m_i or weight concentration c_i, the weight average molecular weight, $\overline{Mw}$ is given by

$$Mw = \frac{\Sigma\, m_i\, M_i^2}{\Sigma\, m_i\, M_i} = \frac{\Sigma\, c_i\, M_i}{\Sigma\, c_i} \qquad (2.8)$$

Many polymers have dimensions which exceed $\lambda/20$, and scattering may occur from several positions within a given particle. When these positions are sufficiently far apart, light scattered from them arrives at the observer out of phase. The scattered light intensity is reduced and the ratio of scattered intensity to the intensity in the absence of interference is $P(\theta)$, the particle scattering factor at a given angle θ.

Modification of equation 2.7 by this particle scattering factor gives

$$\frac{I_s(\theta)\, \sin\theta}{I_o} = A.\ K(\lambda)\ .\ Mw\ .\ c.\ P(\theta) \qquad (2.9)$$

where second and higher virial coefficients are neglected. The $\sin\theta$ factor is included to correct for the change in volume of the illuminated sector observed at each angle (164). The factor A is a geometric constant and like $K(\lambda)$ is constant for a given system. The ratio $I_s(\theta)\ \sin\theta\ .\ I_o^{-1}$ can be determined as described in section 2.2.5 from light scattering experiments.

The $P(\theta)$ approximation is valid for particle radii in the

range $\sim\lambda/20$ to $\sim\lambda/4$, which gives an upper limit for casein micelles of M $\sim 10^9$ using the empirically derived relationship $M = 0.84\ r^3$ (149). The value of the $P(\theta)$ function changes with the shape of solute molecules but for spherical particles with diameter D it is given by

$$P(\theta) = \left(3/x^3\ (\sin x - x \cos x) \right)^2 \qquad (2.10)$$

where $x = 2\pi\lambda^{-1} \sin \theta/2 \ .\ D$. Since there is no phase difference possible in the direction of propagation of the incident electromagnetic field, $P(\theta)$ is reduced to the small particle value of 1 at zero angle. Light scattering data for macromolecules are therefore determined over a series of angles and extrapolated to zero angle where there is no diminution of scattered light intensity.

Molecular weights are frequently determined by a double extrapolation to zero angle and infinite dilution. This is achieved by a Zimm Plot of Kc/R_θ versus $\sin^2 \theta/2 + k'c$ where k' is a constant which gives a convenient spread of data in the grid-like graph obtained. The intercept on the Y-axis is $\overline{Mw}^{-1}$ (167).

In kinetic and multimerization studies the $\overline{Mw}$ of the solute may be concentration dependent so only angular extrapolations are possible (168).

2.2.7. Calculation of molecular weights

From Section 2.2.6 the weight average molecular weight $\overline{Mw}$, can be determined according to

$$\overline{Mw} = (I_s(\theta).\ \sin\theta\ .I_o^{-1}).\ c^{-1}\ .\ P(\theta)^{-1}.A^{-1}.\ K(\lambda)^{-1}.\ e^{\tau 1} \qquad (2.11)$$

neglecting the second and higher virial coefficients.

For the Ca^{2+} - induced aggregation of caseins the scattered light intensity is reduced, particularly at high angles, by the increasing turbidity of reaction mixtures. Parker and Dalgleish (149) found corrections for turbidity necessary at molecular weights greater than

~ 3×10^8. In the present work, the reactions were followed for much shorter times, so that turbidity of the solutions was much less important. In fact the highest molecular weight measured was approximately 10^7 which is well below the size where turbidity becomes a problem.

The factor $I_s(\theta) \sin\theta \cdot I_\theta^{-1}$ can be found from the experimental data. I_o is related to the value stored in channel 2 of the autocorrelator divided by the number of channels, that is the number of photons detected by the monitor per time interval. Since there are 96 channels we obtain the relationship

$$\frac{96 \sin \theta}{\text{Monitor Value}} \propto \sin \theta \; I_o^{-1} \qquad (2.12)$$

To normalise each scattered light value I_s, which is the number of counts in each channel, the above factor is used thereby giving values of $I_s \sin \theta \; I_\theta^{-1} \propto R_\theta$. Both the goemetric constant A and $K(\lambda)$ will be invariant for a given system being studied.

Each experimental run produces a series of 96 successive R_θ values. Each run was repeated three times to reduce the likeliehood of singular results. The three data points corresponding to the same time interval of the reaction were then averaged.

$$\frac{R_\theta^{\,j} + R_\theta^{\,j} + R_\theta^{\,j}}{3} = Av_\theta^{\,i} \qquad (2.13)$$

where j is the channel number. This gives a set of 96 normalised intensities. Further experimental runs were then performed at angles in the 30^o to 130^o range, each being repeated three times. Eleven reaction profiles are thereby produced after averaging which correspond to the eleven angles measured.

The scattering value obtained for buffer alone when injected into the flow system was subtracted from each result ie.

$$Av_\theta^j - \text{Base value} = Av_\theta^j \text{ (adjusted)} \qquad (2.14)$$

At the first few points the value of Av_θ^j (adjusted) is close to the scattering values of the protein solution used. The scattering of each protein concentration was determined as described in Section 2.2.5. Two methods of molecular weight determinations were carried out.

(1) The first method involves an extrapolation to zero angle to eliminate the $P(\theta)$ term as $P(0) = 1$. Measurements of Av_θ^j over eleven different angles were plotted as $(Av_\theta^j)^{-1}$ versus $\sin^2 \theta/2$ as suggested by Zimm (167). There is no extrapolation to zero concentration due to the dependence of reaction kinetics upon concentration. A linear regression on these eleven points allowed extrapolation to zero angle where the intercept has a value of I^{-1} where I is the scattered light intensity produced by the weight average molecular weight.

Dividing this value by the scattering value of the relevant protein concentration and multiplying by the monomeric molecular weight gives the weight average molecular weight

$$\overline{Mw} = \frac{I \times \text{Monomer MW}}{\text{Scattering value of protein concentration used}} \qquad (2.15)$$

This procedure is followed for each of the 96 successive values to give a reaction profile of $\overline{Mw}$ versus time.

Figure 2.4 shows eleven averages obtained at different angles plotted according to

$$I^{-1} \text{ versus } \sin^2 \theta/2 \qquad (2.16)$$

where I^{-1} is the adjusted scattering intensity at angle θ, for a chosen channel, j. The extrapolated value of I at $\theta = 0$ is 5.78 which corresponds in this case to a molecular weight of 1×10^6.

(2) Alternatively the value of I^{-1} was calculated by averaging the eleven Av_θ^j values obtained at different values of θ from 30^o to 130^o

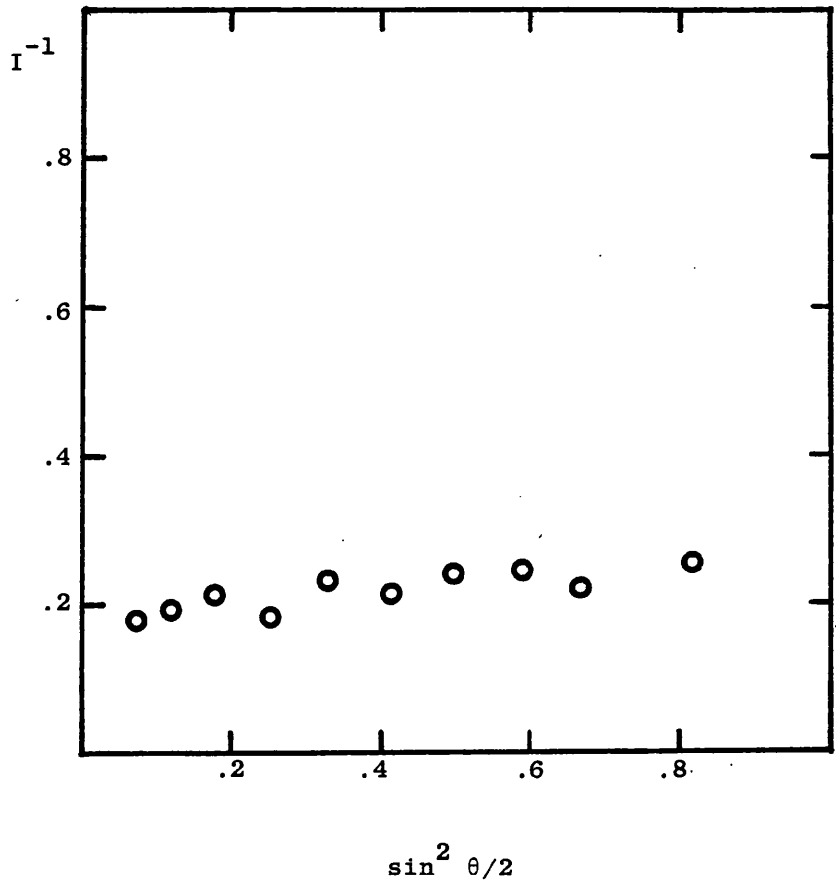

Fig. 2.4 A plot of reciprocal scattered intensity (I^{-1}) versus $\sin^2 \theta/2$ (where θ is the angle at which the scattering was determined) for the 96th point in the reaction of Ca^{2+} (8mM) with α_{s1}-casein (1 mg/ml).

at 10^{o} intervals. This gives values of Av^{j} for j = 1 to 96.

$$\frac{Av^{j}_{30^{o}} + Av^{j}_{40^{o}} + Av^{j}_{50^{o}} + \ldots\ldots Av^{j}_{130^{o}}}{11} = I^{-1} \qquad (2.17)$$

The value of I produced by this method was again multiplied by the factor which relates the scattering intensity for a known monomer concentration to the monomer molecular weight to give the weight average molecular weight (Equation 2.1.5).

Averaging the values of Av_{θ}^{j} over eleven values of θ gives a value of I as 4.51 which for the particular casein concentration corresponds to a molecular weight of 1.28×10^{6}.

There is not a large difference between the molecular weights calculated by averaging or extrapolating the scattering intensity values to zero angle. The particle scattering factor $P(\theta)$ is expected to be close to the small particle value of unity since the molecular weights are predominantly below 10^{7}. The results quoted in this work are those obtained by utilizing the second method described. This method is less sensitive to the reaction profile observed at 30^{o} which tends to have much larger scattered intensities than other angles, and also to be less self consistent.

In practise both molecular weights were calculated and their respective reaction profiles plotted. Although the molecular weights determined by extrapolation to zero angle are generally larger than those determined from the averaged scattering value the trends observed by one method of calculation were replicated by the other method.

2.3. Determination of precipitate concentrations

Calcium and casein solutions form a precipitate when mixed provided that the calcium ion concentration is above a critical level (54). However, even where the calcium ion concentration is above this critical level for a given casein concentration, not all the protein is

precipitated: some protein remains soluble even after long periods of time, suggesting that an equilibrium exists between precipitated and non precipitated material.

2.3.1. Preparation of solutions for centrifugation

Six calcium solutions in the range 13 to 18mM inclusive were prepared as described in Section 2.2.1. Six different α_{s1}-casein solutions in the range 0.5 to 4 mg/ml were also prepared as described in Section 2.2.2. These concentrations of β-casein solutions were also prepared.

Equal volumes (10 mls) of one calcium and one casein solution were mixed and incubated at 23°C for 1 hour. This procedure was followed for all of the possible combinations of the six Ca^{2+} and the six α_{s1}-casein solutions specified. A set of the six α_{s1}-casein solutions (10 mls of each) diluted with an equal volume of 20mM imidazole/50mM NaCl buffer at pH7 were also prepared as standards, and maintained at 23°C for 1 hour.

The same calcium and casein mixtures were also prepared using β-casein solutions and these were incubated at 40°C for 1 hour along with solutions of the six β-casein solutions of different concentrations diluted with an equal volume of 20mM imidazole/50mM NaCl at pH7.

2.3.2. Determination of soluble concentrations

After incubation each α_{s1}-casein/Ca^{2+} or buffer solution was spun in the 6 x 38 ml rotor of a MSE superspeed 65 centrifuge for 2 hours at 22,000 RPM (6.5×10^4 g). The temperature was maintained at 23°C during centrifugation. This process was designed to sediment the high molecular weight material which had precipitated from solution.

Samples of the supernatant liquid were extracted by Pasteur pipette and cooled to approximately 5°C thereby preventing further aggregation taking place. The absorbances of these solutions were determined at 278nm using a Cary 219 spectrophotometer. Although the absorbances varied, use of a 2mm, 5mm or 1cm quartz cell permitted accurate determination of each concentration of soluble material.

The absorbances of those casein solutions which had no Ca^{2+} added were determined as base values for each α_{s1}-casein concentration. The appropriate base values were subtracted from the absorbances of each Ca^{2+}/α_{s1}-casein combination. From the absorbances which are then calculated the concentration of soluble protein was determined. The precipitate concentration for each mixture was then considered to be the initial concentration of α_{s1}-casein in that mixture minus the soluble concentration of protein. These results are presented in TABLE 1.

This procedure for determining the soluble protein concentration was repeated for β-casein/Ca^{2+} solutions but samples were maintained at 40°C during centrifugation. After separation from the precipitate the supernatant liquid was allowed to cool to room temperature (23°C) to ensure that no further aggregation occurs. Since the Ca-β-casein precipitate will redisperse under these conditions the separation must be completed before cooling is allowed.

The concentrations of soluble β-casein were found by multiplying the apparent concentration calculated from the absorbances at 278nm by 0.47 to give the β-casein concentrations in mg/ml.

2.4. Calculation of the extent of binding Ca^{2+} to the protein

Both α_{s1}- and β-casein will bind Ca^{2+}. According to Dalgleish and Parker (58) this binding process can be considered to be

the result of an initial binding constant K^* and a substitution parameter N which modifies the initial binding constant K^* for each Ca^{2+} bound by the protein. The total ligand concentration (where Ca^{2+} is a ligand binding to casein) is defined by

$$[L]_{tot} = [L] + K^* [P][L] + 2 K^{*2} N [P][L]^2 + 3 K^{*3} N^2 [P][L]^3 + 4 \ldots\ldots \quad (2.20)$$

where $[L]$ = concentration of Ca^{2+} and $[P]$ = concentration of protein. Likewise the total protein concentration will be

$$[P]_{tot} = [P] + K^* [P][L] + K^{*2} N [P][L]^2 + \left(K^{*3} N^2 [P][L]^3\right) + K^{*4} N^3 [P][L]^4 \quad (2.21)$$

Thus $$[P]_{tot} = [P] + [P] \sum_{i=1}^{n} K^* N^{(i-1)} i/2 [L]^i \quad (2.22)$$

where n is the total number of binding sites. The total ligand concentration can also be expressed in this form

$$[L]_{tot} = [L] + [P] \sum_{i=1}^{n} i (K^*)^i N^{(i-1)i/2} [L]^i \quad (2.23)$$

The average number of ligands per protein molecule $\bar{\nu}$, is defined by

$$\bar{\nu} = \frac{[L]_{tot} - [L]}{[P]_{tot}} = \frac{\Sigma ix}{1 + \Sigma x} \quad (2.24)$$

where $x = (K^*)^i N^{(i-1)i/2} [L]^i$

To calculate $\bar{\nu}$ for each Ca^{2+} and casein combination i was taken at 20. In practice the average number of ligands bound did not vary greatly for values of i > 16. For α_{s1}-casein K^* has a value of 2100 l/m-mole and N is 0.73 at 23°C (58). The base binding constant K^* for β-casein is 2600 l/m-mole and the substitution parameter 0.56 at 40°C (74). Using these values for K^* and N it is possible to calculate $\bar{\nu}$ for a Ca^{2+}/casein combination at the prescribed temperature. The initial Ca^{2+} and casein concentrations were set as $[L]_{tot}$ and $[P]_{tot}$

respectively.

From the definitions of $\bar{\nu}$ we conclude that

$$[L]_{tot} = [L] + \left([P]_{tot} \times \frac{\Sigma ix}{1 + \Sigma x} \right) \qquad (2.25)$$

A trial value of the free calcium concentration $[L]$ was selected and a value of $[L]_{tot}$ was calculated. The ratio of the actual ligand concentration and that which was calculated can be obtained. Dividing the trial value of $[L]$ by this ratio gives a free ligand concentration which will fit this equation. Recalculation of x allows $\bar{\nu}$ to be determined and thus the free protein concentration $[P]$. The average number of Ca^{2+} bound per α_{s1}-casein molecule ($\bar{\nu}$) is shown as a function of free Ca^{2+} in Fig. 2.5.

The charge on the protein molecule is altered by the binding of calcium. For α_{s1}-casein the charge on the protein molecule Q is given by

$$Q = -22 + 2\bar{\nu} \qquad (2.26)$$

since at pH7 α_{s1}-casein has a negative charge close to 22 (40).

The relationship between the average number of Ca^{2+} bound to β-casein at 40°C and the free $[Ca^{2+}]$ is shown in Fig. 2.6. The net negative change on β-casein at pH7 is only 13 (62). Thus for β-casein the charge per protein molecule will be determined by

$$Q_{\beta} = -13 + 2\bar{\nu} \qquad (2.27)$$

Values of Q^2 for different Ca^{2+}/α_{s1}-casein and Ca^{2+}/β-casein combinations at 23°C and 40°C respectively are given in TABLES 1 and 2.

2.5.1. Temperature variation of Ca/casein combinations

Initially a calcium/α_{s1}-casein combination of medium reactivity was selected. Syringes containing the appropriate Ca^{2+} and α_{s1}-casein combinations were prepared and placed in the water bath which circulated

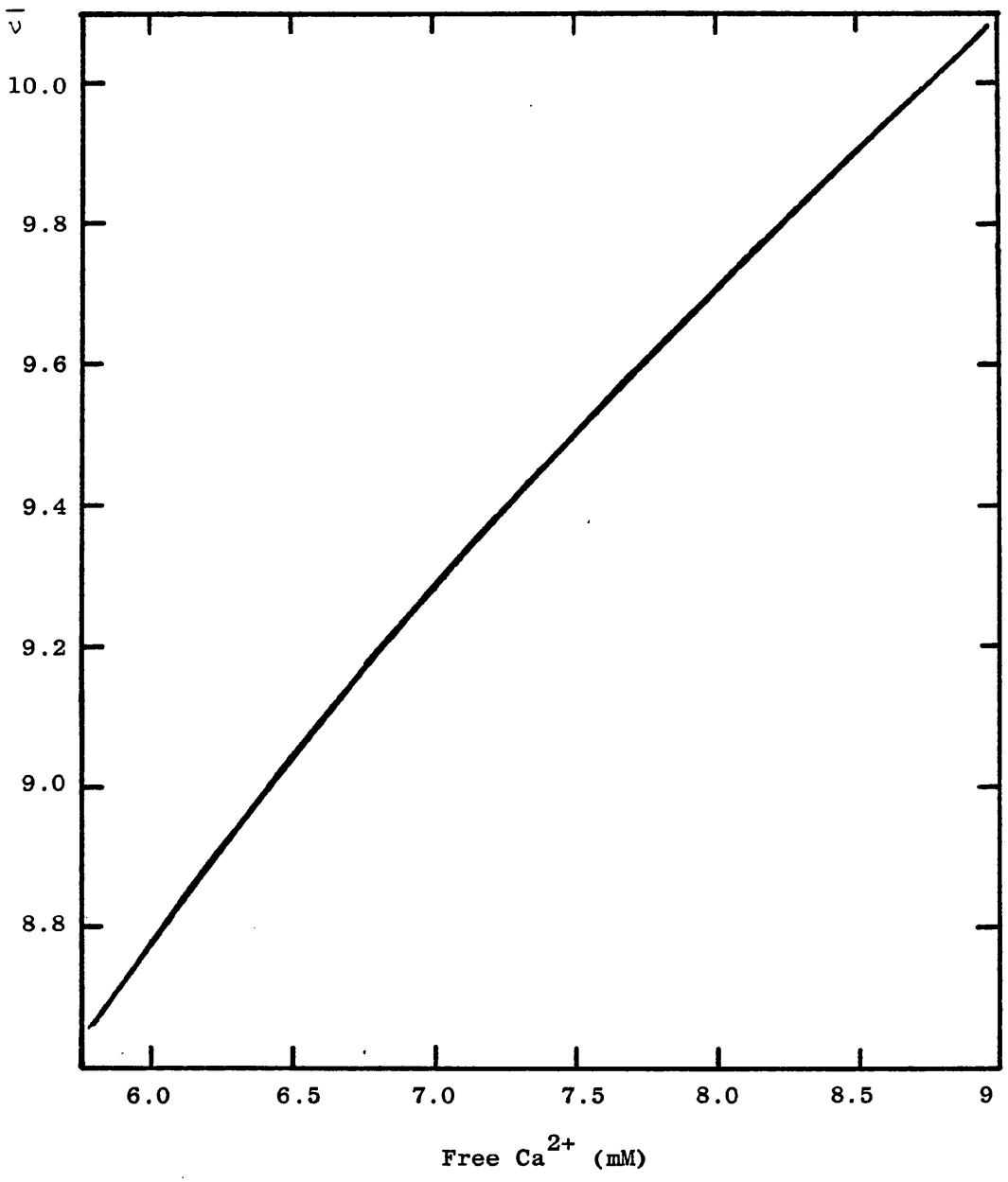

Fig. 2.5. Binding isotherm of Ca^{2+} to α_{s1}-casein at 23°C in 50mM NaCl, 20mM imidazole-HCl buffer at pH7. K^{*} = 2128 N = 0.735.

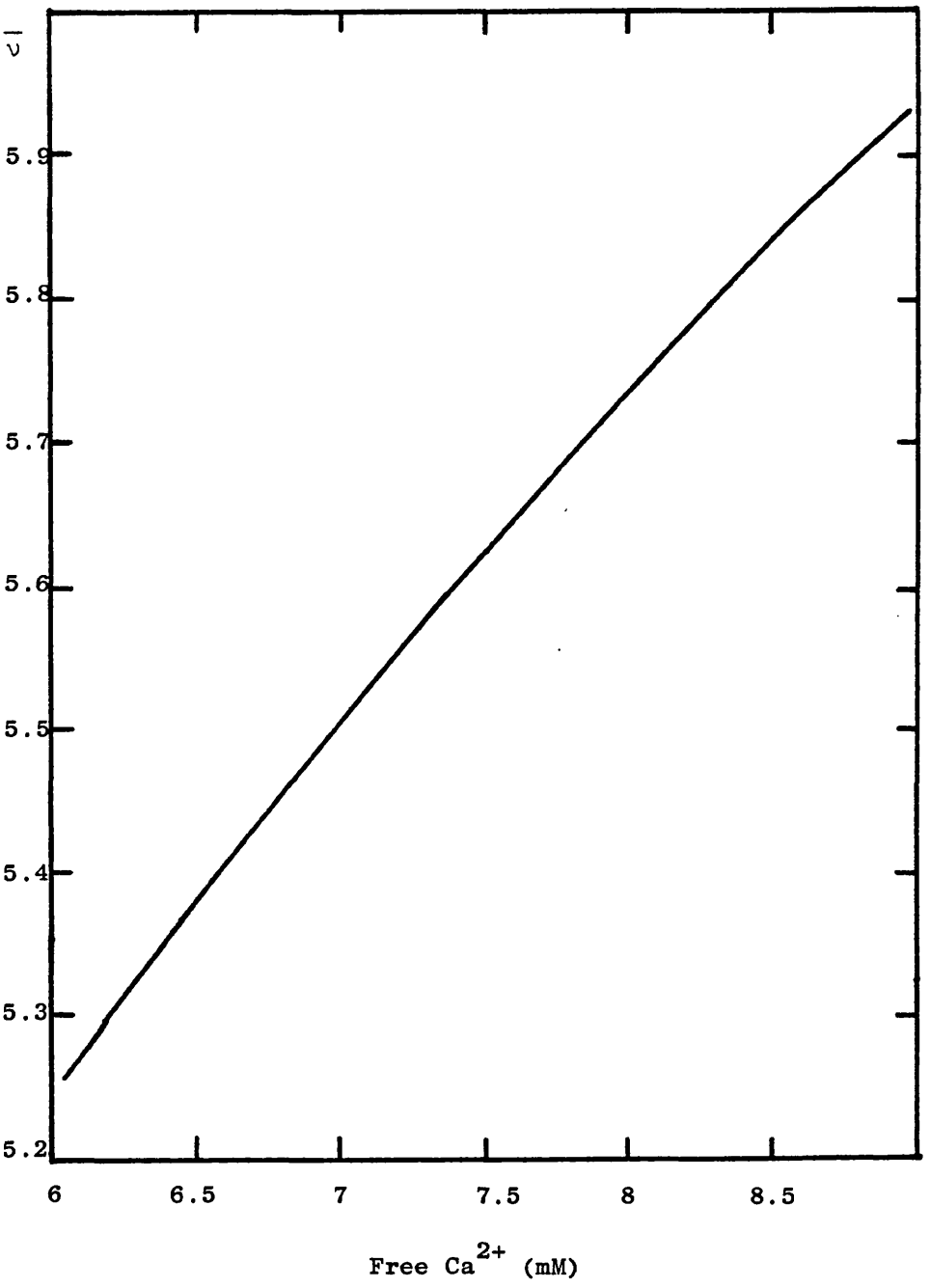

Fig. 2.6. Binding isotherm of Ca^{2+} to β-casein at 40°C in 50mM NaCl, 20mM imidazole-HCl buffer at pH7. K^{*} = 2600, N = 0.56.

water through the stopped flow system. Beginning at around 14°C the temperature was slowly raised until a calcium and casein mixture, of the concentration selected, held in a small vial, became cloudy. At this temperature the kinetics were first determined.

The temperature of the water bath was then raised and the apparatus and solutions given time to equilibrate to this temperature, when the kinetics were again determined as described in Section 2.2.5. This procedure was repeated until the reaction became too fast to measure.

Other lower and higher concentrations of either Ca^{2+} or α_{s1}-casein were then treated in the same way. All temperature measurements quoted are those determined by the calibrated thermistor situated at the base of the reaction cell and not as shown by the thermometer held in the water bath.

A temperature dependence of the reaction of calcium/β-casein mixtures was also carried out. In this case the temperature at which precipitation first occurred for most concentration combinations was about 33°C. Repetition of the kinetic measurements at various temperatures allowed a comparison of results to exhibit the effect of temperature.

2.5.2. Calibration of thermistor

The resistance of a thermistor varies with temperature according to the relationship, $\ln R = AT^{-1} + B$. Hence by measuring the resistance of a thermistor the temperature can be accurately determined provided that each thermistor is first calibrated.

After sealing the thermistor and the wires leading from it in position (see Fig. 2.3(i)) on the stopped flow apparatus, the flow system was completely immersed in a water bath with water also being

circulated from it through the flow system water jacket (see Fig. 2.3 (iii)). As the temperature of the water was gradually raised from $10^{o}C$ to $50^{o}C$ the resistance of the thermistor was noted. Adequate time was allowed between each temperature increase and the moment when this resistance was determined, for the whole system to reach this temperature. The water temperature was accurately determined when the resistance value had been stable for at least 1 minute.

A plot of ln R versus T^{-1}, where temperature is on the Kelvin scale, gave a straight line of gradient 3.842×10^{3} passing through the points ($\ln R = 3.664$, $T^{-1} = 3.5316 \times 10^{-3}$) and ($\ln R = 2.021$, $T^{-1} = 3.104 \times 10^{-3}$) as shown in Fig. 2.7.

From this line the temperature of the reaction mixture, at the time that the kinetics were measured, can be accurately determined by the resistance of the thermistor situated in the reaction cell.

2.6. Preparation of casein solutions containing subcritical levels of calcium

To establish whether or not the rate of reaction is dependent upon the time required for casein to bind Ca^{2+}, subcritical levels of Ca^{2+} were included with casein prior to kinetic measurements being made. Comparison between experiments carried out with Ca^{2+} and casein in separate syringes, as per normal, and these experiments where some Ca^{2+} was included with casein prior to mixing will show no rate increase as a result of preaddition of Ca^{2+} if Ca^{2+} binding to the protein is very fast.

A calcium/casein combination was selected. The calcium solution was then diluted to 0.75 of its original concentration. In preparation of the casein solution a calcium chloride solution was used

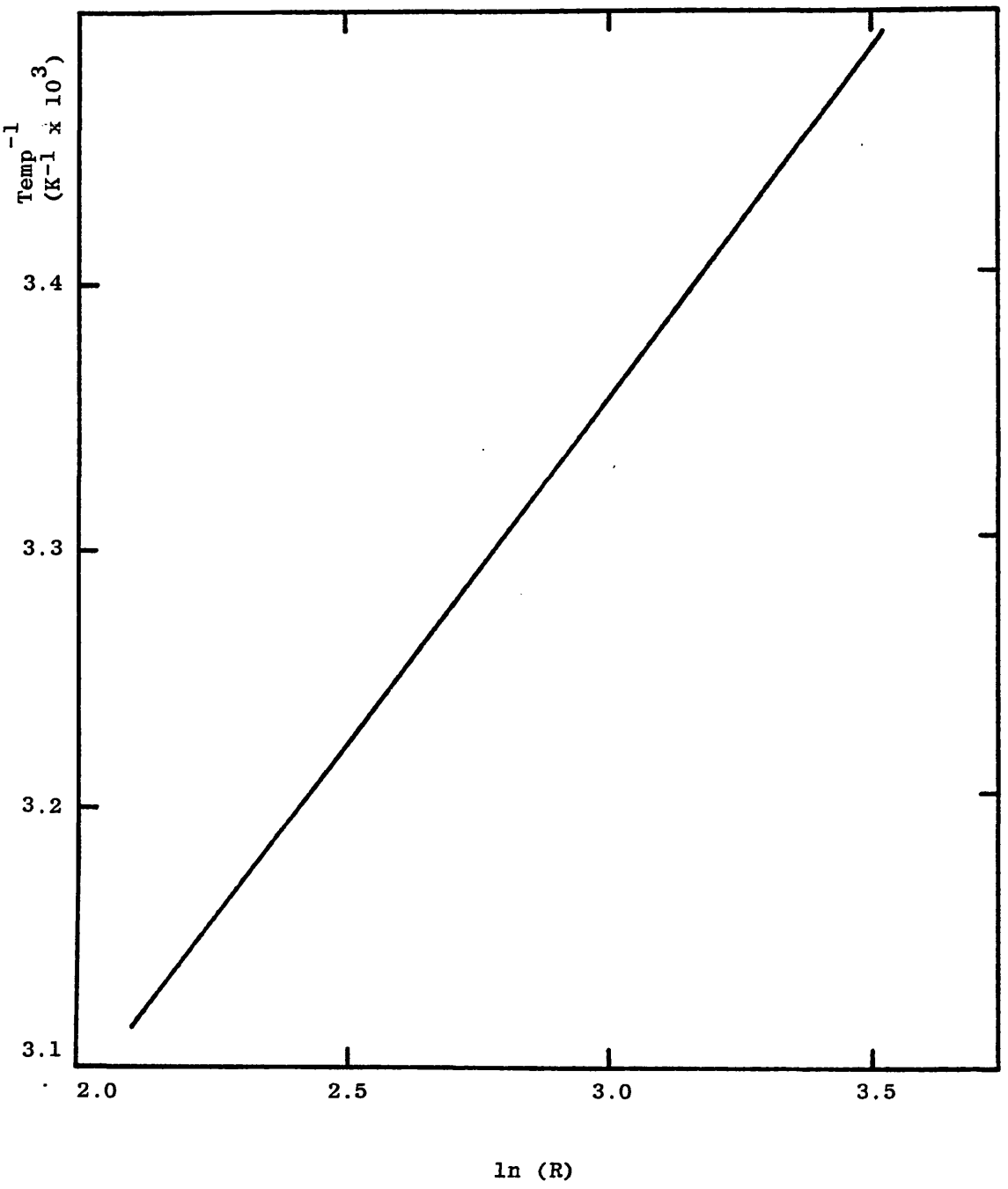

Fig. 2.7. Calibration line for thermistor temperature as shown by the resistance R, measured.

for dilution, rather than the simple 20mM imidazole/50mM NaCl pH7 buffer normally used. The final concentration of Ca^{2+} in the mixture was 0.25 of the selected calcium concentration: this was not sufficient to precipitate the casein. Combination of these two solutions results in total $[Ca^{2+}]$ and [casein] identical to those selected for comparison.

This procedure was followed for α_{s1}-casein solutions and for β-casein solutions. The rate of reaction was determined at several temperatures for each.

3. Experimental Results

3.1.1 Reaction of Ca^{2+} with α_{s1}-casein

After addition of Ca^{2+} to α_{s1}-casein solutions the scattered light intensity increases with time. Calculation of weight average molecular weights from the measured light scattering produced reaction profiles as shown in Fig. 3.1.

The profile labelled C was obtained at $23^{o}C$ for a 7.5mM calcium and 1.5mg/ml casein solution. The weight average molecular weight increased from the monomer value of 23,600 to approximately 1.3×10^{6} in three seconds, demonstrating that species up to and above a degree of polymerization of 55 are present at that time.

However this reaction profile was calculated by averaging the profiles obtained at each of the 11 scattering angles rather than by extrapolation to zero angle. The latter method tends to produce larger molecular weights although at the same stage for this reaction the two methods are in very close agreement. Aggregation continues beyond the stage shown in Fig. 3.1 and molecular weights of up to 5×10^{7} can be obtained, which is consistent with polymers containing greater than 1000 monomer units.

At the start of the reaction the rate of increase in molecular weight is slow but this gradually increases until a stage is reached when molecular weight growth is linear with time. This continues until the molecular weight is about 10^{7}, then the rate of change of apparent molecular weight is no longer constant, but becomes gradually less. This is attributable to the effect of increasing turbidity of the solution, and appropriate correction for this shows that the molecular weight does continue to increase linearly with time (149). The study of the reactions in this work was confined to the region where

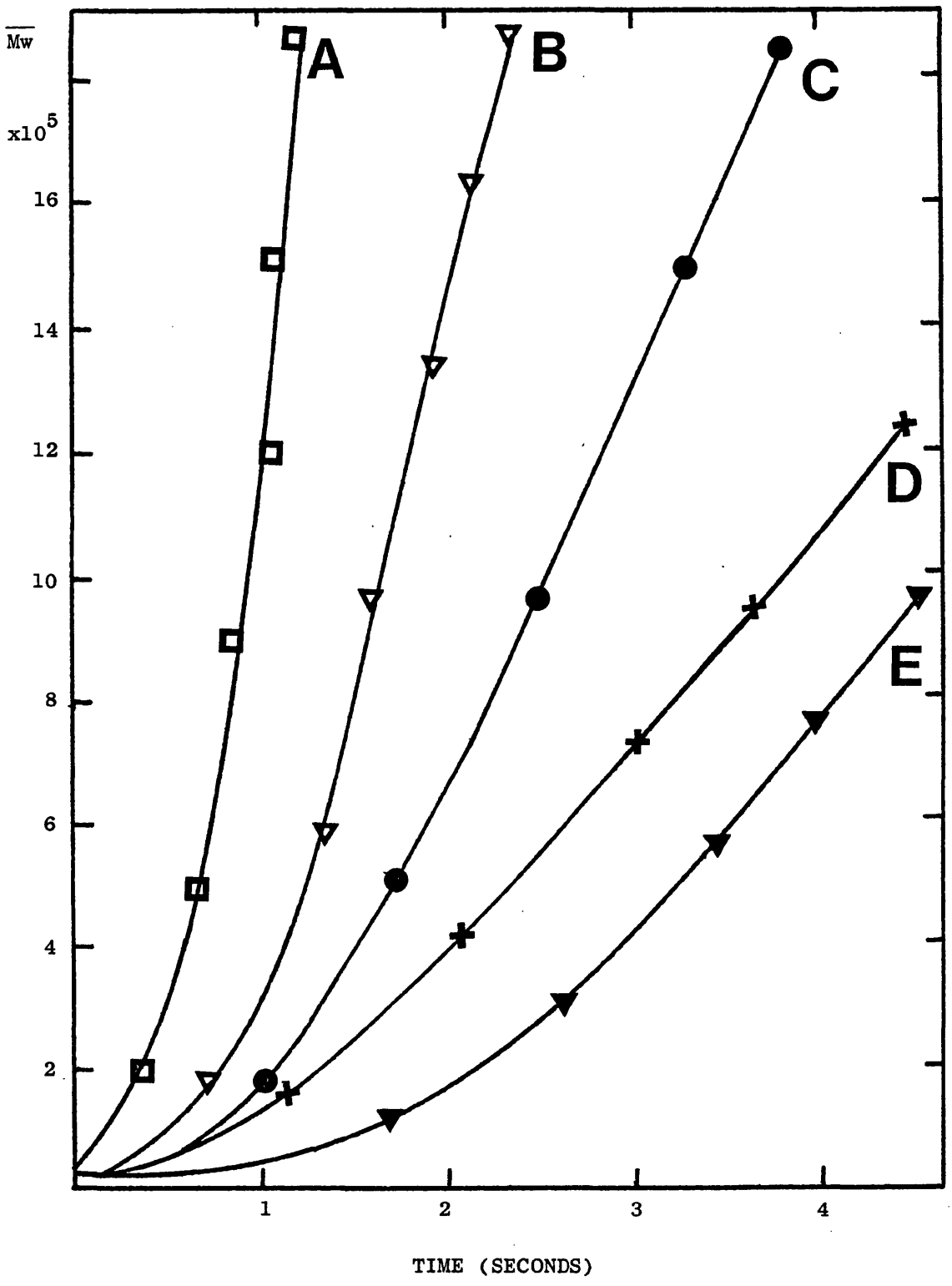

Fig. 3.1. Reaction profiles of various Ca^{2+}/α_{s1}-casein concentration combinations at 23°C. A, 8.5mM Ca^{2+}/1.5 mg/ml α_{s1}-casein; B, 7.5mM Ca^{2+}/2 mg/ml α_{s1}-casein; C, 7.5mM Ca^{2+}/1.5 mg/ml α_{s1}-casein; D, 7mM Ca^{2+}/1.5 mg/ml α_{s1}-casein; E, 7.5mM Ca^{2+}/1 mg/ml α_{s1}-casein.

turbidity effects were not important, i.e. when $\overline{Mw} < 10^7$.

Two parameters are necessary to define the reaction profile, namely the gradient of the linear portion ($d\overline{Mw}/dt$), and the time obtained by extrapolating this line to the monomer molecular weight of 23,600, that is the molecular weight at time zero, t = 0. This second parameter is defined as the critical time, t_c. The slope of reaction profile C in Fig. 3.1 is found to be 9.18×10^5 S^{-1}, the critical time being 1.15 seconds.

The general shape of the molecular weight-time plots was similar for all Ca^{2+}/α_{s1}-casein reactions studied. All of these profiles showed an initial stage during which molecular weight growth was slow, followed by a stage when the rate of molecular weight growth increases over a short time interval until it becomes constant.

3.1.2 Effect of $[Ca^{2+}]$ on reaction rate

Increasing the calcium ion concentration increases the rate of the aggregation reaction. The reaction profiles for solutions containing 1.5mg/ml of α_{s1}-casein with 7,7.5 and 8.5 mM Ca^{2+} are shown in Fig. 3.1. The limiting slopes (gradients of linear sections) increased as the $[Ca^{2+}]$ increased and the initial times correspondingly decreased.

Measurements were made of the reaction profile for six different concentrations of α_{s1}-casein (0.25, 0.5, 0.75, 1, 1.5 and 2mg/ml) each covering the range of Ca^{2+} from 6.5 to 9mM at 0.5mM intervals. A few of the combinations of lowest $[Ca^{2+}]$ and/or lowest $[\alpha_{s1}\text{-casein}]$ did not react sufficiently to be measured, within the 96 second maximum reaction time. The results confirmed that for a given α_{s1}-casein concentration, the limiting slope increased and the critical time decreased as calcium ion concentration increased. Natural

logarithms of the limiting slopes and critical times determined for each Ca^{2+}/α_{s1}-casein combination are presented in TABLE 1, where all the reaction rates were determined at 23°C.

Since all reaction rates increased with $[Ca^{2+}]$ a relationship between these seemed likely. A plot of the logarithm of the reaction rate (as defined by limiting slope) versus the logarithm of the calcium ion concentration is shown in Fig. 3.2. A series of curves, each one corresponding to a different α_{s1}-casein concentration are obtained. A double logarithmic plot of rate as determined by critical time versus $[Ca^{2+}]$ shows an inverted type of curvature at each α_{s1}-casein concentration. Thus

$$\ln (\text{limiting slope}) \not\propto \ln [\text{total } Ca^{2+}] \qquad (3.1)$$

Similarly

$$\ln (t_c) \not\propto \ln [\text{total } Ca^{2+}] \qquad (3.2)$$

Since neither slope nor t_c show any direct proportionality to $[\text{total } Ca^{2+}]$ it was clear that there is no simple correlation between the total calcium ion concentration and the rate of growth of $\overline{Mw}$.

3.1.3 Effect of α_{s1}-casein concentration on reaction rate

The rate of reaction increased when the concentration of α_{s1}-casein increased as shown by curves B, C and E in Fig. 3.1. This rate increase observed with increasing $[\alpha_{s1}\text{-casein}]$ is also evident from Fig. 3.2 in which the curves corresponding to higher concentrations of α_{s1}-casein are positioned above those of lower α_{s1}-casein concentrations, at higher intercept values on the ln (slope) axis.

From the data given in TABLE 1 a double logarithmic plot of rate versus the total concentration of α_{s1}-casein can be constructed. Such a plot is shown in Fig. 3.3 where the limiting slope is again used

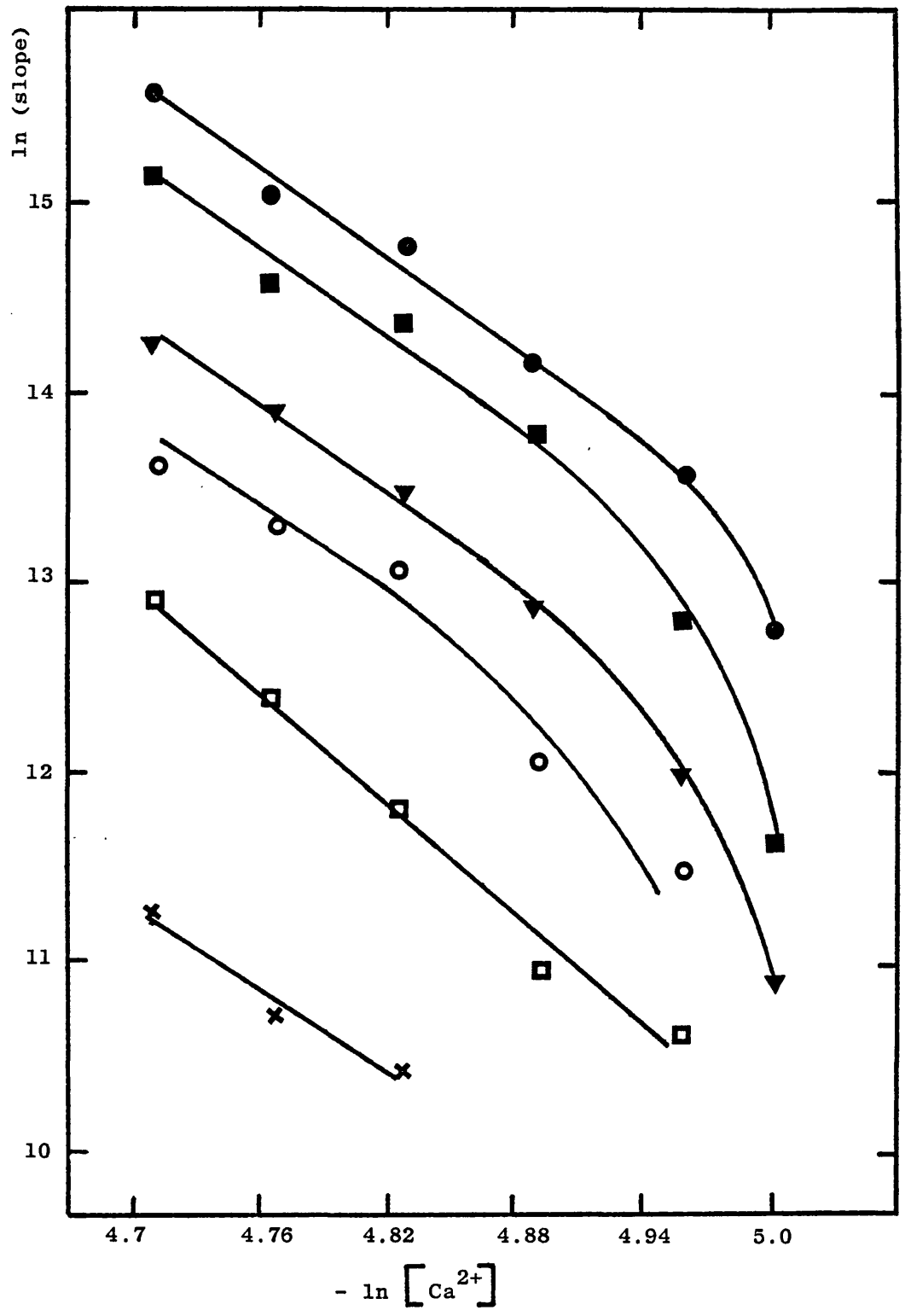

Fig. 3.2. Effect of total $[Ca^{2+}]$ on the rate of reaction as shown by limiting slope. The symbols ●, ■, ▼, ○, □, × represent α_{s1}-casein of 2, 1.5, 1, 0.75, 0.5 and 0.25 mg/ml respectively.

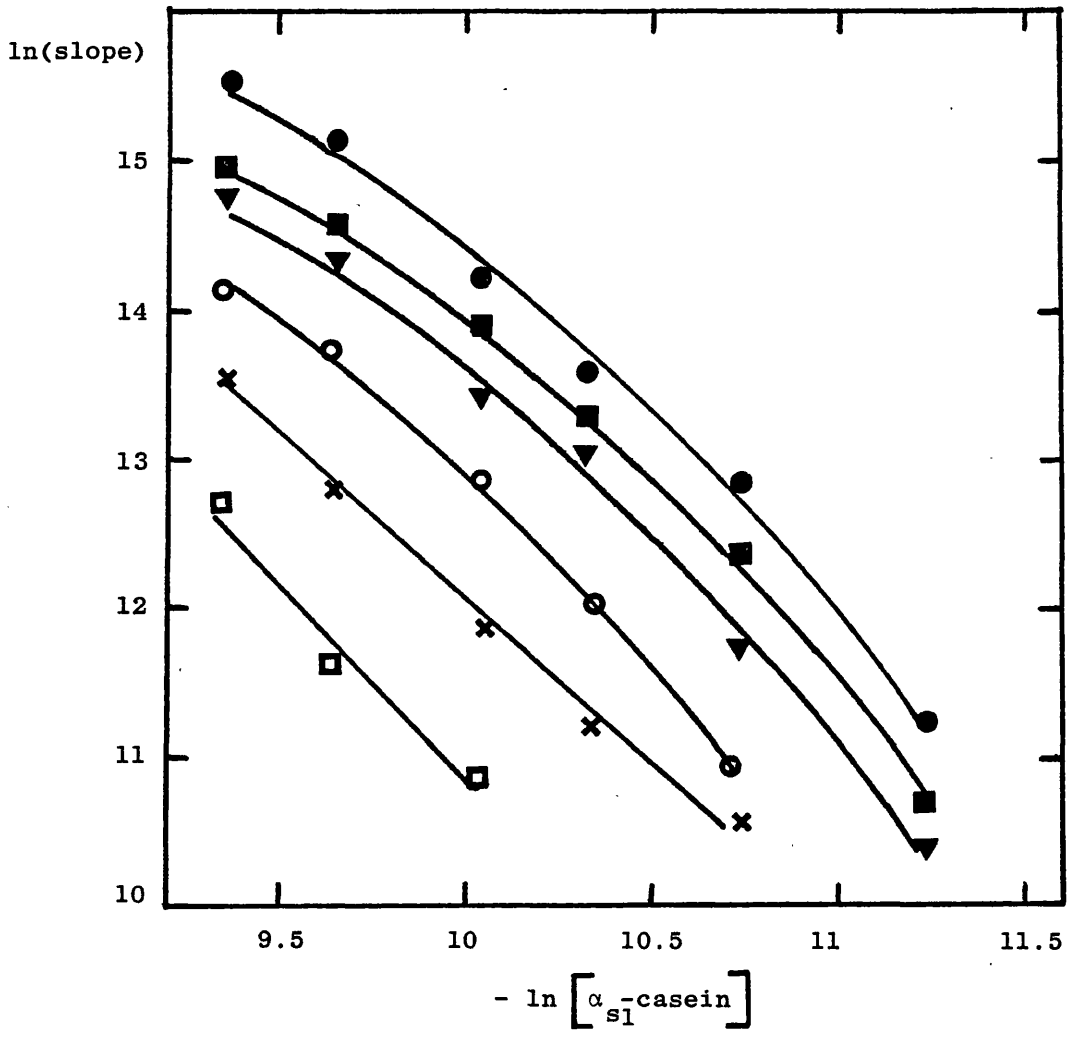

Fig. 3.3. Effect of $[\alpha_{s1}\text{-casein}]$ on the rate of reaction as indicated by limiting slope. The symbols ●, ■, ▼, ○ ✖, and □ represent Ca^{2+} solutions of 9, 8.5, 8, 7.5, 7, and 6.5mM respectively.

as being the diagnostic parameter for the reaction rate. A series of curves, each representing a given calcium ion concentration, can be drawn through the appropriate points. Once again an inverted curvature was obtained when critical time was used as the rate diagnostic parameter. Thus

$$\ln (\text{slope}) \not\propto \ln \quad \text{total } \alpha_{s1}\text{-casein} \tag{3.3}$$

Similarly

$$\ln (t_c) \not\propto \ln \quad \text{total } \alpha_{s1}\text{-casein} \tag{3.4}$$

Since neither limiting slope nor t_c exhibit any direct proportionality to $\left[\text{total } \alpha_{s1}\text{-casein}\right]$ it was concluded that there is no simple relationship between $\left[\text{total } \alpha_{s1}\text{-casein}\right]$ and the rate of growth of $\overline{Mw}$.

3.1.4 Relationship between limiting slope and critical time

In all of the reactions between calcium and α_{s1}-casein studied, the critical time decreased as the limiting slope increased. Changing the reaction rate by varying $\left[Ca^{2+}\right]$ or $\left[\alpha_{s1}\text{-casein}\right]$ altered the limiting gradient and critical time in an inverse fashion. A plot of the logarithm of limiting slope versus the logarithm of the critical time is shown in Fig. 3.4.

A linear relationship was found to exist between the logarithm of the critical time such that

$$\ln (\text{limiting slope}) = \ln (a) - \ln (t_c) \tag{3.5}$$

where a is a constant. The gradient of this line was found to be -1. Therefore

$$\text{limiting slope} \propto {}^{1}/t_c \tag{3.6}$$

Both of the rate diagnostic parameters therefore are equally affected by changes in $\left[Ca^{2+}\right]$ or $\left[\alpha_{s1}\text{-casein}\right]$. Any relationship

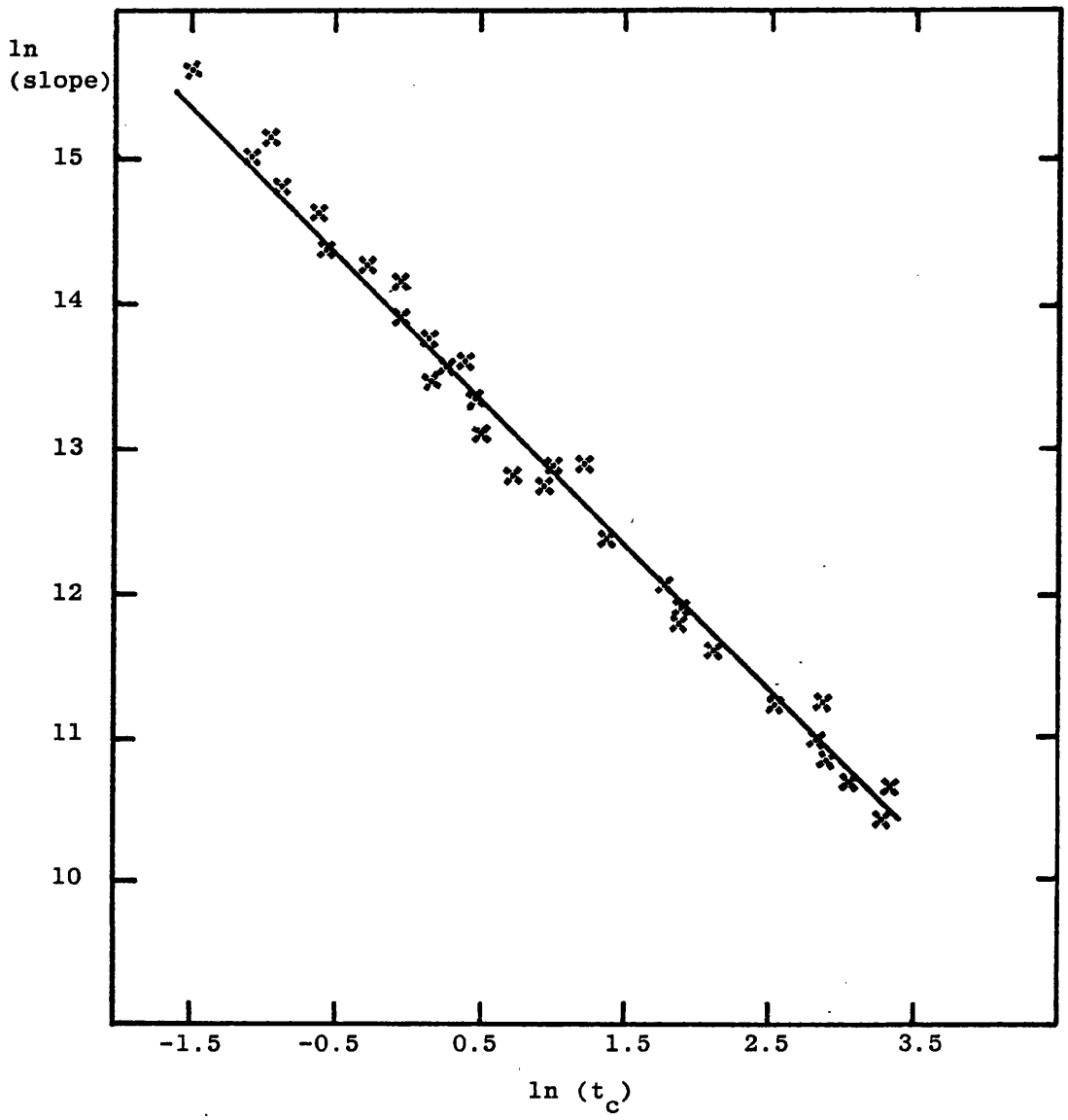

Fig. 3.4. Relationship between limiting slope and the critical time t_c, of reactions of α_{s1}-casein with Ca^{2+} at 23°C.

exhibited by one parameter to a factor influencing the rate of reaction will be inverted for the other. This refers to results at a fixed temperature - it will be seen later that changing temperature affects this relationship.

As suggested by equation 3.5, it was found that the reaction profiles obtained for reaction between α_{s1}-casein and calcium at different concentrations of the respective reactants (but at a fixed temperature) can be fitted to one unique profile, using a reduced time scale.

For any chosen molecular weight, real time is divided by the time taken to attain this molecular weight in each individual reaction profile. A molecular weight of 10^6 was generally reached by the growing particles before the end of the period over which the reaction was monitored. The time taken to reach 10^6 was selected as the reduction factor for each profile. Each time axis of the individual profiles was then reduced by the appropriate factor such that the time taken to attain the selected $\overline{Mw}$ becomes unity. All experimental curves, for results obtained at a fixed temperature, when plotted on this reduced time scale, superimposed to give a single reaction profile as shown in Fig. 3.5.

The particular value of $\overline{Mw}$ selected for production of these composite curves was unimportant: any value may be used, and the result remains the same, namely that the curves for all α_{s1}-casein/Ca^{2+} combinations will superimpose when plotted in this manner. In an earlier publication, Horne and Dalgleish (156) used the t_c value to reduce the time-scales, producing equivalent results. However, this earlier work was restricted to variation of Ca^{2+} concentration only, and the results presented here, show that, no matter whether the variation in rate is caused by changing the casein or Ca^{2+} concentration,

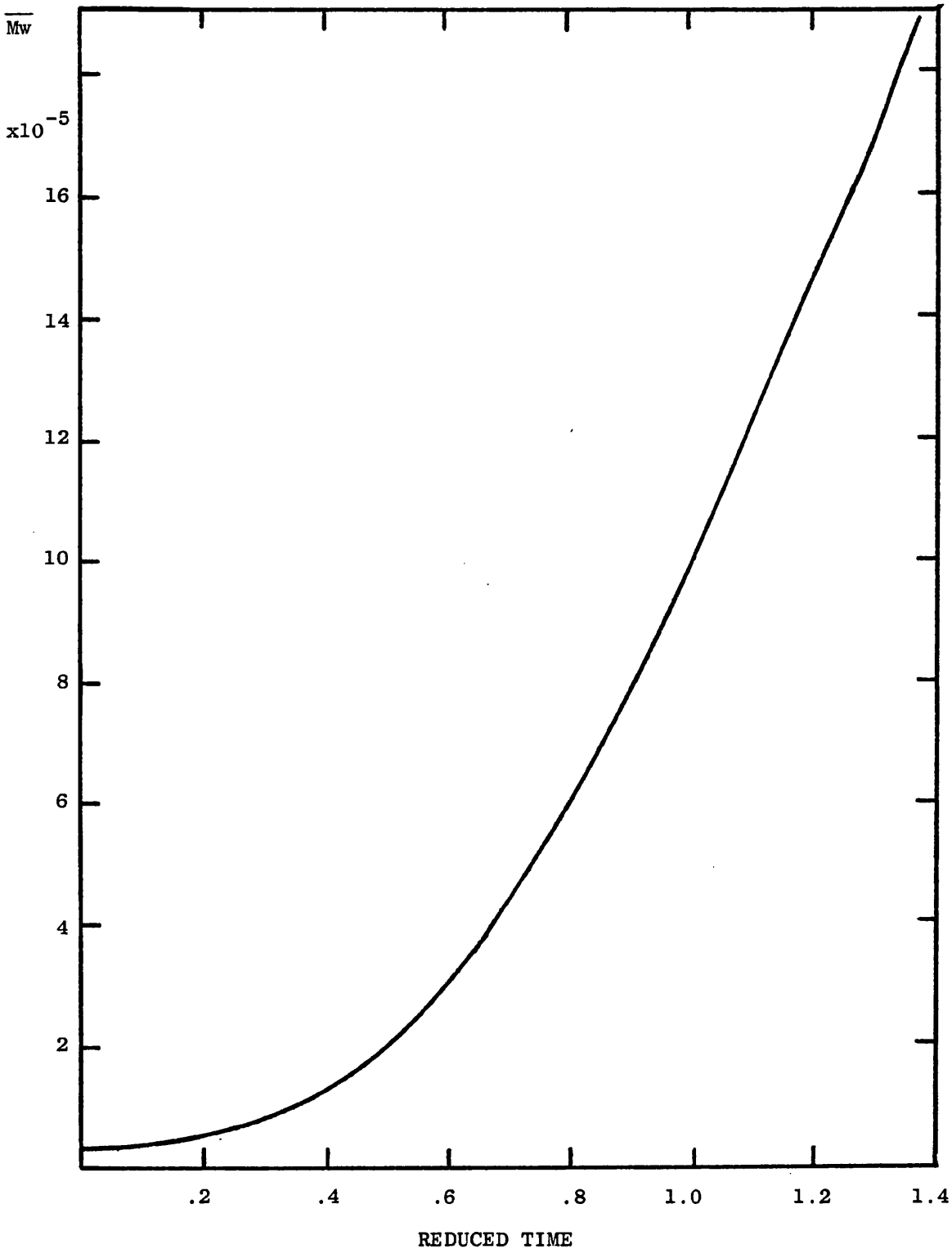

Fig. 3.5. Reaction profiles of all Ca^{2+} and α_{s1}-casein combinations at 23°C plotted on a reduced time scale where $\frac{}{Mw} = 10^6$ was selected as $t_{red} = 1$.

the single curve for all results is obtained when they are plotted on the reduced-time scale.

3.2.1 Reaction of Ca^{2+} with β-casein

Using the same concentrations of calcium and β-casein which had been used previously in experiments with α_{s1}-casein, no reaction was observed at 23°C, and it was necessary to raise the temperature to 40°C to obtain a comparable rate of reaction. As with α_{s1}-casein the scattered light intensity increases as the reaction proceeds. The $\overline{Mw}$ versus time reaction profile for several calcium and β-casein combinations at 40°C are shown in Fig. 3.6.

The reaction profiles for the β-casein aggregation are qualitatively similar to those of α_{s1}-casein. There is a section where the rate of growth in molecular weight is linear with time, preceeded by an initial stage in which the molecular weight is increasing more slowly, although this is considerably less pronounced than for α_{s1}-casein reactions.

The molecular weights in the aggregation reactions of β-casein are considerably larger in comparison to those obtained in reactions of α_{s1}-casein. Plots of the particle scattering factor, $P(\theta)$ (i.e. $(\text{scattering})^{-1}$ versus $\sin^2 \theta/2$) for β-casein show no distinct $P(\theta)$ variation as demonstrated in Section 2.2.7 for α_{s1}-casein. The reaction profiles shown are those produced by averaging the results over 11 angles and not by extrapolation. This allows comparison of the molecular weights and the reactions of α_{s1}- and β-casein.

Over the same time intervals, with the same concentrations of reactants, β-casein aggregates have much higher molecular weights than the α_{s1}-casein aggregates, but afterall, the temperature is much

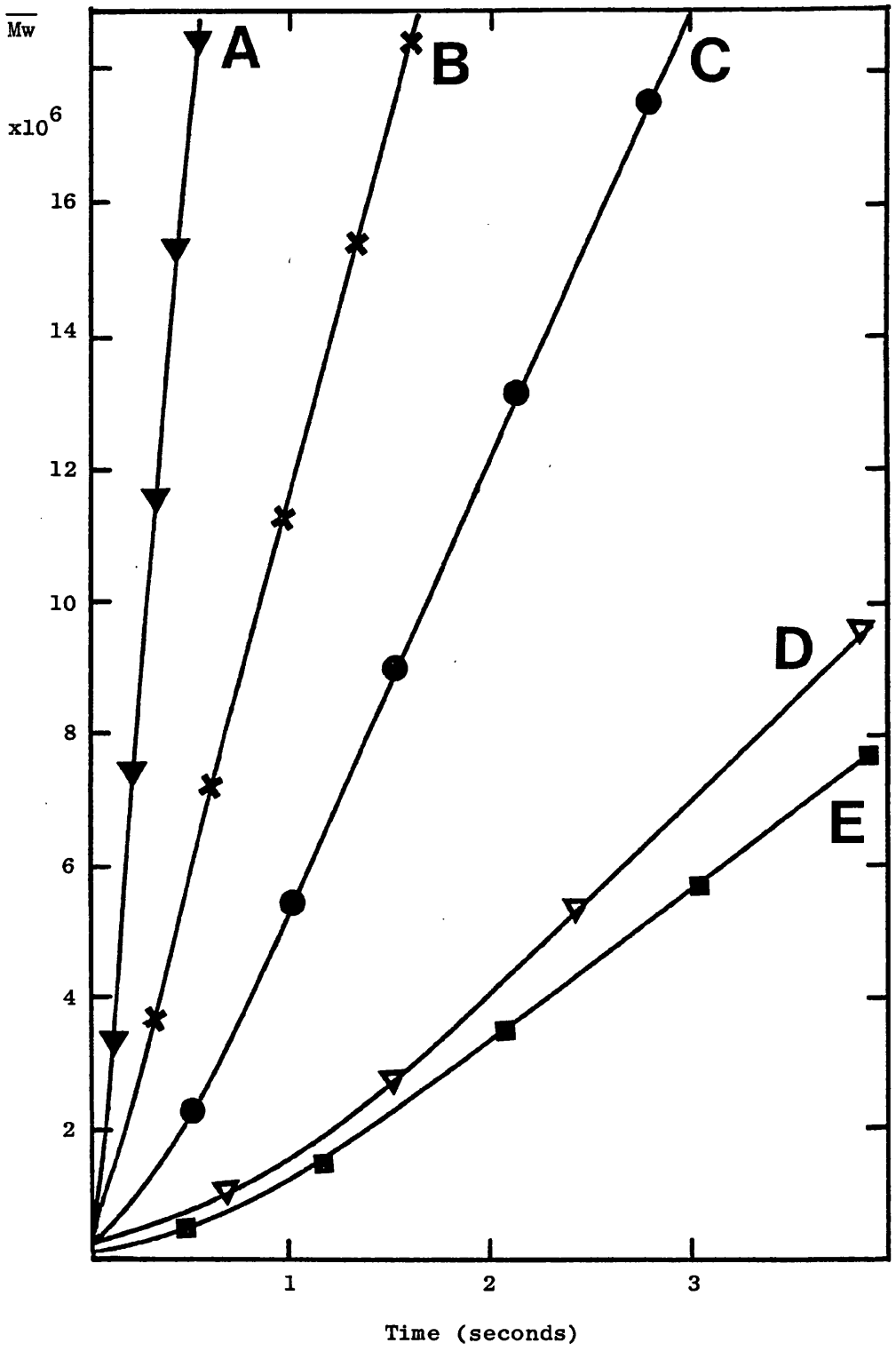

Fig. 3.6. Reaction profiles of various Ca^{2+}/β-casein concentration combinations at 40°C. A, 9mM Ca^{2+}/ 1 mg/ml β-casein; B, 7.5mM Ca^{2+}/1.5 mg/ml β-casein; C, 7.5mM Ca^{2+}/ 1 mg/ml β-casein; D, 7mM Ca^{2+}/1 mg /ml β-casein; E, 7.5mM Ca^{2+}/0.5 mg/ml β-casein.

higher.

The original scattering intensity of β-casein solutions without added calcium is greater than for α_{s1}-casein. The scattered intensity of a 2mg/ml α_{s1}-casein solution at 23°C was 0.14 whereas the value for a 2mg/ml β-casein solution at 40°C was 0.22 per channel. These protein scattering values are dependent upon the concentration of the protein solutions and the value at 0.25 mg/ml β-casein is 0.022 per channel. The monomer molecular weight of β-casein is 24,000, slightly greater than that of α_{s1}-casein, but it is known that β-casein is subject to a temperature dependent association (29,71). Evans et al. (69) predict that polymeric species with degree of association of approximately 25 will be present in 5mg/ml β-casein solutions at 40°C, however this will be significantly reduced with the lower concentrations used in this study.

Upon addition of Ca^{2+} the β-casein further associates. The profile labelled B in Fig. 3.6 is that for a 7.5mM calcium and 1.5mg/ml β-casein solution. The molecular weight reaches 1.7×10^7 in 1.5 seconds. The critical times of β-casein reactions obtained by extrapolating the limiting slopes to a monomer molecular weight of 24,000 are much shorter than the equivalent times for α_{s1}-casein. Critical times for 7.5mM Ca^{2+}/1.5mg/ml casein are 1.15 and 0.07 seconds for α_{s1}-casein and β-casein respectively at the different temperatures of determination.

3.2.2 Effect of $[Ca^{2+}]$ on the rate of reaction of β-casein

The rate of reaction increased as the calcium ion concentration increased. This effect is shown by curves A, C and D in Fig. 3.6 in which the decrease of $[Ca^{2+}]$ from 9 to 7.5 and 7mM respectively (all reacting with 1mg/ml β-casein) results in a decrease in the limiting slopes with corresponding increases in critical times.

Measurements were made of the reaction profile for six concentrations of β-casein (0.25, 0.5, 0.75, 1, 1.5 and 2mg/ml) each covering the range of $[Ca^{2+}]$ from 6.5mM to 9mM at 0.5mM intervals. At the highest of these calcium and β-casein combinations the reaction rate was very fast and a reaction profile could not be effectively determined within the shortest possible total reaction time of 0.1 second. All of these experiments were conducted at 40°C and the results are presented in TABLE 2. An increase in reaction rate with $[Ca^{2+}]$ is observed at each β-casein concentration as indicated previously.

Again a relationship between the reaction rate and the calcium ion concentration is suggested, but in fact the double logarithmic plot of limiting slope versus $[\text{total } Ca^{2+}]$ shown in Fig. 3.7 reveals a similar type of curvature to that shown in Fig. 3.2 for α_{s1}-casein results. No linear relationship is observed between ln (limiting slope) and ln $[\text{total } Ca^{2+}]$. Similarly using the critical time as the rate diagnostic parameter, no direct proportionality between the rate and $[\text{total } Ca^{2+}]$ was observed.

3.2.3 Effect of β-casein concentration on reaction rate

The reaction rate increases with increasing β-casein concentration. This is illustrated in Fig. 3.6 by curves B, C and E which are the reaction profiles of 1.5, 1 and 0.5mg/ml β-casein solutions respectively when reacted with 7.5mM Ca^{2+} at 40°C. The limiting slopes decrease and the critical times increase with decreasing $[\beta\text{-casein}]$. This effect is confirmed by the results given in TABLE 2 and by the observation that those curves in Fig. 3.7 which correspond to higher β-casein concentrations are positioned at higher values of ln (limiting slope).

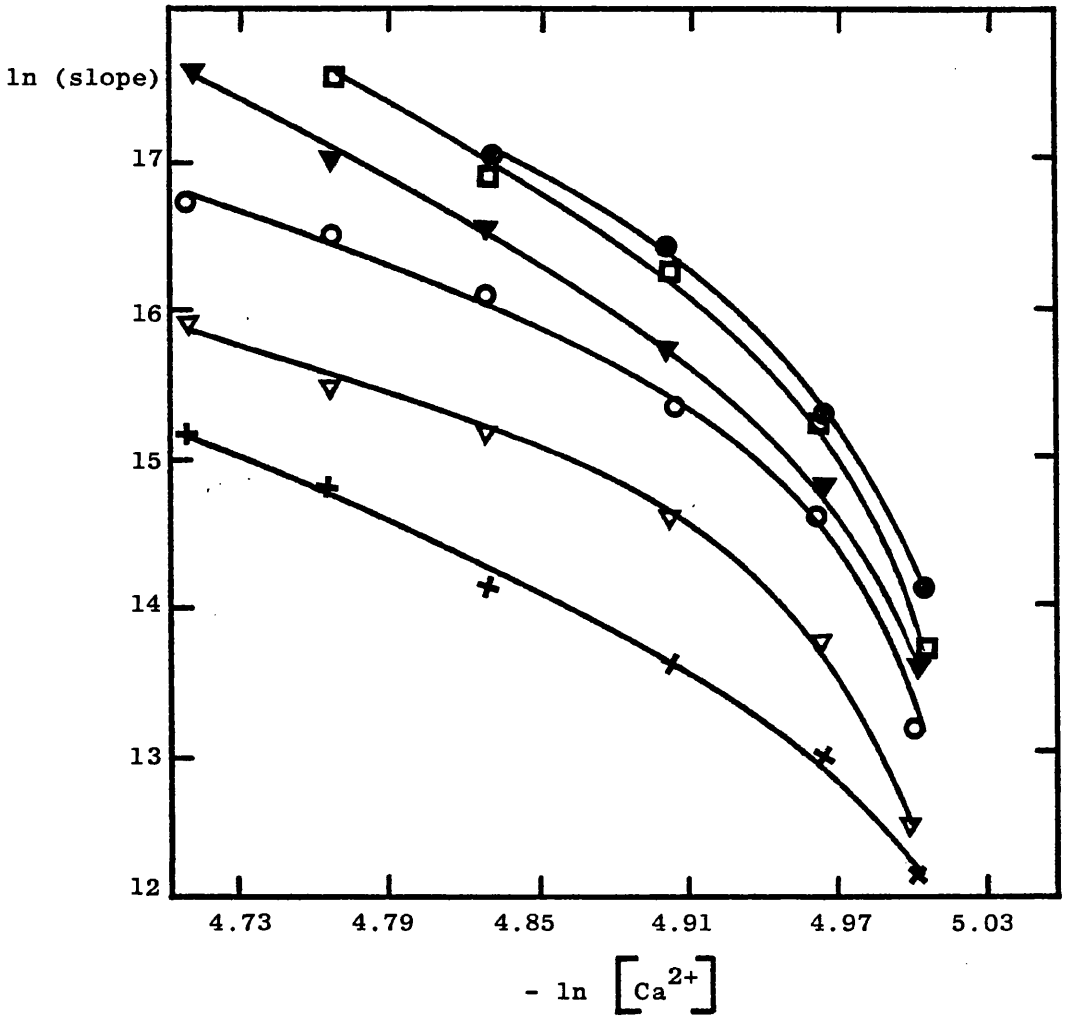

Fig. 3.7. Effect of total $[Ca^{2+}]$ on the rate of reaction as shown by the limiting slope. The symbols ●, □ , ▼, ○ , ▽ , × represent β-casein of 2, 1.5, 1, 0.75, 0.5, and 0.25 mg/ml respectively.

A double logarithmic plot of critical time versus β-casein concentration is shown in Fig. 3.8. A series of curves each representing a different calcium ion concentration is depicted where that corresponding to lowest $[Ca^{2+}]$ is positioned at higher values of ln (t_c). Since there is no linear relationship observed between ln (t_c) and ln [total β-casein] or the inverted ln (limiting slope) versus ln [total β-casein] plot it was concluded that, as with α_{s1}-casein, there is no simple correlation between the total β-casein concentration and the reaction rate.

3.2.4 Relationship between limiting slope and critical time for β-casein

The two rate diagnostic parameters, limiting slope and critical time, were affected in opposite ways by changes in reactant concentrations. Where a reaction condition caused the gradient of the linear section of the reaction profile to increase, the critical time decreased correspondingly.

A plot of ln (limiting slope) versus ln (t_c) of the results given in TABLE 2 produced a straight line with a gradient of -1. Thus

$$\text{limiting slope} = \text{constant} \times t_c^{-1} \qquad (3.7)$$

The limiting slope varies inversely with critical time for all the β-casein/ca^{2+} combinations which were studied at 40°C. As a consequence of this result, any relationship observed between a reaction condition and one rate diagnostic parameter would be inverted for the other parameter. Like α_{s1}-casein, it follows from this result, that each of the Ca^{2+}/β-casein reaction profiles will be related to a standard reaction profile by a simple factor. The standard Ca^{2+}/β-casein reaction profile at 40°C was determined as described in Section 3.1.4. but with a $\overline{Mw}$ of 6×10^6 when the reduced time is unity. (This molecular weight was arbitrarily chosen as a convenient $\overline{Mw}$ reached by all of the reactant

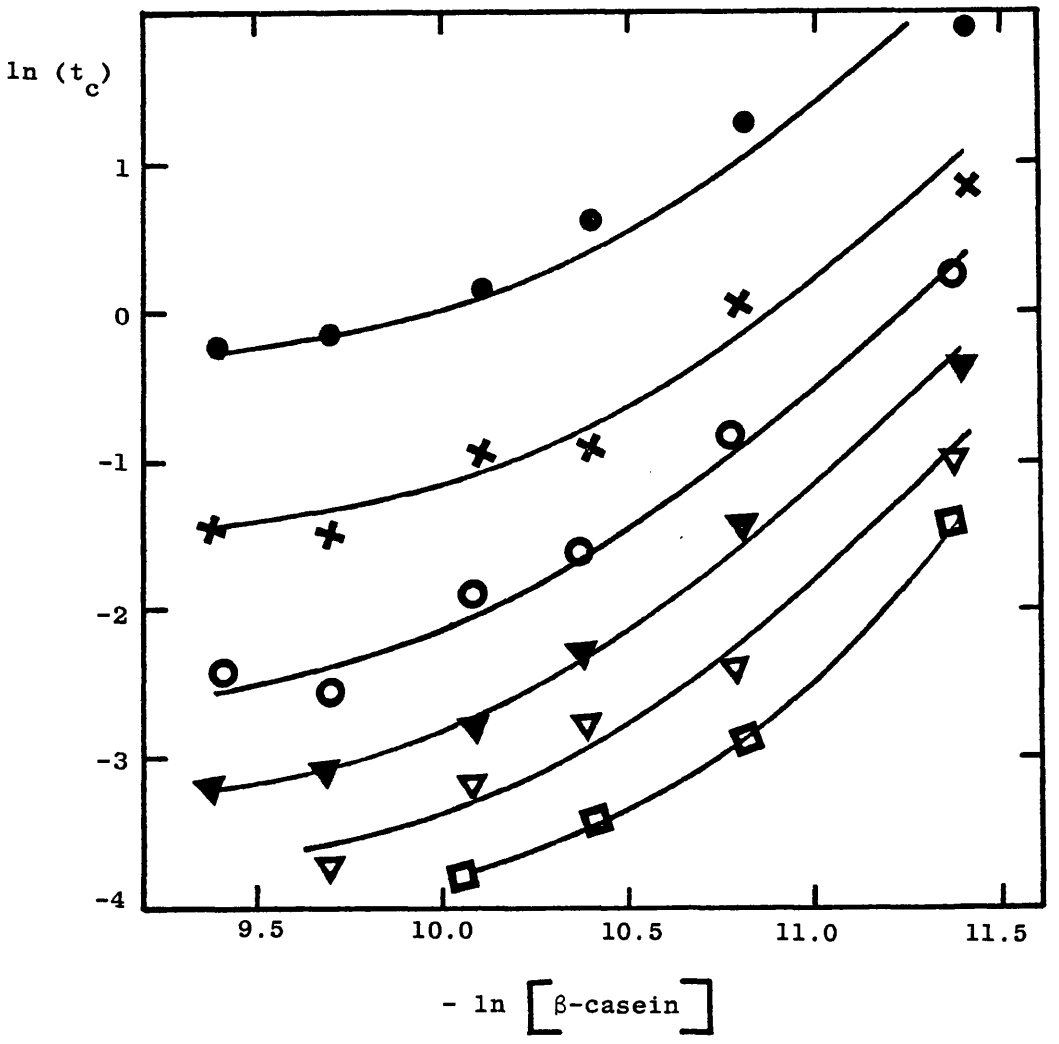

Fig. 3.8. Relationship between rate of reaction as diagnosed by critical time, and the [initial β-casein].
□, 9mM Ca^{2+}; ▽, 8.5mM Ca^{2+}; ▼, 8mM Ca^{2+}; ○, 7.5mM Ca^{2+}; ×, 7mM Ca^{2+}; ●, 6.5mM Ca^{2+}.

combinations before the end of kinetic measurements).

The definitive β-casein/Ca^{2+} reaction profile at 40°C is shown in Fig. 3.9. The essential differences between reaction profiles of α_{s1}-casein and β-casein with Ca^{2+} are still maintained. The critical time is smaller and the slopes are greater, although the β-casein curve pertains to measurements at 40°C while the definitive α_{s1}-casein curve (Fig. 3.5) was derived from measurements made at 23°C. The temperature will have an effect on the reaction and this is examined in Sections 3.3 and 3.4.

3.3.1. Effect of temperature on the reaction of Ca^{2+} with α_{s1}-casein

To determine the effect of temperature on the reaction of α_{s1}-casein with Ca^{2+}, reaction profiles were obtained for the reaction of 7mM $CaCl_2$ with 1mg/ml α_{s1}-casein at selected temperatures. As before, all of the reaction profiles had the same characteristics. Initially molecular weight increase was relatively slow becoming faster until the growth in molecular weight was linear with time. Each reaction was characterised by the two parameters of limiting slope and critical time. The results are given in TABLE 3.

As would be expected the rate of the aggregation reaction increases with temperature, indicated by the increasing gradients of the linear section and corresponding decreases in critical times. If the limiting slope or $1/t_c$ are taken to be simply relatable to rate constants, then an Arrhenius-type of plot of ln (limiting slope) or ln $(1/t_c)$ against reciprocal temperature should be linear. The plot is shown in Fig. 3.10 for a temperature range of 16 to 30°C. The inverse type of relationship between the two parameters is again illustrated by this graph, the slope increasing and the critical time decreasing with increasing temperature.

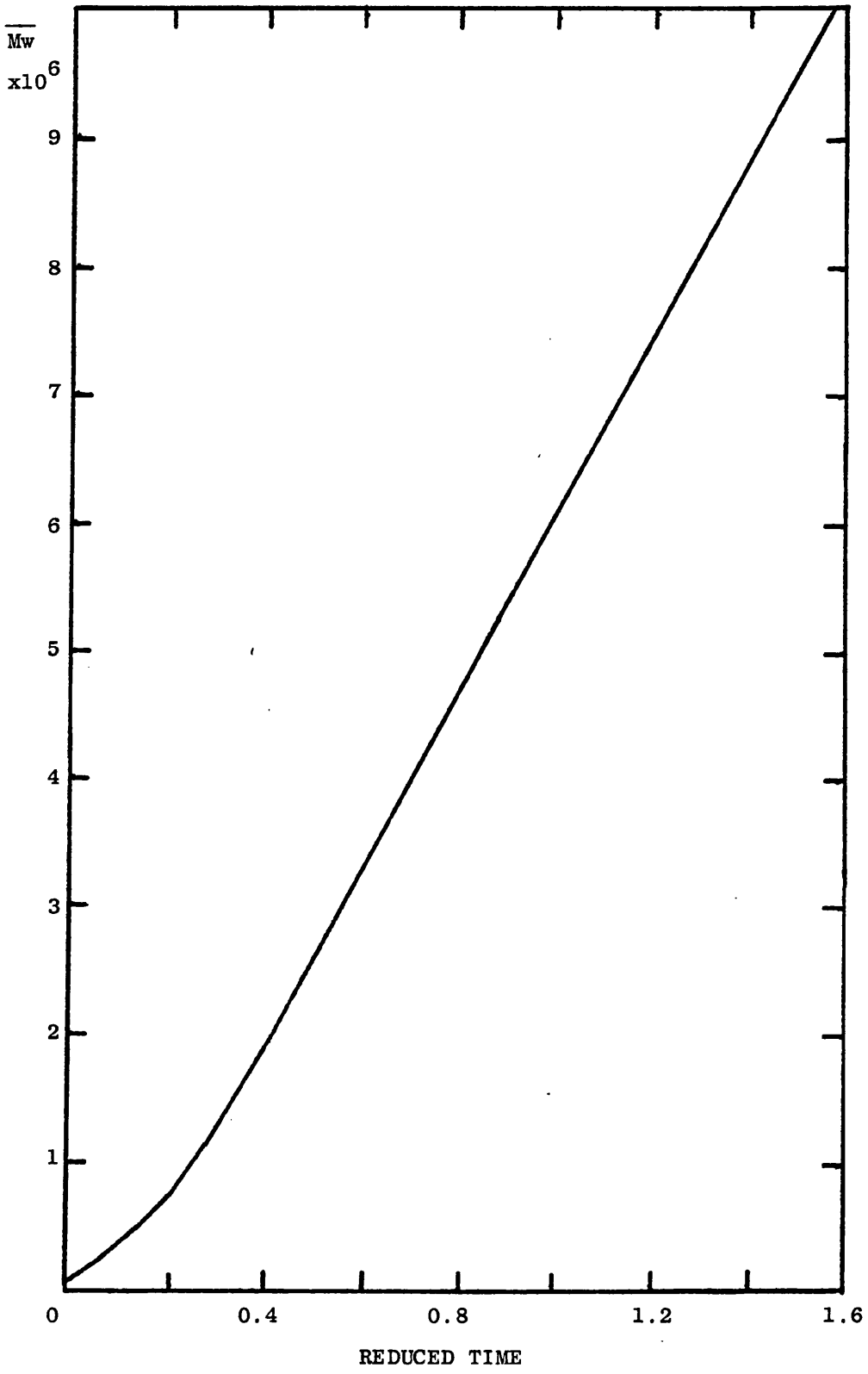

Fig. 3.9. Reaction profiles of all Ca^{2+}/β-casein combinations at 40°C plotted on a reduced time scale where $\overline{Mw}$ = 6 x 10^6 was selected as t_{red} = 1.

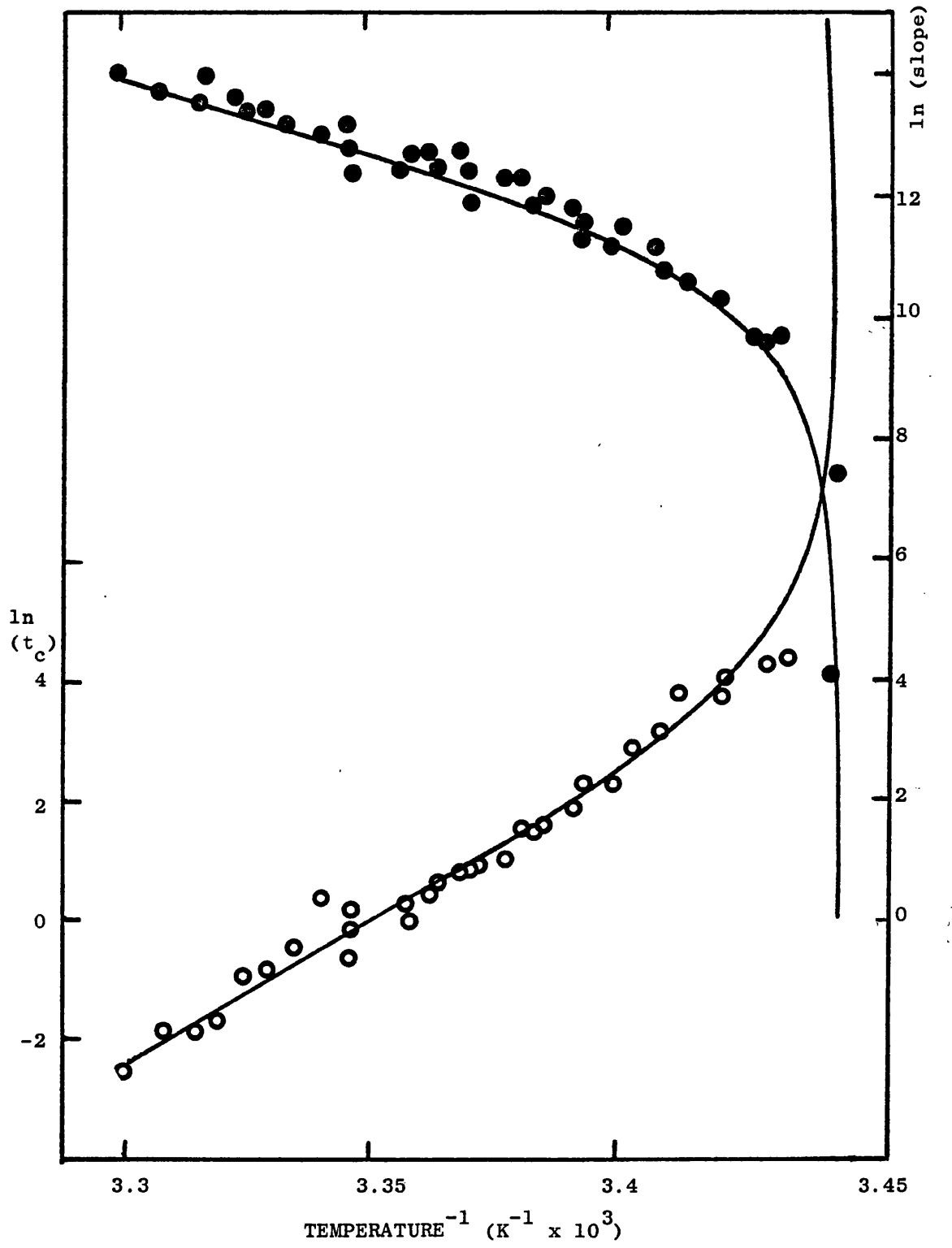

Fig. 3.10. Arrhenius plot of limiting slope, (right hand axis) and critical time (left hand axis) for the reaction of 7mM Ca^{2+} with 1 mg/ml α_{s1}-casein.

Below 16.7°C no reaction would take place for this concentration combination. The reaction then rapidly became faster and continuously increased over the range 17.5°C to 30°C. Above the higher temperature the reaction was too fast to measure. The Arrhenius plot is non-linear, tending to a decreasing slope as the temperature was increased. This non-linearity can be taken as an indication that the reaction mechanism is not simple. The gradient of the Arrhenius plot of the slope at the highest temperature (30°C) gave an apparent activation energy of 1.4×10^5 J/mole. Conversely at 16 to 17°C the slope of the Arrhenius plot was virtually infinite. Even at the highest temperature, the apparent activation energy appears very high for what is in effect a very efficient and fast reaction.

The apparent activation energy at 30°C is approximately 2.4×10^5 J/mole when calculated from the Arrhenius plot of critical time, which suggests some difference in the effect of temperature on the first and second stages of the reaction.

3.3.2. Comparison of curves obtained at different temperatures on a reduced time scale

In exactly the same manner as described in Section 3.1.4 reaction profiles obtained for the same calcium/α_{s1}-casein combination (7mM Ca^{2+}/1 mg/ml α_{s1}-casein) at different temperature can be plotted on a single reduced time scale. A molecular weight of 4×10^5 was arbitrarily chosen as that weight corresponding to a reduced time of one because this molecular weight was reached on all the individual reaction profiles. However, similar results can be achieved by selecting other values of $\overline{Mw}$ as corresponding to a reduced time of one.

In contrast to the single curve obtained by this procedure for all α_{s1}-casein/Ca^{2+} combinations, variation of temperature produces

a family of curves which are ordered according to the temperature at which they were measured (Fig. 3.11). The curves shown range from one measured at 18.6°C to one at 29.3°C which was much faster as indicated by the increase in limiting slope and shorter critical time described in the previous section. In the centre of those curves drawn is the definitive curve previously obtained for combination of calcium and α_{s1}-casein at 23°C.

The critical times of each of the experiments becomes smaller as the temperature increases on this reduced time scale in the same way as observed for real time. However the gradients of the linear sections of the curves plotted on the reduced time scale decrease with increasing temperature although the gradient on a real time scale increases with temperature. As the temperature is raised the critical time is therefore reduced by a greater extent relative to increases in the limiting gradient, i.e., temperature changes appear to have a relatively greater effect on the lag phase of the reaction than on the linear phase.

3.3.3. Effect of temperature on several Ca/α_{s1}-casein combinations

Reaction profiles were obtained for six calcium and α_{s1}-casein concentration combinations over a temperature range of 16°C to 30°C. The temperature at which the aggregation reaction became extensive enough to be measured varied according to the concentrations of reactants. Using a solution containing 7.5mM Ca^{2+} and 1.5 mg/ml α_{s1}-casein, for example, the reaction is sufficiently rapid to allow the rate to be measured at 16°C whereas a similar solution with 6.5mM Ca^{2+} and 0.5 mg/ml α_{s1}-casein does not have a similar reaction rate until it is heated to about 21°C.

A summary of the results is given in TABLE 4, and Arrhenius

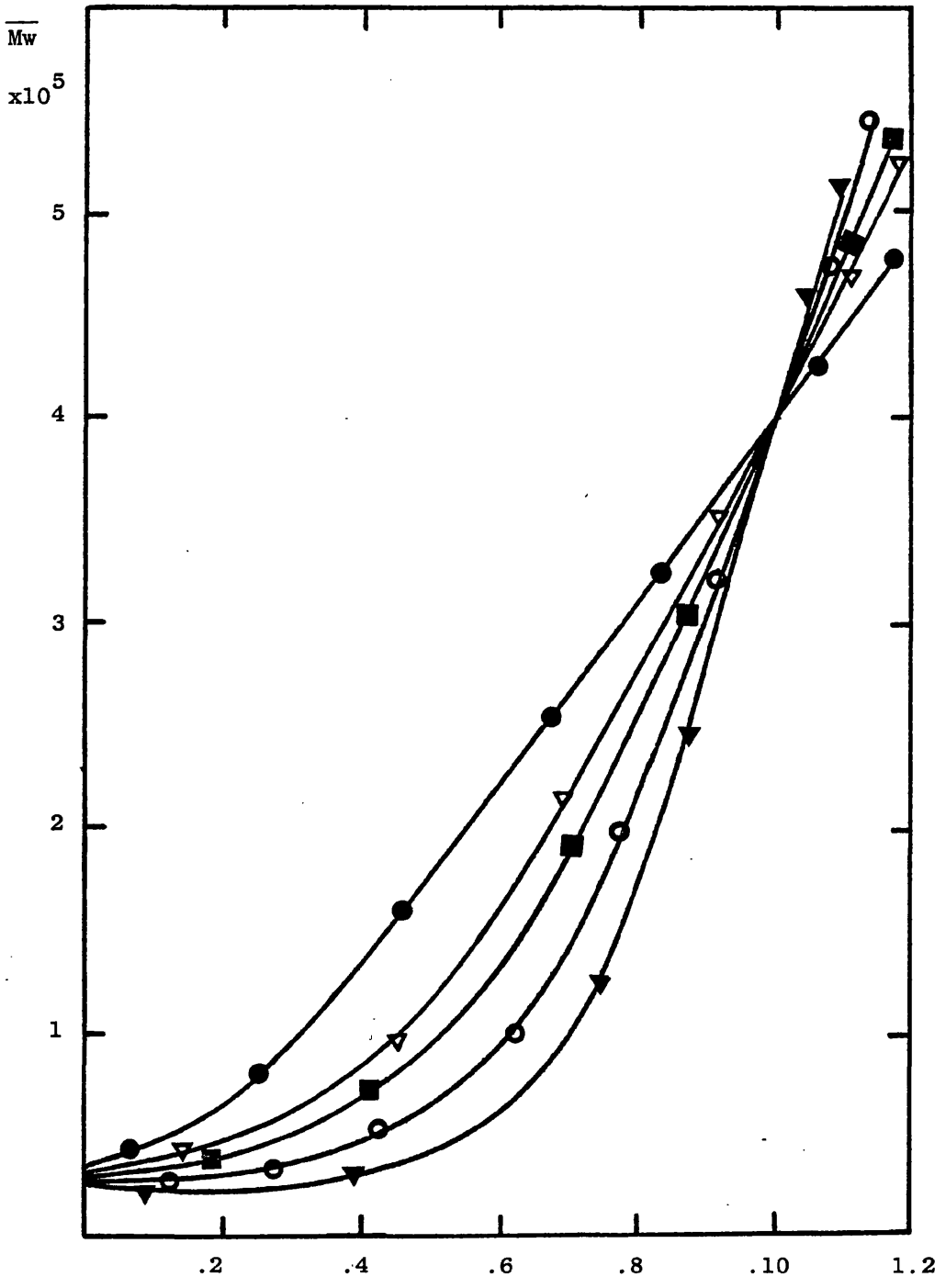

Fig. 3.11. Reaction profiles obtained at various temperatures for 7mM Ca^{2+} and 1 mg/ml α_{s1}-casein on a reduced time scale where $\overline{Mw} = 4 \times 10^5$ at $t_{red} = 1$. The temperatures at which these profiles were obtained are ▼, 18.6°C; ○, 20.7°C; ■, 23°C; ▽, 26.2°C; and ●, 29.3°C.

plots are illustrated in Fig. 3.12, in which a series of approximately parallel lines show the effect of increasing temperature on several Ca^{2+}/α_{s1}-casein combinations. These lines correspond to the approximately linear behaviour shown in Fig. 3.10 for temperatures some way above the minimum temperature at which measurements could be made. Since the lines are approximately parallel the apparent activation energies do not greatly change when casein and calcium concentrations are changed. The apparent activation energies were the same as that determined for the more detailed study in Section 3.3.1.

The position of each line is affected by the concentrations of calcium and casein. Increasing either $\left[Ca^{2+}\right]$ or $\left[\alpha_{s1}\text{-casein}\right]$ displaces the lines to higher positions i.e. increases the apparent intercept of the Arrhenius plots.

At 20°C the reaction of 7.5mM Ca^{2+} with 0.5 mg/ml α_{s1}-casein gives a limiting slope, $d\overline{Mw}/dt$ of 4.2×10^4 S^{-1} and a critical time of 9.0 seconds. Increasing the casein concentration to 2 mg/ml results in a reaction having a limiting slope of 4.7×10^5 S^{-1} and t_c of 1.5 s as rate parameters. To attain the same limiting slope with the lower concentration of casein requires the temperature to be raised to 25.9°C, at which temperature the critical time would be 0.37 seconds. The changes in temperature apparently affect the critical time to a greater extent than changes in concentration which agrees well with the observation made in Section 3.3.2 that on a reduced time scale the reaction profile changes with temperature.

The gradients of the lines in the ln (t_c) versus temperature^{-1} series have a higher absolute value than those in the equivalent ln (limiting slope) series and suggests that the apparent activation energy for the lag phase of the reaction is greater than for the section where $\overline{Mw}$ is linear with time. The apparent activation energy of the

Fig. 3.12. Arrhenius plots of the rate of reaction as determined by limiting slope (upper scale) and critical time (lower scale) for various reactions of Ca^{2+} with α_{s1}-casein.

Symbol	Ca^{2+} (mM)	α_{s1}-casein (mg/ml)
○	7.5	0.5
□	7.5	1.5
▽	7.5	2
■	6.5	1
●	8.5	1
▼	9.0	1

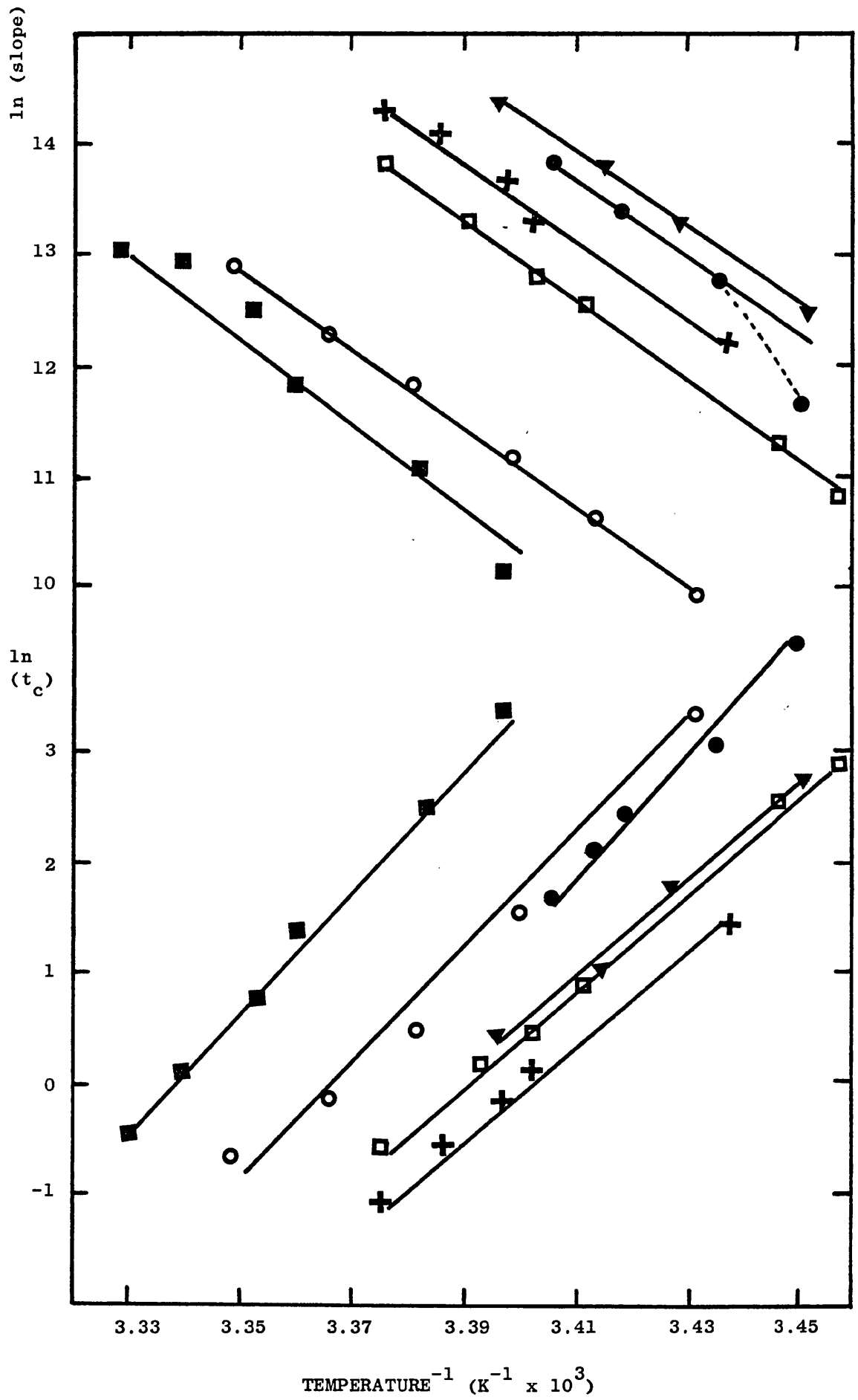
ln (slope)
14
13
12
11
10
ln
(t_c)
3
2
1
0
-1
3.33
3.35
3.37
3.39
3.41
3.43
3.45
TEMPERATURE^{-1} (K^{-1} x 10^3)

first stage of α_{s1}-casein aggregation is calculated to be 4.5×10^5 J/mole over the temperature range where each of the reactions is measured, whereas the apparent activation energy of the second stage is 2.9×10^5 J/mole^{-1}.

3.4.1. Effect of temperature on several calcium and β-casein concentration combinations

As the temperature of the reaction mixture was raised the rate of reaction increased as shown by increased slopes and reduced critical times. This behaviour of β-casein is comparable to that of α_{s1}-casein except that reaction with calcium did not initiate appreciable β-casein aggregation until the temperature was raised to about 32°C using the concentrations of 0.25 to 2 mg/ml β-casein and 6.5 to 9mM calcium. The lower concentration combinations required even higher temperatures before aggregation became measurable.

From the results presented in TABLE 5 an Arrhenius plot of ln (limiting slope) was constructed (see Fig. 3.13) and a linear relationship is demonstrated for any given Ca^{2+}/β-casein concentration combination. As with α_{s1}-casein, different combinations of $[Ca^{2+}]$ and [β-casein] result in a series of lines having approximately the same gradient when rate measurements are made at a number of different temperatures. The gradients of the Arrhenius plots of limiting slope and critical time were individually determined by linear regression. The average gradient of the limiting slope and critical time plots gave apparent activation energies of 7.5×10^5 J/mole and 1.3×10^6 J/mole respectively.

These apparent activation energies are in fact greater than the equivalent values for α_{s1}-casein which were 2.9×10^5 J/mole and 4.5×10^5 J/mole for the Arrhenius plots of limiting slope and critical

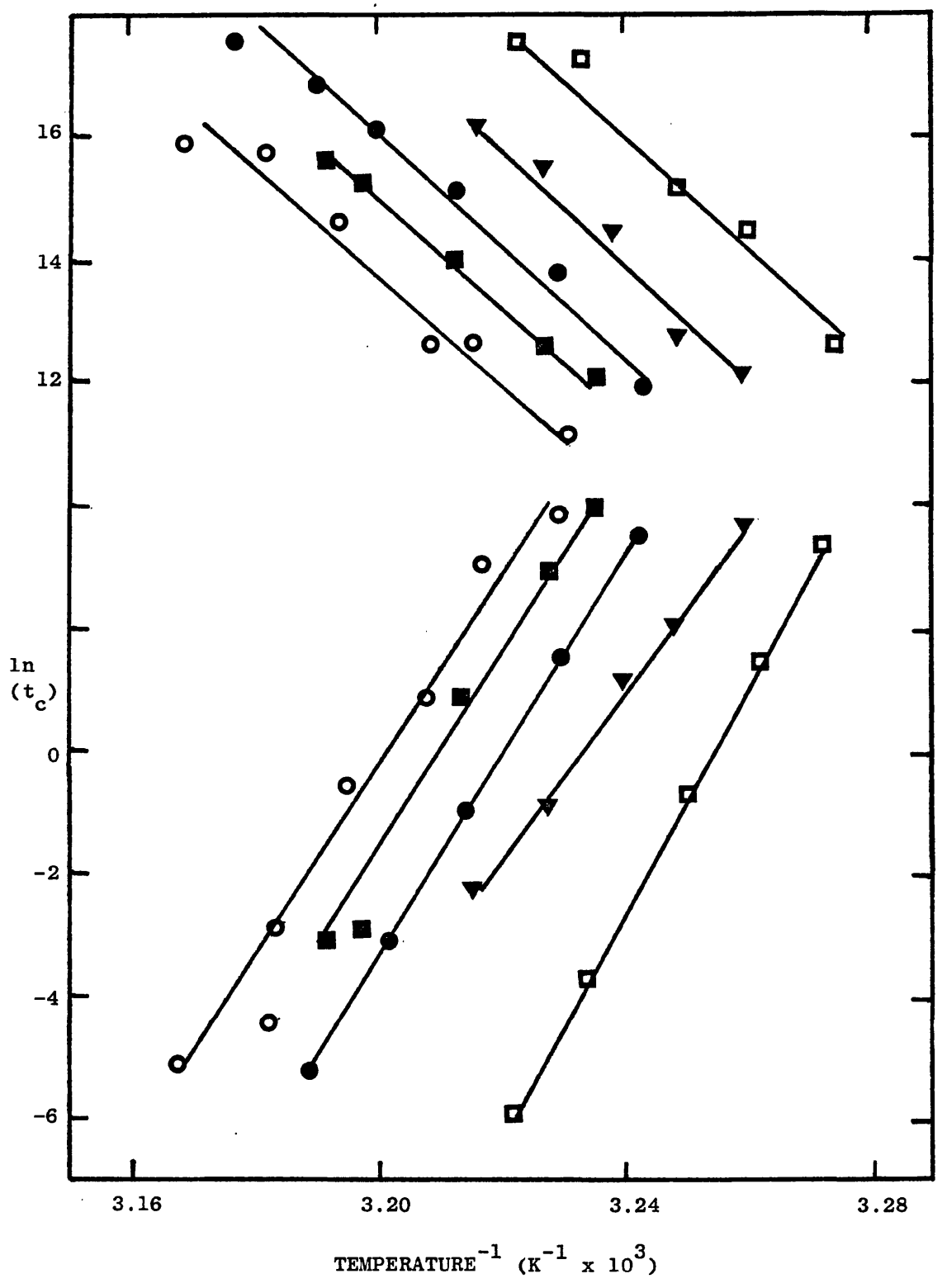

Fig. 3.13. Arrhenius plot rate of reaction as indicated by limiting slope (upper scale) and critical time (lower scale) for various reactions of Ca^{2+} with β-casein. □, 9mM Ca^{2+}/2 mg/ml β-casein; ▼, 8mM Ca^{2+}/1.5 mg/ml β-casein; ●, 7.5mM Ca^{2+}/1.5 mg/ml β-casein; ■, 7mM Ca^{2+}/2 mg/ml β-casein; ○, 6.5mM Ca^{2+}/1.5 mg/ml β-casein.

time respectively.

Temperature has a greater effect on the critical time than on the limiting slope and hence the apparent activation energies derived from t_c are larger than those derived from the plots of limiting slope; for both caseins. The apparent activation energies for the aggregation reaction of β-casein in the presence of Ca^{2+} are approximately five times greater than for α_{s1}-casein. The different temperatures at which these values were calculated would in fact be expected to favour reduced activation energies for the β-casein aggregation reaction since the gradient of the Arrhenius plot of the α_{s1}-casein aggregation (see Fig. 3.10) is in fact gradually decreasing with increasing temperature. Thus the activation energy for the association of β-casein upon addition of Ca^{2+} is indeed greater than for α_{s1}-casein.

3.4.2. Reaction profiles of calcium and β-casein at several temperatures plotted on a reduced time scale

The aggregation reaction of 6.5mM calcium with 1.5 mg/ml β-casein was observed at several temperatures from 36°C to 43°C. Below 36°C the association reaction was insiginificant. An increase in reaction rate was observed with increasing temperature as shown by both rate diagnostic parameters in Fig. 3.13.

The reaction profiles obtained can be plotted on a reduced time scale as described in Section 3.1.4. In this case a molecular weight of 2×10^6 was arbitrarily chosen as the $\overline{Mw}$ at a reduced time of one.

At 36.5°C the reduction factor was 72 while the factor required to place the reaction profile obtained at 42.5°C on a reduced time scale was only 0.27, thereby reflecting the difference in the

extent and rate of reaction over the time interval of measurement. Figure 3.14 shows the curves obtained at different temperatures on a reduced time scale. As was found for α_{s1}-casein, a single definitive β-casein curve is not obtained, but rather a series of reaction profiles which are changing with temperature.

The critical times are longer at lower temperatures, rapidly decreasing with increases in temperature. However, the limiting slopes, although increasing with temperature on a real time scale, apparently decrease with temperature on this reduced time scale. This verifies that the two rate diagnostic parameters are not equally affected by temperature changes unlike the results of altering $[Ca^{2+}]$ or $[\beta\text{-casein}]$ at a fixed temperature (see Section 3.2.4). The critical time is reduced by more than the slope is increased when the temperatures of the reactants is raised.

3.5.1. Effect of including subcritical levels of calcium with α_{s1}- and β-casein prior to mixing

It seems clear that the first stage in the overall reaction must be the binding of calcium to α_{s1}-casein, and it was necessary to establish whether this was an important factor in determining the critical time of the reactions; i.e. whether it was a rate determining step.

It is well known that α_{s1}-casein remains completely soluble in calcium solutions of low concentration (see Fig. 1.2). For any given α_{s1}-casein concentration there is a critical calcium concentration below which there is no decrease in protein solubility. Above the critical calcium concentration some of the protein will flocculate. Inclusion of a subcritical level of calcium with α_{s1}-casein prior to kinetic measurements would allow time for an appreciable level of calcium

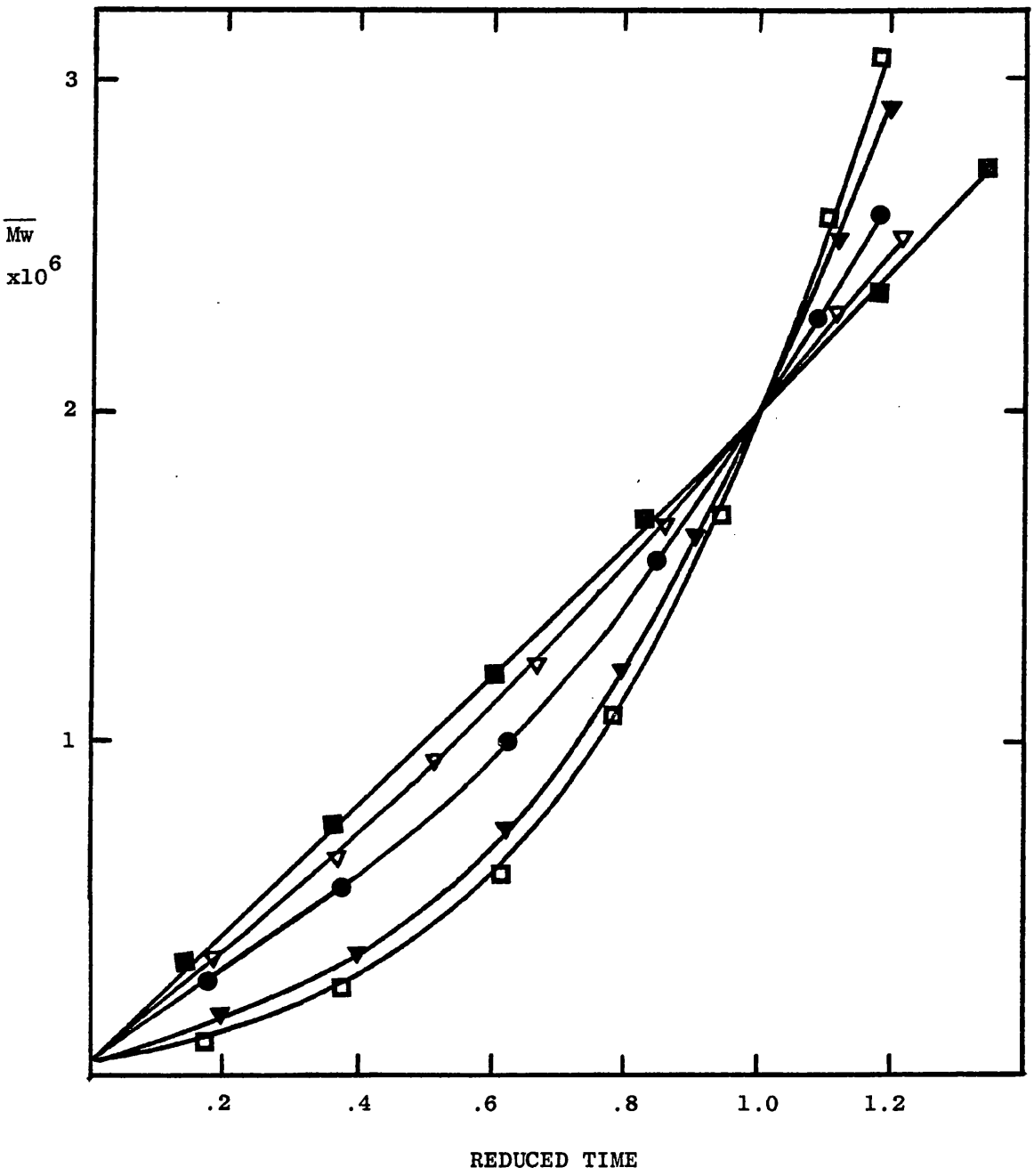

Fig. 3.14. Reaction profiles of 6.5mM calcium and 1.5 mg/ml β-casein at various temperatures plotted on a reduced time scale for $\overline{Mw} = 2 \times 10^6$ at $t_{red} = 1$. □, 36.5°C; ▼, 37.8°C; ●, 38.5°C; ▽, 40°C; ■, 42.5°C.

binding to α_{s1}-casein, without inducing flocculation.

In the event that calcium binding to α_{s1}-casein controls the rate of precipitation then an increase in the rate would be predicted for a given calcium/α_{s1}-casein concentration combination having a proportion of the calcium ion concentration included with the α_{s1}-casein prior to mixing. The appropriate Ca^{2+} and α_{s1}-casein solutions were prepared as described in Section 2.6.

Using 7mM total calcium and 1 mg/ml α_{s1}-casein the reaction profiles determined at various temperatures could be compared to the results presented in Section 3.3.1. The reaction profile was not altered by having subcritical levels of Ca^{2+} included with α_{s1}-casein prior to kinetic measurements. Both the critical time and the limiting slope could still be used as rate diagnostic parameters. An Arrhenius plot of ln (limiting slope) from the data given in TABLE 6 showed the same approximately linear relationship previously observed above a critical temperature of about $16^{o}C$ (see Fig. 3.15). There was no increase in the position of this line which was close to that previously obtained. The rate of reaction, as determined by the limiting slope, was not increased by the preaddition of calcium.

The lag phase was still present in all reaction profiles, and the critical times measured were again plotted according to Arrhenius. This plot of ln (t_c) versus temperature^{-1} (shown in Fig. 3.15) exhibits the same relationship observed in Fig. 3.10 for 7mM Ca^{2+} and 1 mg/ml α_{s1}-casein where no calcium was added to the protein prior to complete mixing. Once again, no decrease in the critical time was observed which would have indicated an increase in the rate of reaction due to premixing of calcium.

Since no rate increase was observed by preaddition of calcium ions to α_{s1}-casein, the rate determining step in the aggregation

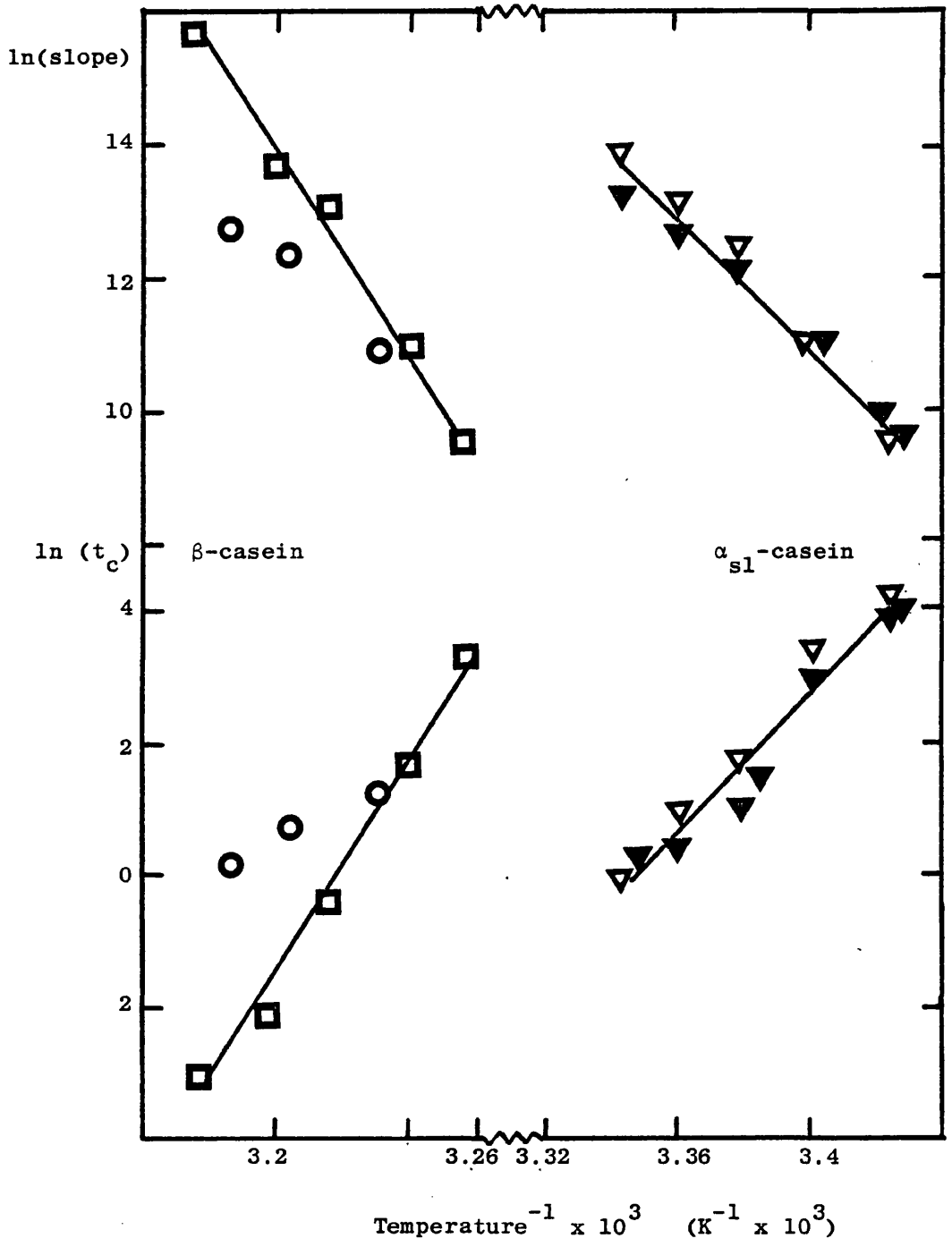

Fig. 3.15. Effect of adding subcritical levels of calcium prior to measurement of reaction rate. The α_{s1}-casein (1 mg/ml) and β-casein (0.5 mg/ml) were combined with 7mM Ca^{2+} and 8.5mM Ca^{2+} respectively. ▽○, Subcritical levels of Ca^{2+} included prior to mixing; ▼□, Casein and Ca^{2+} only mixed during experiment.

of α_{s1}-casein cannot be simply calcium binding. Calcium binding to α_{s1}-casein is apparently faster than the rate of limiting process.

Similar arguments apply to β-casein, which also has a critical calcium concentration below which it remains soluble. This critical calcium concentration varies according to $[\beta\text{-casein}]$ and the temperature. Inclusion of subcritical calcium concentrations with β-casein prior to kinetic measurement did not increase the rate of aggregation of β-casein as shown by the Arrhenius plots of limiting slope and critical time in Fig. 3.15 for a combination of 8.5mM total calcium and 0.5 mg/ml β-casein. No significant changes in the reaction profile were made by preaddition of Ca^{2+} to β-casein. Calcium binding to β-casein thus appears to be faster than the rate limiting step in the aggregation process.

Therefore, these results demonstrate that there is no possibility that the initial stage of the observed aggregation can be explained in terms of the kinetics of binding of Ca^{2+} to the proteins, and that the answers to this problem must be sought in the behaviour of the proteins themselves.

3.6.1. Relationship between precipitate concentration of α_{s1}-casein and Ca^{2+}

The solubility of α_{s1}-casein is reduced by addition of calcium ions as shown in Fig. 1.2 (56). After a critical concentration of Ca^{2+} has been attained (which varies with α_{s1}-casein concentration) the decrease in solubility is rapid over a short increase in $[Ca^{2+}]$ becoming gradually less marked until it levels off where most of the α_{s1}-casein has been precipitated. The precipitate concentration of each Ca^{2+}/α_{s1}-casein combination given in TABLE 1 was determined at $23^{o}C$.

As expected, increasing the calcium ion concentration produces a higher precipitate concentration at any fixed α_{s1}-casein concentration, but higher protein concentrations contain lower ratios of soluble material than lower protein concentrations at the same $\left[\text{total } Ca^{2+}\right]$ (see Fig. 3.16). For any Ca^{2+}/α_{s1}-casein combination, there is some soluble material which remains unaggregated even after a considerable length of time. Complete precipitation is not attained under any of the reaction conditions used in these experiments.

The relationship between the precipitate concentration or the precipitate fraction with $\left[Ca^{2+}\right]$ is similar to that observed for the rate of reaction (c.f. Fig. 3.2). From the results given in Fig. 3.16, it appears that not all of the protein can take part in the aggregation reaction. The effect of changing $\left[Ca^{2+}\right]$ may therefore be simply to alter the concentration of protein which can aggregate or it may alter not only the amount but also the properties of the protein, since changing $\left[Ca^{2+}\right]$ will also alter the extent of binding of Ca^{2+} to the protein. In the first of these two cases, it would be expected that the rate of aggregation would change according to the law of mass action, but in the second, more complex factors will come into play. This is discussed more fully in the next section.

3.6.2. Relationship between reaction rate and precipitate concentration of α_{s1}-casein

The rate of reaction was found to be influenced by the concentration of α_{s1}-casein (Section 3.1.3) but no direct proportionality was indicated. Since not all of the α_{s1}-casein present in any of the casein/Ca^{2+} combinations, for which reaction profiles were determined at 23°C, was actually taking part in the aggregation reaction, it was suggested that the rate might be directly proportional to the amount of

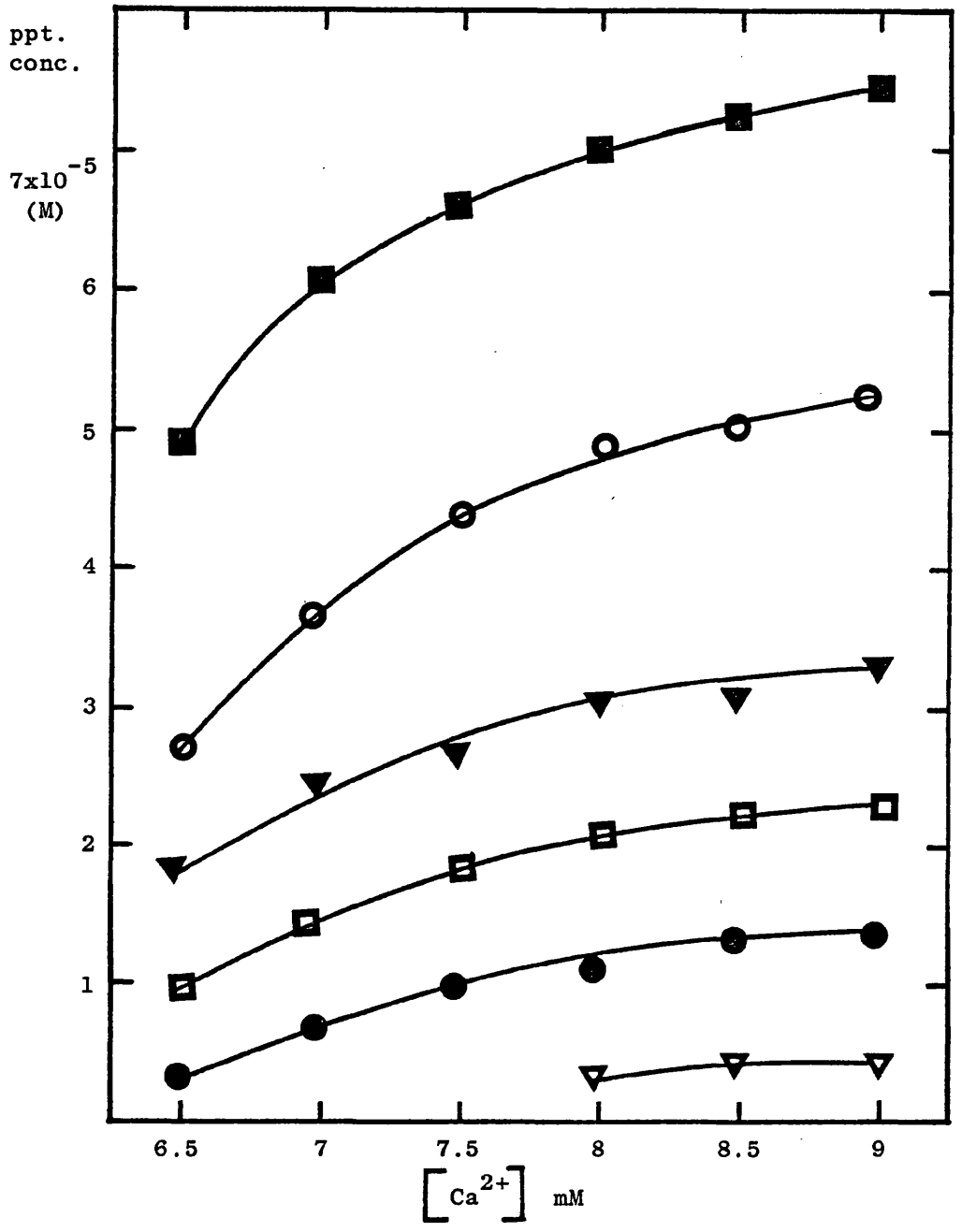

Fig. 3.16. Precipitate concentration of α_{s1}-casein as a function of $[Ca^{2+}]$ where ■ is 2 mg/ml; ○, 1.5 mg/ml; ▼, 1 mg/ml; □, 0.75 mg/ml; ●, 0.5 mg/ml and ▽= 0.25 mg/ml α_{s1}-casein. (1 mg/ml = 4.24 M α_{s1}-casein).

α_{s1}-casein which could actually be precipitated.

A double logarithmic plot of slope versus precipitate concentration showed a strong linear relationship between these two variables as illustrated in Fig. 3.17. In general, the rate of reaction increased with precipitate concentration of α_{s1}-casein.

Results at a single Ca^{2+} concentration indicate a direct proportionality between the rate of reaction and the concentration of α_{s1}-casein precipitate, raised to a power, the value of which may be two since the gradient of the line for 9mM Ca^{2+} in the logarithmic plot is approximately 1.7. However, a second line may be drawn, representing a range of calcium ion concentrations at a fixed concentration of α_{s1}-casein (as shown by the dotted line joining those results produced from an initial concentration of α_{s1}-casein of 2 mg/ml in Fig. 3.17) which indicates another rate controlling factor influenced by $\left[Ca^{2+}\right]$.

From these observations it was concluded that

$$\frac{d\overline{Mw}}{dt} \propto \left[\alpha_{s1}\text{-casein precipitating}\right]^{a} \qquad (3.8)$$

where the value of constant a is not defined.

Thus, it appears that the effect of changing Ca^{2+} concentration is not simply to increase the amount of precipitate, and hence the rate, by the law of mass action. Had that been so, the variation of reaction rate with Ca^{2+} should not be present in Fig. 3.17. It is to be concluded that Ca^{2+} affects the reaction by more than simply altering the amount of precipitate formed.

3.6.3. Relationship between the precipitate concentration of β-casein and the $\left[Ca^{2+}\right]$

As was found for α_{s1}-casein, not all of the protein present

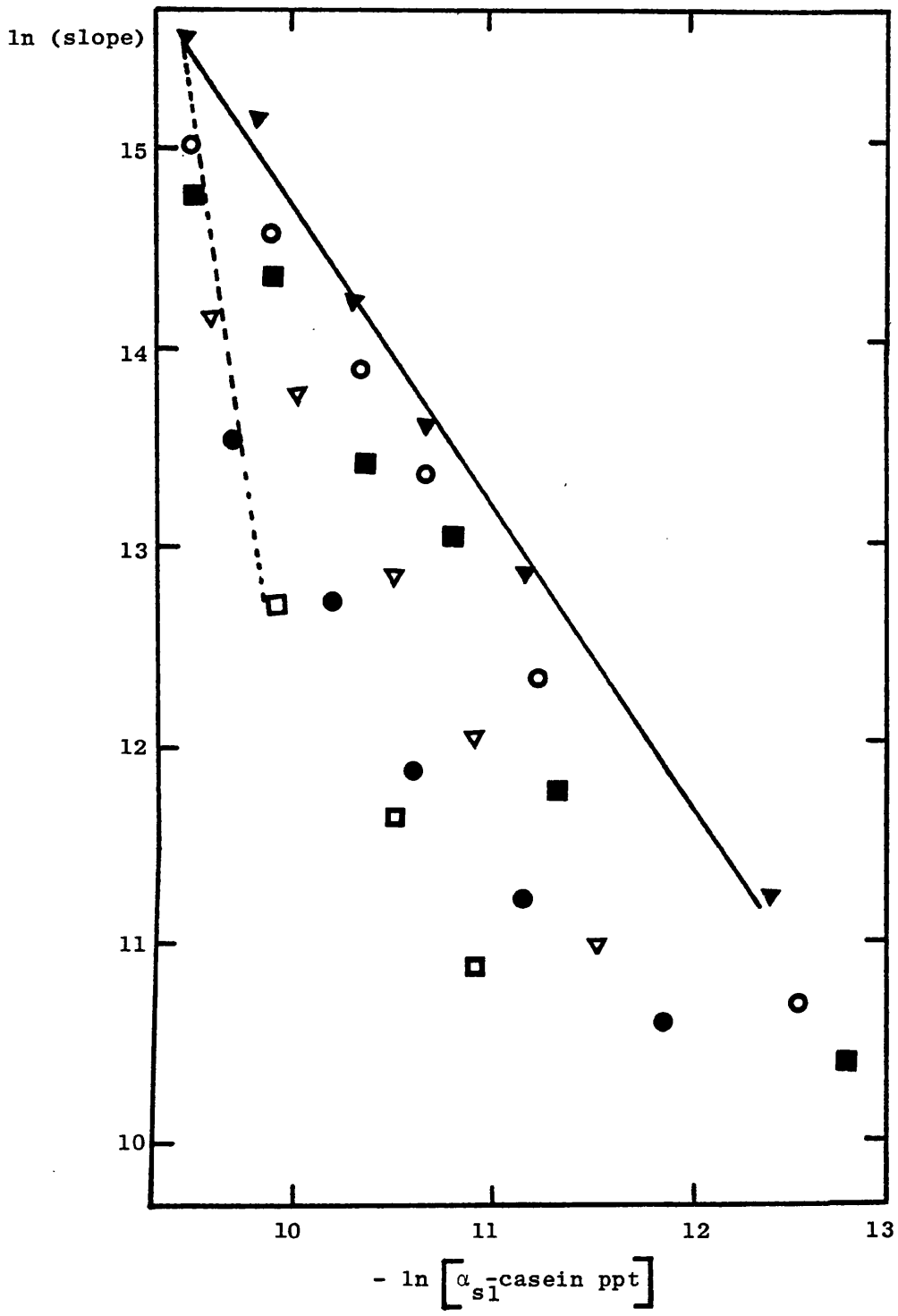

Fig. 3.17. Relationship between reaction rate, as shown by limiting slope, and the precipitate concentration of α_{s1}-casein. Results at 9mM Ca^{2+} are indicated by ▼ and those at 2 mg/ml α_{s1}-casein joined by ---.

in the reaction mixture is aggregable material. Some β-casein remained soluble even after long reaction times.

The soluble and precipitating concentrations of β-casein obtained for combinations with Ca^{2+} were determined at 40°C. The precipitate fractions of most of the Ca^{2+}/β-casein combinations were found to be greater than 70% with many being close to 90% as inspection of the data in TABLE 2 reveals. However, the precipitate concentration still increased with increasing calcium concentration but only slightly as shown in Fig. 3.18. For example, the precipitable protein concentration obtained from an 8.33×10^{-5}M β-casein solution increased from 7.41×10^{-5} to 7.87×10^{-5} with a calcium ion increase from 6.5mM to 9.0mM which represents an increase in precipitate of less than 6% from 88.8% to 94.4%. Comparable changes in calcium with the same $[\alpha_{s1}\text{-casein}]$ at 23°C produced an increase in precipitable protein from 56.6 to 86.1%.

The actual precipitate concentration of β-casein depended predominantly upon the initial β-casein concentration. Compared to α_{s1}-casein the extent of β-casein precipitation is much less dependent upon $[Ca^{2+}]$. If the initial state of aggregation of the protein, in the absence of Ca^{2+}, is important in defining its precipitation, then the differences between the proteins may be explained. When Ca^{2+} is absent, β-casein is known to have a much stronger tendency to aggregate than α_{s1} (64,69), and this tendency may be important when the aggregating agent, Ca^{2+} is present also.

3.6.4. Relationship between the rate of reaction and the concentration of precipitable β-casein

The fraction of β-casein which precipitates at 40°C is very high for those concentrations used in this work. However, not all the

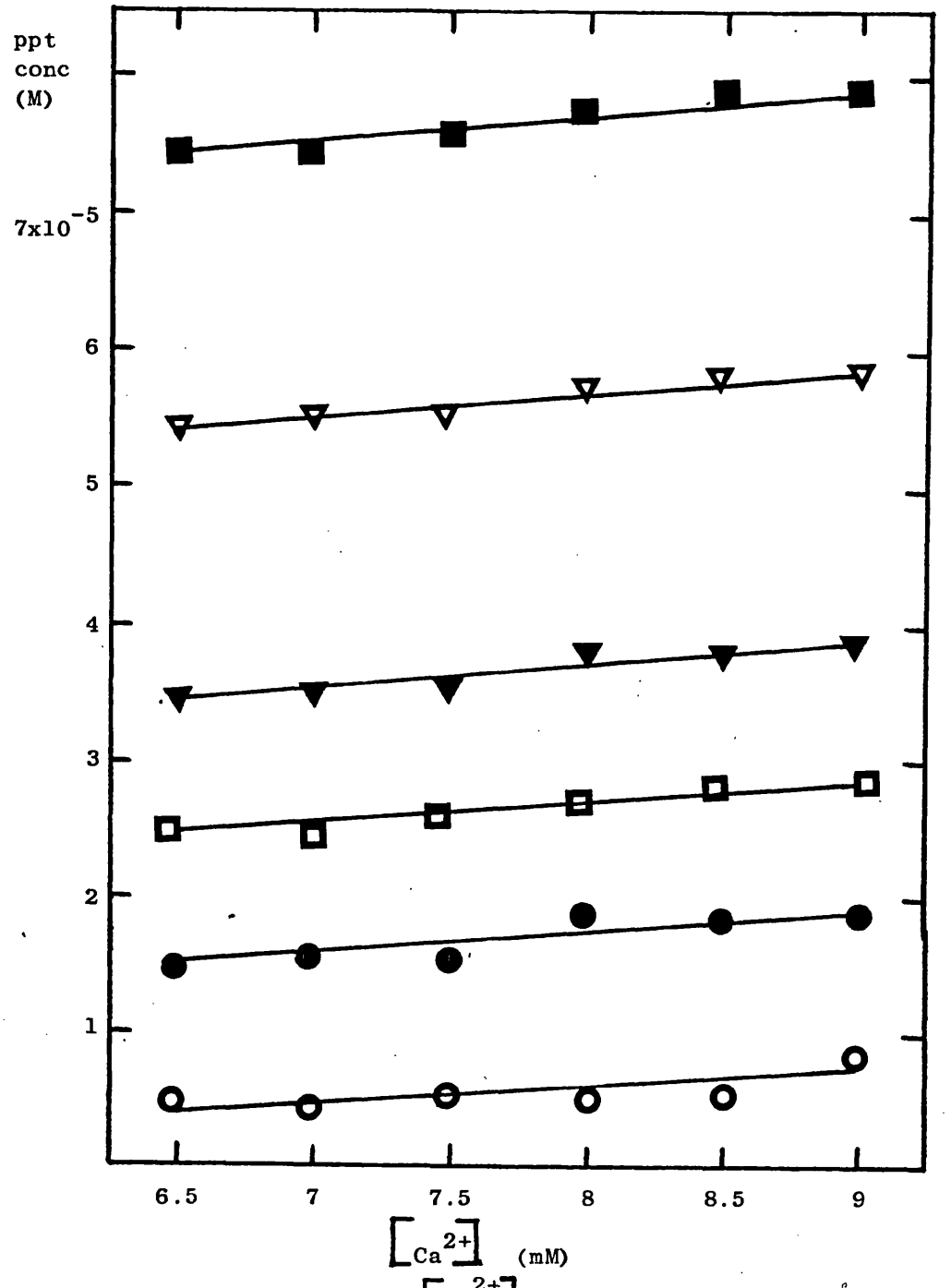

Fig. 3.18. Effect of $[Ca^{2+}]$ on the precipitate concentration by β-casein where the initial [β-casein] is represented by ■ for 2mg/ml; ▽, 1.5 mg/ml; ▼, 1 mg/ml; □, 0.75 mg/ml; ●, 0.5 mg/ml; ○, 0.25 mg/ml. (1mg/ml = 4.17×10^{-5}M).

protein was precipitable even for the highest calcium concentrations after a considerable reaction time.

Although no direct proportionality was found between the rate of reaction and the total concentration of β-casein (Section 3.2.3), it did have a pronounced effect upon both the limiting slope and critical time. A double logarithmic plot of limiting slope versus precipitate concentration presented as Fig. 3.19 shows that the rate of reaction did increase as the precipitate concentration increased for a given calcium ion concentration. At a constant $[Ca^{2+}]$ there is a linear relationship between these two variables.

There is however a spread of reaction rates within a given initial [β-casein] which is a consequence of the $[Ca^{2+}]$. It would seem therefore that the rate of reaction of β-casein is directly relatable to the concentration of precipitable β-casein and to a second factor controlled by $[Ca^{2+}]$.

These results are analogous to those from α_{s1}-casein/Ca^{2+} mixtures, namely that the mass action effect of changing the precipitate protein by altering the calcium concentration is not sufficient to explain the changes in reaction rates which are observed experimentally.

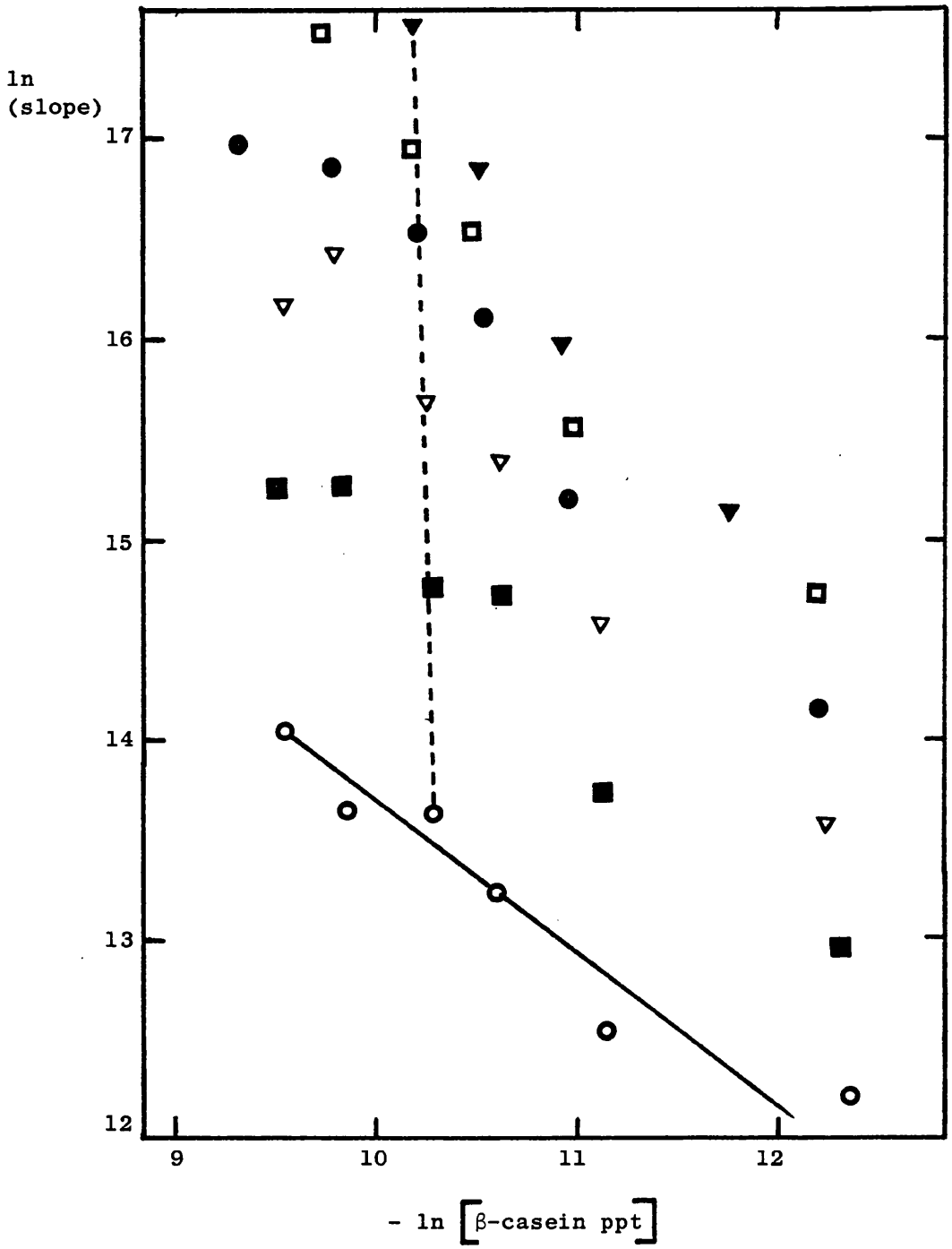

Fig. 3.19. Relationship between reaction rate as shown by limiting slope and the precipitate concentration of β-casein. ▼, 9mM Ca^{2+}; □, 8.5mM Ca^{2+}; ●, 8mM Ca^{2+}; ▽, 7.5mM Ca^{2+}; ■, 7mM Ca^{2+}, and ○, 6.5mM Ca^{2+}. The almost vertical dotted line joins those points obtained with 1 mg/ml β-casein solutions.

4. Discussion

4.1 Charge

Results already available show the dependence of the rate of aggregation of α_{s1}-casein upon the protein charge (156,169): reducing the charge on α_{s1}-casein increases the rate of aggregation. The charge on α_{s1}-casein can be altered by chemical modification or by interaction with species such as H^+ or Ca^{2+}. Precipitation of α_{s1}-casein occurs when the pH is reduced to 4.6 (160). Addition of Ca^{2+} also induces precipitation of the protein. The protein fraction which remains soluble has been shown to be a function of the calcium ion concentration (56, and Section 3.6.1). Since the net charge on the protein is in turn dependent upon $\left[Ca^{2+}\right]$ via the number of Ca^{2+} bound to each protein molecule, then the variation in soluble fraction with changing $\left[Ca^{2+}\right]$ may be explained by the change in the charge carried by each monomer casein unit.

It was shown in the previous chapter that the rates of aggregation of both α_{s1}- and β-casein were dependent upon both the calcium ion concentration and the casein concentration (sections 3.1 and 3.2). This also suggests that protein charge is involved in determining the reaction rate, since increasing $\left[Ca^{2+}\right]$ will reduce the protein charge and hence the rate of aggregation by reducing the electrostatic repulsion between protein molecules. Although the net charge on the casein molecule is reduced at a given $\left[Ca^{2+}\right]$ by lowering the casein concentration, the rate does not increase but instead decreases.

At pH7 the charge on the α_{s1}-casein monomer is close to -22 (19, 57). Binding of Ca^{2+} will reduce this negative charge by 2 units for each ion of calcium bound and thus decrease the electrostatic repulsion between particles. If the amount of Ca^{2+} bound to each casein molecule is

known then the charge can be calculated. The average number of Ca^{2+} bound per casein molecule $\bar{\nu}$, can be determined from dialysis experiments (58). The free calcium ion concentration can be determined for a given Ca^{2+}/casein combination. The difference between the initial concentration of Ca^{2+} and the free Ca^{2+} concentration after time for equilibrium, is the quantity of Ca^{2+} which is bound to the casein molecules.

Analysis of such binding isotherms for α_{s1}-casein and Ca^{2+} has allowed their quantitative description in terms of an initial binding constant K^* and a substitution parameter N which represents, in effect, the interaction between binding sites (58). Values of K^* and N determined from measured isotherms can be used to calculate $\bar{\nu}$ and hence the average charge (Q), for any solution containing Ca^{2+} and α_{s1}-casein.

Simple interaction theory relates the energy of repulsion Er, of two particles held in colloidal suspension to the respective charges Q_1 and Q_2 on these particles.

$$Er = \frac{Q_1 Q_2}{4\Pi \varepsilon r} \qquad (4.1)$$

where ε is the dielectric constant of the medium and r is the distance between particle centres.

Precipitation or aggregation is the result of a series of interaction steps between particles, each step involving at least two particles which adhere by some mechanism. In the case of casein aggregation the charge on any individual molecule cannot be determined but the average charge remaining on each molecule can be calculated from the average binding parameter $\bar{\nu}$. Since $Q_1 = Q_2$ in this case, then $Er \propto Q^2$. The important function is therefore Q^2.

According to Arrhenius the rate constant k for a reaction is related to an activation energy, Ea by the equation

$$\ln k = \ln A - Ea/RT \qquad (4.2)$$

The activation energy is the sum of attractive and repulsive components i.e. $Ea = E_{attraction} + E_{repulsion}$, since two molecules approaching one another will experience both attractive and repulsive forces between them. After thorough consideration of the forces which are operative between approaching particles Horne and Dalgleish (156) concluded that the attractive energy term could be reasonably considered to be approximately independent of the charge carried by the particle while the repulsive term, Er is proportional to Q^2 (see Section 1.7.3). A linear relationship between the logarithm of the rate constant and Q^2 is predicted by combining equations 4.1 and 4.2.

The charges on the α_{s1}-casein molecules for the Ca^{2+}/α_{s1}-casein combinations used in this work were calculated as described in section 2.4. A plot of the logarithm of reaction rate (as diagnosed by limiting slope) versus Q^2 is shown in Fig. 4.1. A series of lines is produced such that the predicted relationship is true for a given α_{s1}-casein concentration at different concentrations of Ca^{2+}. The rate constant for aggregation is therefore of the expected form

$$k = Ae^{\frac{-bQ^2}{RT}} \qquad (4.3)$$

From the calcium binding results of Parker and Dalgleish (74) the average charge per β-casein molecule was also calculated, incorporating the fact that β-casein has a charge of -13 at pH7. The logarithm of the rate constant (as diagnosed by the limiting slope) for β-casein/Ca^{2+} combinations were also plotted against Q^2 (see Fig. 4.2). A linear relationship is again demonstrated between ln k and Q^2 for a given β -casein concentration

Any mechanistic pathway proposed to describe aggregation of α_{s1}- or β-casein must therefore incorporate and explain the rate/charge

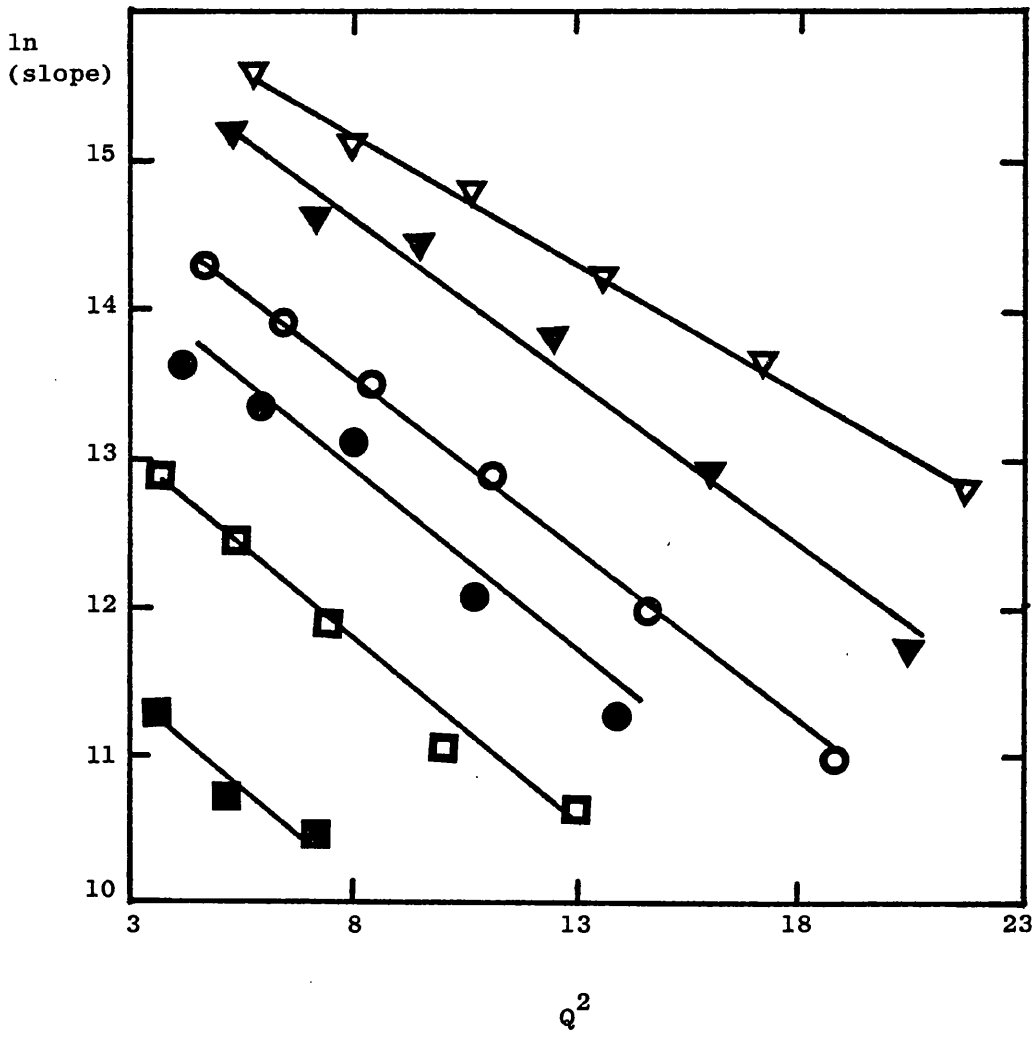

Fig. 4.1 Relationship between the rate of reaction as diagnosed by limiting slope and the square of the charge on the α_{s1}-casein molecule. ▽ represents 2mg/ml; ▼, 1.5mg/ml; ○, 1mg/ml; ●, 0.75mg/ml; □, 0.5mg/ml and ■, 0.25mg/ml α_{s1}-casein.

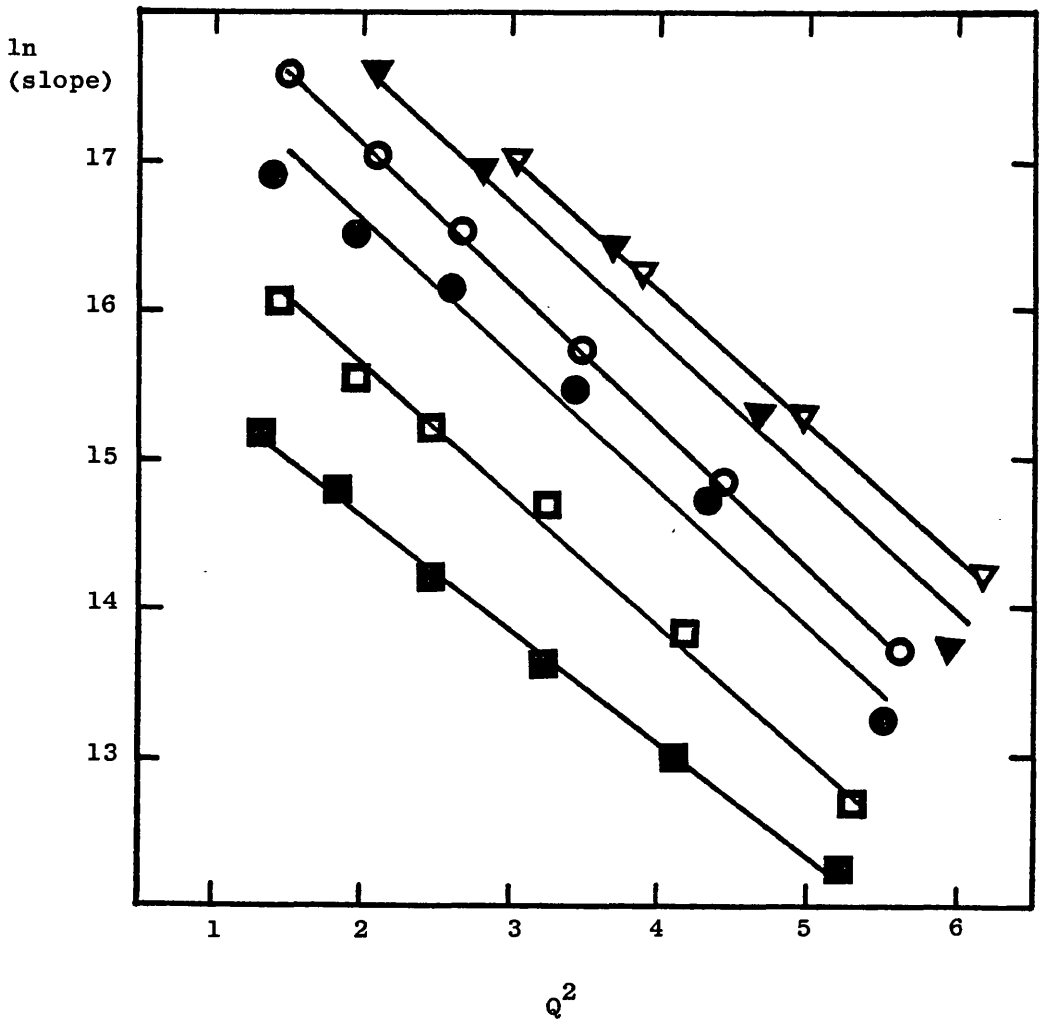

Fig. 4.2. Relationship between the rate of reaction of β-casein as diagnosed by limiting slope and the square of the charge on the protein molecule. ▽ represents 2mg/ml; ▼, 1.5mg/ml; ○, 1mg/ml; ●, 0.75mg/ml; □, 0.5mg/ml and ■, 0.25mg/ml.

relationship. This concept will be used throughout the discussion.

4.2 Soluble/precipitable protein equilibrium

In section 3.6.1 it was shown that not all of the casein in a given reaction mixture is precipitable. The extent of precipitation is dependent upon $[Ca^{2+}]$, $[\text{casein}]$ and temperature. These facts suggest that there is an equilibrium between soluble and precipitable protein.

$$Ca^{2+} + \text{casein} \rightleftharpoons \text{Ca-casein complex (soluble)} \rightleftharpoons \text{Ca-casein complex (precipitate)} \qquad (4.4)$$

Other caseins form "micelles" in the absence of Ca^{2+} (40,64,80). The kinetics of "micelle" formation also exhibited a lag phase which was adequately explained as the time required to form aggregable particles (149). Adopting this approach led to consideration that precipitable material may result from a formation of intermediate "micellar" aggregates. Thus, the first stage in the precipitation may be the production of oligomers, formed in equilibrium by aggregation of monomer casein molecules, and it is these oligomeric particles which form the actual precipitate. That is

$$n\ M_1 \rightleftharpoons M_n \rightarrow \text{precipitate} \qquad (4.5)$$

where M_1 represents monomeric casein and M_n is an oligomer composed of n units of α_{s1}-casein-Ca^{2+}. The equilibrium constant for formation of M_n is thus given by

$$K_n = \frac{[M_n]}{[M_1]^n} \qquad (4.6)$$

At equilibrium, the monomer concentration will be the concentration of soluble casein, while the precipitate concentration of protein gives a measure of $[M_n]$. The equilibrium constant K_n must be independent

of the initial monomer concentration of casein, so that if K_n is calculated according to

$$K_n = \left[\text{precipitate}\right] \left[\text{soluble protein}\right]^{-n} \qquad (4.7)$$

equation 4.7 it should not vary with protein concentration, although it may be Ca^{2+}-dependent. Since the equilibrium is dependent on the concentrations of Ca^{2+} and α_{s1}-casein, and since the kinetics of equilibration must be charge-dependent, it was reasonable to assume that a major factor in defining K_n was the charge on the monomer α_{s1}-casein-Ca^{2+} complex. When ln K_n, calculated from experimental results by the relationship in equation 4.7, was plotted against Q^2, straight lines were produced for individual casein concentrations, and varying $\left[Ca^{2+}\right]$, irrespective of the value of n which was chosen (see Fig. 4.3). However, plots for different casein concentrations were not superimposable. The correct value of n is that which allows the plots of ln K_n versus Q^2 for all the casein concentrations to be superimposed. Taking the experimental results of soluble casein at different α_{s1}-casein/Ca^{2+} combinations, K_n was calculated for all values of n from 2 to 16. The value of n which gave the best superimposition of the plots of ln K_n versus Q^2 was n = 8. The unit of aggregation was, as a result, taken to be octamer, so that the precipitation was taken to be:

$$8M_1 \rightleftharpoons M_8 \rightarrow \text{precipitate} \qquad (4.8)$$

Fig. 4.4 shows the plot of ln K_8 against Q^2 for the experimental points. In kinetic terms, such a reaction scheme, which nominally involves a collision between 8 particles to form the product is not feasible, and 8-body collision being a highly improbable event. Thus formation of octamer units must in reality involve a series of steps, such as

$$M_1 + M_1 \rightleftharpoons M_2 + M_1 \rightleftharpoons M_3 + M_1 \rightleftharpoons M_4 \ldots\ldots \rightleftharpoons M_8 \qquad (4.9)$$

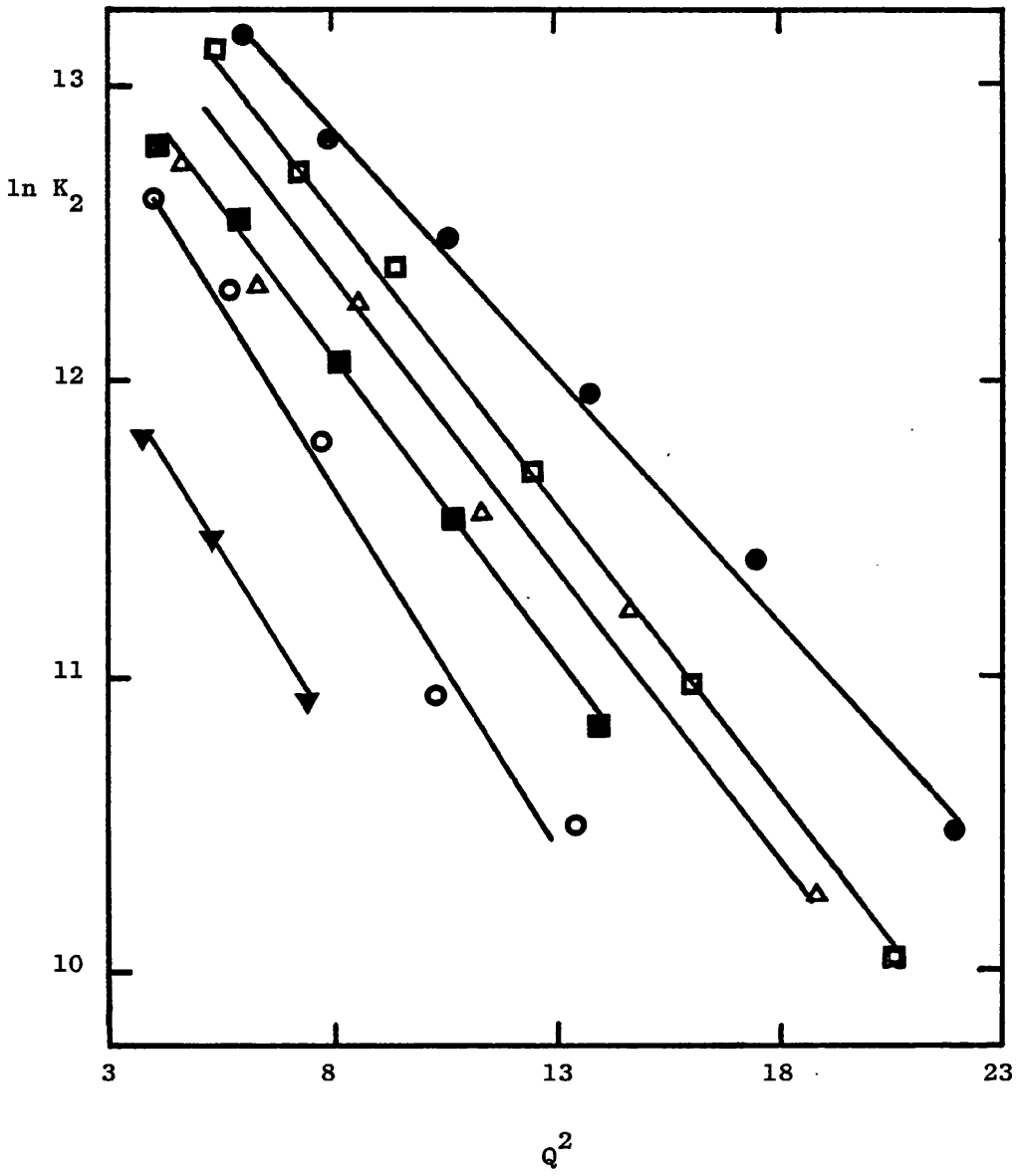

Fig. 4.3. Plot of the logarithm of the equilibrium constant K_n against Q^2 (n is the number of monomers in the precipitating unit, in this case 2) ● represents 2mg/ml; □, 1.5mg/ml; △, 1mg/ml; ■, 0.75mg/ml; ○, 0.5 mg/ml and ▼, 0.25mg/ml α_{s1}-casein.

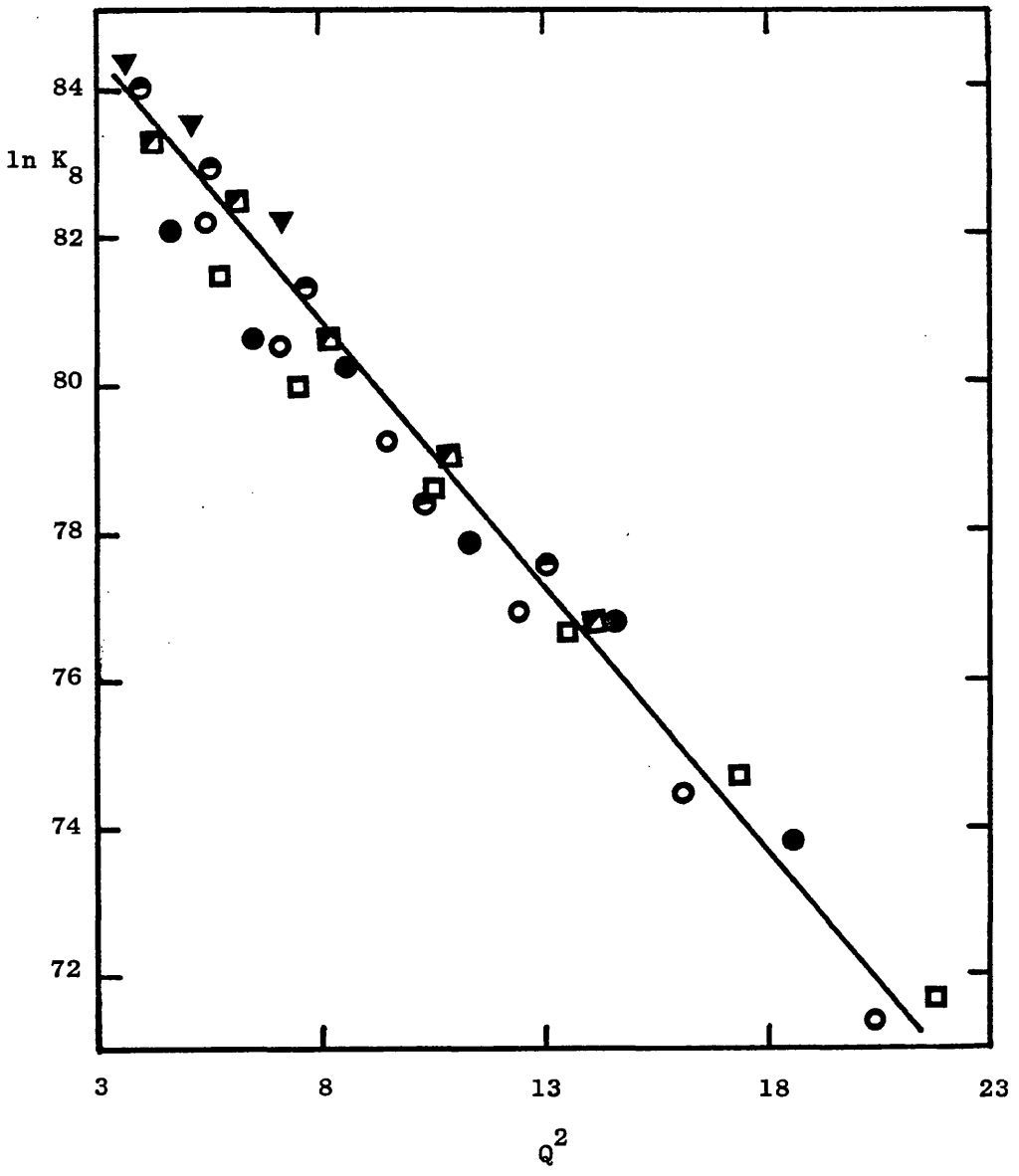

Fig. 4.4. Plot of the logarithm of the equilibrium constant K_n against Q^2 (n is the number of monomers in the precipitating unit, in this case 8) ◘ represents 2mg/ml; ○, 1.5mg/ml; ●, 1mg/ml; ◪, 0.75mg/ml; ◓, 0.5mg/ml and ▼, 0.25mg/ml α_{s1}-casein.

Other association steps such as $M_2 + M_2 \rightleftharpoons M_4$ and $M_4 + M_4 \rightleftharpoons M_8$ are also possible. A further simple scheme might be that given below.

$$M_1 + M_1 \overset{1}{\rightleftharpoons} M_2 + M_2 \overset{2}{\rightleftharpoons} M_4 + M_4 \overset{3}{\rightleftharpoons} M_8 \qquad (4.10)$$

In this, intermediate species such as M_3 and M_5 are not ruled out but merely omitted to simplify calculation. Each of the three association steps will have equilibrium constants K_1, K_2 and K_3

$$K_1 = \frac{[M_2]}{[M_1]^2} \qquad K_2 = \frac{[M_4]}{[M_2]^2} \qquad K_3 = \frac{[M_8]}{[M_4]^2} \qquad (4.11)$$

"Micellisation" ie $M \rightleftharpoons M_n$ must occur in this way, but the concentration of intermediates in such reactions is known to be low.

Combining the equations in 4.11 gives

$$[M_8]_{eq} = K_3 \; K_2^{\,2} \; K_1^{\,4} \; [M_1]_{eq}^{\,8} \qquad (4.12)$$

where $[M_8]_{eq} = [M_8]$ at equilibrium and $[M_1]_{eq} = [M_1]$ at equilibrium.

The soluble fraction is considered to be composed of all species M_n with $n < 8$ and for the above equilibria (equation 4.10) this will be $[M_1]_{eq} + [M_2]_{eq} + [M_4]_{eq}$. The precipitatable protein concentration is $[M_8]_{eq}$. It is possible to calculate the values of $K_1 - K_3$ by a more complex least-squares procedure, using the experimental values of the soluble fraction (see Section 4.4.1).

This type of analysis could not proceed for β-casein/Ca^{2+} combinations as a consequence of the very large percentage of β-casein which will precipitate in most of the Ca^{2+}/β-casein combinations used (see Section 3.6.3). Plots of ln K_n versus Q^2, where K_n is the equilibrium constant defined in equation 4.6, for all the β-casein/Ca^{2+} combinations were again constructed for values of n between 2 and 16. Unfortunately no value of n produced a single straight line for varying $[Ca^{2+}]$ and thereby eliminating any dependence upon the β-casein concentration. Thus, in

the case of β-casein the unit of aggregation could not be defined by the same method as for α_{s1}-casein.

4.3.1 Second stage of α_{s1}-casein aggregation

The second stage of α_{s1}-casein aggregation begins when the precipitable material is formed. By using the model of von Smoluchowski (see Section 1.7.2), it can be shown that the rate of change of weight average molecular weight, $d\overline{Mw}/dt$ is constant for this type of reaction in solution. In the reaction profiles of α_{s1}-casein association in the presence of Ca^{2+} which were obtained experimentally, a linear growth of $\overline{Mw}$ with time was observed only after an initial lag phase. It therefore is likely that a von Smoluchowski type of mechanism is being followed during the linear stage, since other possible aggregation mechanisms do not predict a linear growth.

Second order reaction kinetics were assumed in such a reaction process, giving the following expression for $\overline{Mw}$.

$$\overline{Mw} = M_o (1 + 2\nu_o k_s t) \qquad (4.13)$$

where M_o and ν_o are the molecular weight and concentration respectively of the aggregating species. Precipitable casein is therefore believed to be formed during the lag phase by the equilibrium described in the previous section, and precipitation subsequently occurs by a mechanism similar to the Smoluchowski model.

In the previous section the smallest unit taking part in precipitation was defined as M_8. Thus if M_o is the molecular weight of M_8^o and ν_o the concentration of M_8 ie C_8 then

$$\overline{Mw} = M_8^o (1 + 2 C_8 . k_s . t) \qquad (4.14)$$

Smaller species such as M_1, M_2 etc are also present in these particular solutions and must also be included in the expression for the

weight average molecular weight.

$$\overline{Mw} = w_1M_1 + w_2M_2 + w_4M_4 + w_8M_8$$

$$= w_1M_1 + w_2M_2 + w_4M_4 + w_8M_8^{o} (1 + 2 k_s C_8 t) \qquad (4.15)$$

where w_i is the weight fraction of species i and M_i the molecular weight. At equilibrium, w_1 - w_4 are constant and differentiating with respect to time gives

$$\frac{d\overline{Mw}}{dt} = w_8M_8^{o} \cdot 2 k_s \cdot C_8$$

$$= \frac{8C_8}{C_o} M_8^{o} \cdot 2 k_s \cdot C_8 \qquad (4.16)$$

where C_o is the total concentration of all species in solution. Rearranging equation 4.16 gives

$$\frac{d\overline{Mw}}{dt} \cdot C_o = 8C_8^{2} \cdot M_8^{o} \cdot 2 k_s \qquad (4.17)$$

Plotting ln $C_o \cdot d\overline{Mw}/dt$ versus ln C_8^{2} should therefore give a straight line of unit gradient. Such a plot for the aggregation reaction of Ca^{2+} with α_{s1}-casein is shown in Fig. 4.5. A series of closely parallel lines are distinguishable. Each line corresponds to a constant calcium ion concentration and has a gradient very close to one. Since the lines do not superimpose, it again appears that the aggregation constant is charge dependent. For all experiments, values of k_s were then calculated for equation 4.17 and these were then plotted against Q^2 to determine whether k_s itself was dependent upon the monomer charge. This is shown in Fig. 4.7. It is also evident from figure 4.7 that there is indeed a dependence of k_s upon Q^2 (although less so than for the initial equilibrium) such that k_s can be expressed in the form $\ln k_s = 14.8 - 0.154\ Q^2$.

The reaction mechanism is now describable as consisting of two stages, the first being a charge dependent equilibrium to form the

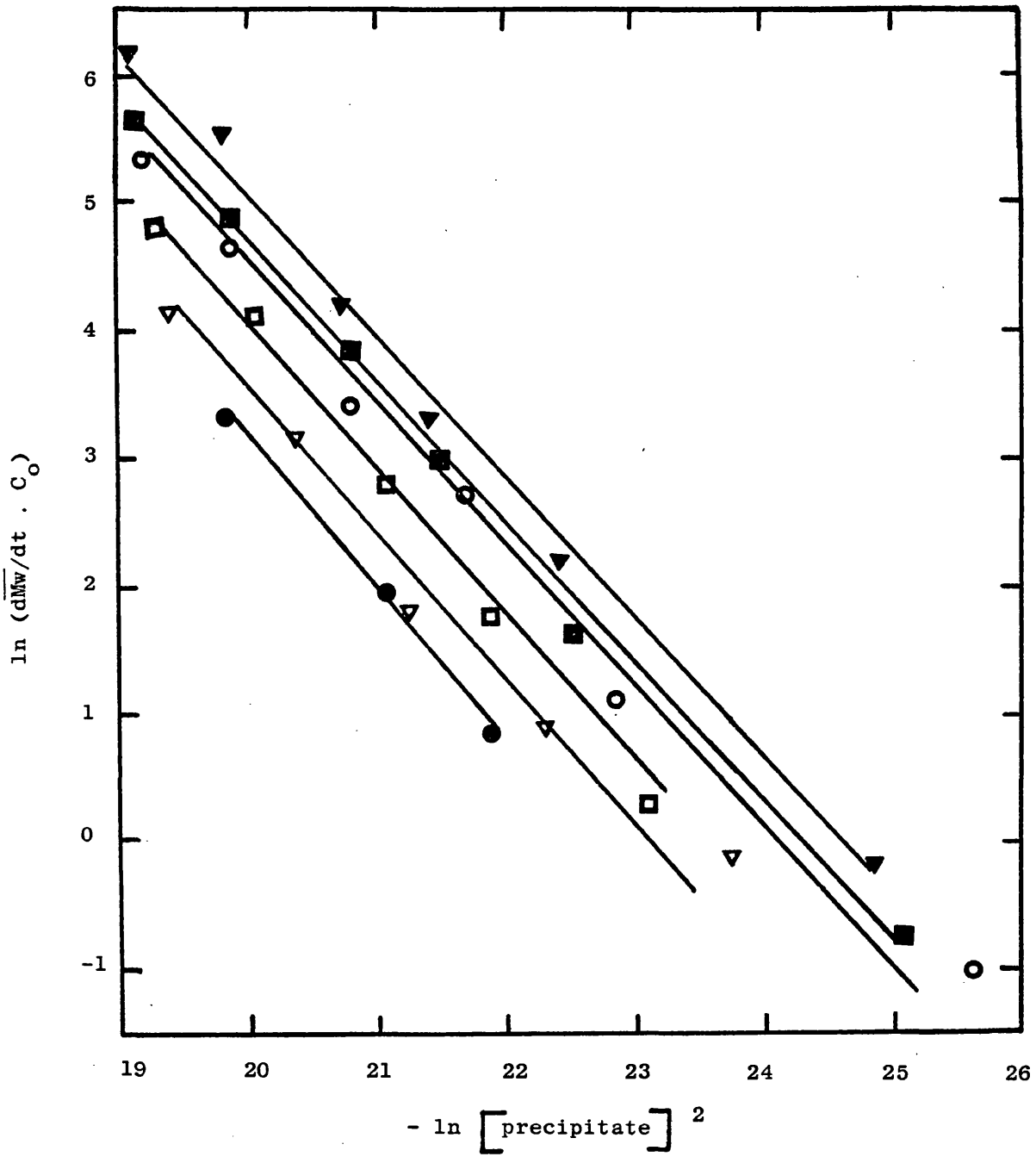

Fig. 4.5. Double logarithmic plot of the product of the limiting slope and [initial α_{s1}-casein] versus the square of the precipitate concentration of α_{s1}-casein. ▼, represents 9mM; ■, 8.5mM; O, 8mM; □, 7.5mM; ▽, 7mM and ●, 6.5mM Ca^{2+}.

precipitable fraction. In the second stage, this precipitatable fraction consisting of particles of the order of octamer then aggregates with a Smoluchowski rate constant k_s which is dependent upon Q^2. As equilibrium is being established the amount of precipitable material increases with time, thereby effectively increasing C_8 in equation 4.14, so that the value of $d\overline{Mw}/dt$ will start at a low value (since C_8 is low) and will gradually increase to a limiting value as C_8 approaches its equilibrium value.

The Smoluchowski rate constant, k_s is therefore a charge dependent variable which has values in the range 1.23×10^6 ℓ/mol sec to 1.65×10^5 ℓ/mol sec for the set of α_{s1}-casein and calcium concentrations used in our experiments at 23°C.

4.3.2 Second stage of β-casein aggregation

In the reaction profiles for the aggregation of β-casein upon addition of Ca^{2+} a linear growth of molecular weight with time is also observed. To ascertain whether the theory of von Smoluchowski is again applicable a plot of $\ln C_o \cdot d\overline{Mw}/dt$ versus $\ln C_8^2$ was constructed and is shown in Fig. 4.6.

The gradients of the lines which are obtained are all close to one: each line corresponding to a constant Ca^{2+} concentration. Using equation 4.17 the k_s value for each experiment was calculated and plotted against Q^2 (see Fig. 4.8). There is no longer a series of parallel lines but rather a single line, indicating that the lines obtained in the $\ln C_o \cdot d\overline{Mw}/dt$ versus $\ln C_8^2$ plot were distinct rather than superimposed due to charge effects. The rate constant k_s for the second stage of β-casein aggregation is therefore dependent upon Q^2 and the relationship is given by the expression $\ln k_s = 13.83 - 0.79\ Q^2$.

However, the value of C_8 used in this analysis is the experimentally

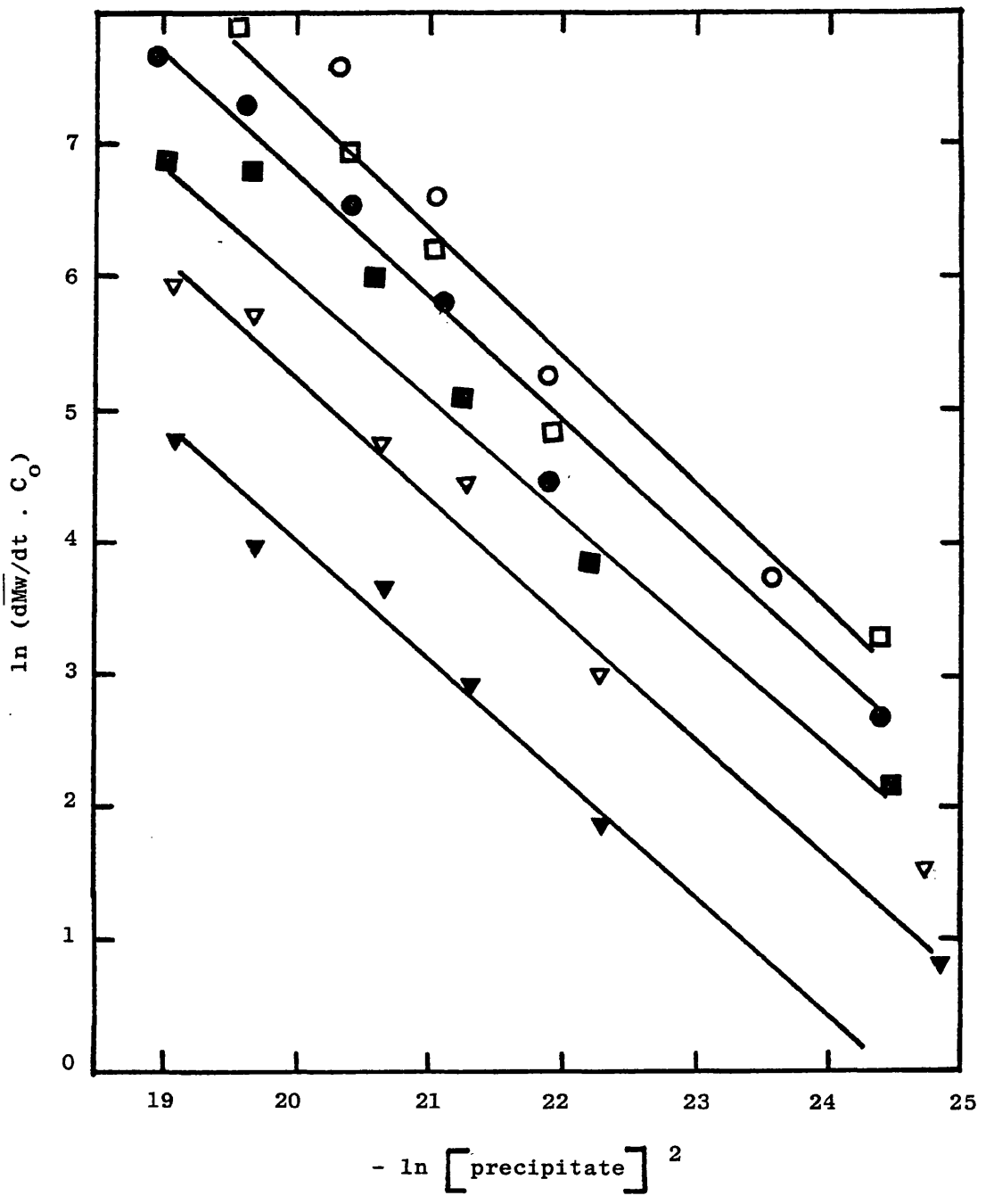

Fig. 4.6. Double logarithmic plot of the product of the limiting slope and the initial β-casein concentration versus the square of the precipitate concentration of β-casein. ○ represents 9mM; □, 8.5mM; ●, 8mM; ■, 7.5mM; ▽, 7mM and ▼, 6.5mM Ca^{2+}.

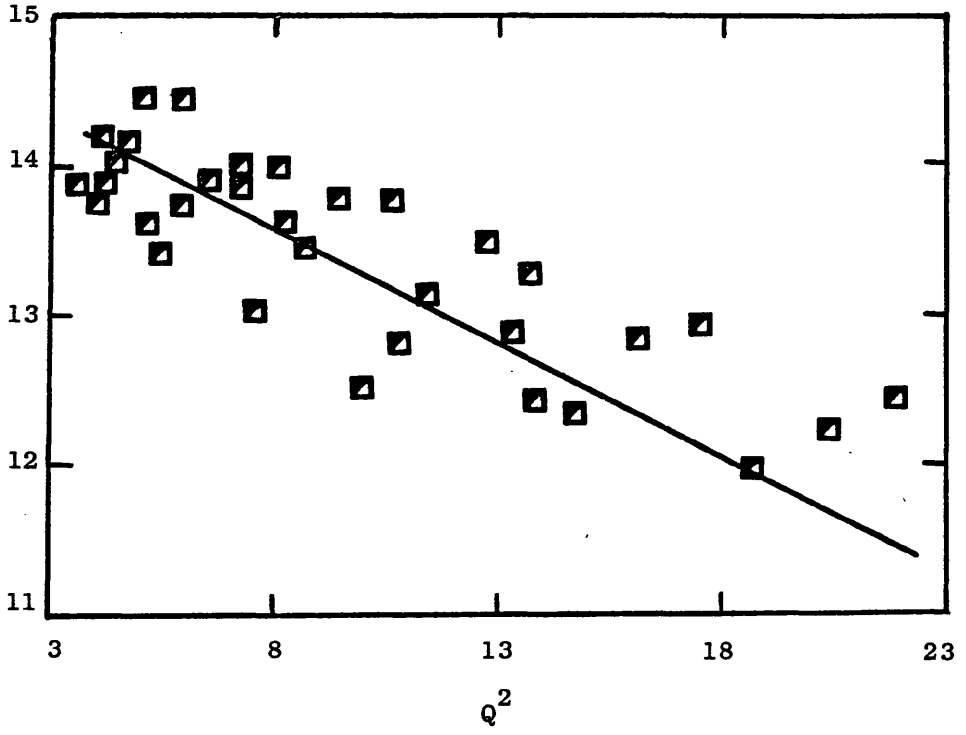

Fig. 4.7. Relationship between ln (k_s) and Q^2 for Ca^{2+}/ α_{s1}-casein combinations at 23°C.

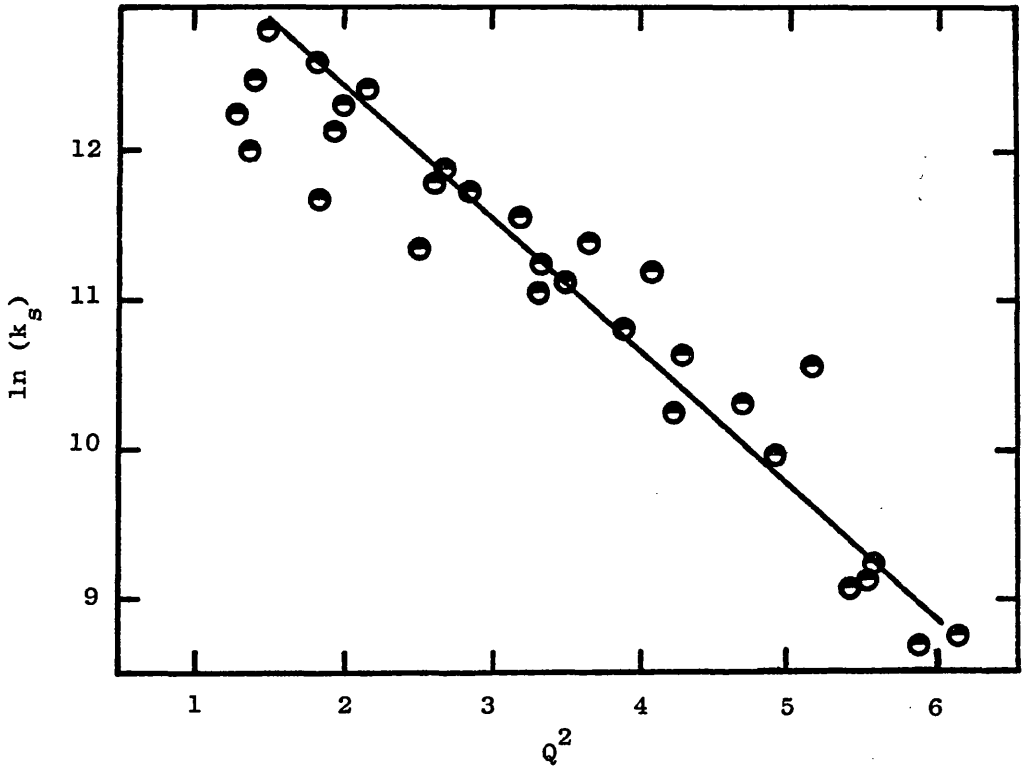

Fig. 4.8. Relationship between ln (k_s) and Q^2 for Ca^{2+}/ β-casein combinations at 40°C.

determined precipitate concentration, quoted in monomer rather than oligomer terms. Consequently the value of k_s obtained from this expression should be multiplied by an appropriate factor which is n^2 for an aggregating unit of M_n. The value of k_s ranges from $(4.1 \times 10^5) \times n^2$ ℓ/mol sec to $(5.8 \times 10^3)\ n^2$ ℓ/mol sec for the range of concentrations used in this work at 40°C. Unfortunately the large precipitate fractions of β-casein does not allow n to be determined satisfactorily.

4.4.1 First stage of α_{s1}-casein aggregation

Prior to the linear growth of molecular weight with time, it was hypothesized (section 4.2) that equilibrium is established between monomer and other intermediate species up to octamer. This equilibrium controls the rate of formation and the amount of precipitable protein. The rate determining step in this equilibrium therefore determines the length of the lag phase. In section 3.5.1 it was demonstrated that calcium binding was not the rate limiting step, and that the cause of the lag phase must be attributed to the protein.

In considering the equilibrium described in section 4.2 in kinetic terms it must be recognised that each equilibrium constant is composed of a forward and reverse rate constant, k_1 and k_2 respectively such that

$$K_{eq} = k_1 k_2^{-1} \qquad (4.18)$$

with the rate constants k being defined as

$$k = Ae^{-Ea/RT} \qquad (4.19)$$

where A is a constant, Ea is the activation energy, R is the gas constant and T is temperature. The rate of aggregation of α_{s1}-casein is shown in section 4.1 and also in other published work (156,169) to be dependent upon the square of the charge on the protein. This defines the energy

term in equation 4.19 as arising mainly from charge repulsion. The equilibrium constants K_n were also shown in section 4.2 to be a function of Q^2, as might be expected since combining equations 4.18 and 4.19 gives

$$\ln K_{eq} = (\ln A_1 - \ln A_2) - \frac{(E_1 - E_2)}{RT} \qquad (4.20)$$

so that simply K_{eq} is established to be of the form

$$K_{eq} = Ae^{-bQ^2/RT} \qquad (4.21)$$

An equilibrium constant K_8 which obeyed the relationship in equation 4.21 was found to be truly independent of α_{s1}-casein concentration (section 4.2). This equilibrium constant is that which applies to the formation of octamers from monomers. However direct formation of an octamer via an eight body collision is deemed highly improbable and several reaction steps are envisaged which lead to the final production of this species. The simple scheme postulated is that shown in equation 4.22, and is consists of a series of equilibria each of which have a constant associated with it.

$$8M_1 \overset{K_1}{\rightleftharpoons} 4M_2 \overset{K_2}{\rightleftharpoons} 2M_4 \overset{K_3}{\rightleftharpoons} M_8 \qquad (4.22)$$

Each of the individual equilibrium constants K_1, K_2 and K_3 for the above multiple equilibrium will have the same form as the overall equilibrium constant K_8 (Equation 4.21). (This was shown to be true in section 4.2). Six unknown constants, A_1, A_2, A_3, b_1, b_2 and b_3 are therefore generated which determine the values of the three equilibrium constants K_1, K_2 and K_3.

To try to determine suitable values for these constants the soluble and precipitate concentrations of α_{s1}-casein at equilibrium were used. The precipitate concentration of α_{s1}-casein gives a value of $[M_8]_{eq}$ which is related to $[M_1]_{eq}$ by equation 4.12, such that

$$\left[M_1\right]_{eq} = P_o / 8K_1^4 K_2^2 K_3 \qquad (4.23)$$

where P_o is the precipitate concentration. Using trial values of the six unknown constants it is possible to calculate $\left[M_1\right]$ at equilibrium from which the concentration of soluble material can also be calculated. The soluble fraction consists of all protein in monomer, dimer and tetramer form. The soluble concentration of protein (in monomer terms) S_o is related to $\left[M_1\right]_{eq}$ by the following equation

$$\begin{aligned} S_o &= \left[M_1\right] + 2\left[M_2\right] + 4\left[M_4\right] \\ &= \left[M_1\right]_{eq} + 2K_1\left[M_1\right]^2_{eq} + 4K_1^2K_2\left[M_1\right]^4_{eq} \end{aligned} \qquad (4.24)$$

A calculated value of S_o is obtained by inserting the values of the equilibrium constants derived from the trial constants in equation 4.24. This value is then compared to the experimental value of S_o. This procedure was then repeated, using the same trial values of the unknown constants, for all of the Ca^{2+}/α_{s1}-casein combinations studied. The differences between experimental and calculated values of S_o were then summed.

Recalculation of soluble concentrations was repeated with adjusted values of the unknown constants till a minimum was obtained in the function

$$\sum_{i=1}^{n} (S_o \text{ experimental} - S_o \text{ calculated})^2 \qquad (4.25)$$

where n is the number of Ca^{2+}/casein combinations studied. Three equilibrium constants, K_1, K_2 and K_3 can then be determined for a given amount of calcium binding to casein using the best values determined for the constants. The best values calculated for the constants were as follows

$A_1 = 8.134 \times 10^4$ $\quad A_2 = 4.136 \times 10^6$ $\quad A_3 = 5.101 \times 10^6$

$b_1 = 0.183$ $\quad b_2 = 0.067$ $\quad b_3 = 0.056$

This equilibrium determines the rate of formation of M_8 which then aggregates by a Smoluchowski type of mechanism. Since rate of production of precipitatable material is not constant but is dependent upon the equilibrium in the first stage of the reaction, the second stage must be modified to account for this. The concentration of M_8 for a given reaction can be calculated using the appropriate equilibrium constants K_1, K_2 and K_3. Equilibrium however is not established during the time intervals for which the kinetics were measured. The $[M_8]$ was still increasing when the reaction profile for a given reaction was completed. Hence $[M_8]$ at any time in the reaction is not approximately equal to $[M_8]_{eq}$ but must be continually adjusted as it approaches the equilibrium value.

Using the equilibrium first stage followed by the postulated Smoluchowski type of second stage as the overall mechanism for this aggregation reaction, attempts were then made to fit the reaction profiles individually. The overall reaction scheme adopted was

$$M_1 \overset{K_1}{\rightleftharpoons} M_2 \overset{K_2}{\rightleftharpoons} M_4 \overset{K_3}{\rightleftharpoons} M_8 \xrightarrow{k_s} \text{precipitate} \qquad (4.26)$$

The rate constant k_s for each Ca^{2+}/α_{s1}-casein combination was calculated as described in section 4.3 and the equilibrium constants, K_1, K_2 and K_3 used were those obtained from the best values of the constants A and b given above. Each equilibrium constant is composed of a forward and reverse rate constant which means that there are six rate constants to be determined.

By a similar procedure to that used in determining the values of A and b for the equilibrium constants, attempts were made to obtain individual rate constants. From equation 4.15 the weight average molecular weight for the system can be calculated as follows

$$\overline{Mw} = \frac{M_1^{o}\left[M_1\right]}{C_o} + \frac{2M_2^{o}\left[M_2\right]}{C_o} + \frac{4M_4^{o}\left[M_4\right]}{C_o} + \frac{8M_8^{o}}{C_o}\left(1 + 2\,k_s \,.\, C_8 .\, t\right) \qquad (4.27)$$

The concentrations of monomer, dimer and tetramer can be calculated numerically over successive time intervals from the equations

$$\frac{d\left[M_1\right]}{dt} = -\,k_1\left[M_1\right]^2 + 2\,k_2\left[M_2\right] \qquad (4.28)$$

$$\frac{d\left[M_2\right]}{dt} = \tfrac{1}{2}\,k_1\left[M_1\right]^2 + 2\,k_4\left[M_4\right] - k_2\left[M_2\right] - k_3\left[M_2\right]^2$$

$$\frac{d\left[M_4\right]}{dt} = \tfrac{1}{2}\,k_3\left[M_2\right]^2 - k_4\left[M_4\right] - k_5\left[M_4\right]^2 + 2\,k_6\left[M_8\right] \qquad (4.29)$$

where $K_1 = \frac{k_1}{k_2}$, $K_2 = \frac{k_3}{k_4}$ and $K_3 = \frac{k_5}{k_6}$ (4.30)

Using trial values of the rate constants k_1 to k_6 the changing concentrations of monomer, dimer and tetramer can be calculated from equations 4.28 to 4.30 by successively adding these increments in concentration to the starting values.

The concentration of M_8 is not constant but increases during the time for which any reaction profile was determined. Thus the equation derived for the Smoluchowski mechanism (equation 4.13) which gives the weight average molecular weight of aggregating species at a fixed concentration is no longer valid. Two research groups have independently obtained another equation for $\overline{Mw}$ by modifying equation 4.13 to allow input of aggregating material with time (170-172). The modified equation is

$$\overline{Mw} = Mw\,(o)\left(1 + 2\,k_s \frac{\int_o^t \left(\int_o^t \frac{d\left[M_8\right]}{dt}\right)^2 dt}{\int_o^t \frac{d\left[M_8\right]}{dt}\, dt}\right)$$

$$= Mw\ (o)\left(1 + 2\ k_s \int_o^t \frac{C_8^{\,2}}{C_8}\ dt \right) \qquad (4.31)$$

From the values of $[M_1]$, $[M_2]$ and $[M_4]$ calculated over successive small time intervals dt, values of $[M_8]$ can be obtained by

$$[M_8] = (C_o - [M_1] - 2\ [M_2] - 4\ [M_4]\ )/8 \qquad (4.32)$$

The rate of change of C_8 with time can then be determined such that integration (using Simpson's method) required in equation 4.31 can be performed using the appropriate value of C_8 at any given instant. Thus molecular weight averages for the particular reaction can be calculated as a function of time. The shape of the reaction profile produced by this calculation can be altered by adjusting the individual rate constants. The values of k_1 to k_6 which minimize the function

$$\sum_{i=1}^{96} (\overline{Mw}\ \text{experimental} - \overline{Mw}\ \text{calculated})^2 \qquad (4.33)$$

were then computed.

For any Ca^{2+}/casein combination a curve could be theoretically produced which fitted the individual reaction profile extremely well. For example with values of $k_1 = 8 \times 10^4$ ℓ/mol sec, k_2 = 1.56 ℓ/mol sec, $k_3 = 2.0 \times 10^6$ ℓ/mol sec, $k_4 = 3.7 \times 10^{-1}$ ℓ/mol sec, $k_5 = 2.5 \times 10^6$ ℓ/mol sec, and $k_6 = 3.5 \times 10^{-1}$ ℓ/mol sec, the experimental reaction profile for the reaction of 8.5mM Ca^{2+} with 1mg/ml α_{s1}-casein is very closely matched by that calculated. (see figure 4.9).

All the other reaction profiles could be fitted by this procedure but examination of the rate constants produced revealed no consistent trends in any of the rate constants for a given set of reaction conditions. In fact numerous combinations of k_1 to k_6 produced excellent curve fits for any given reaction. Changes in the individual rate constants could be compensated for by altering one or more of the other rate constants. It was not therefore very meaningful to attempt

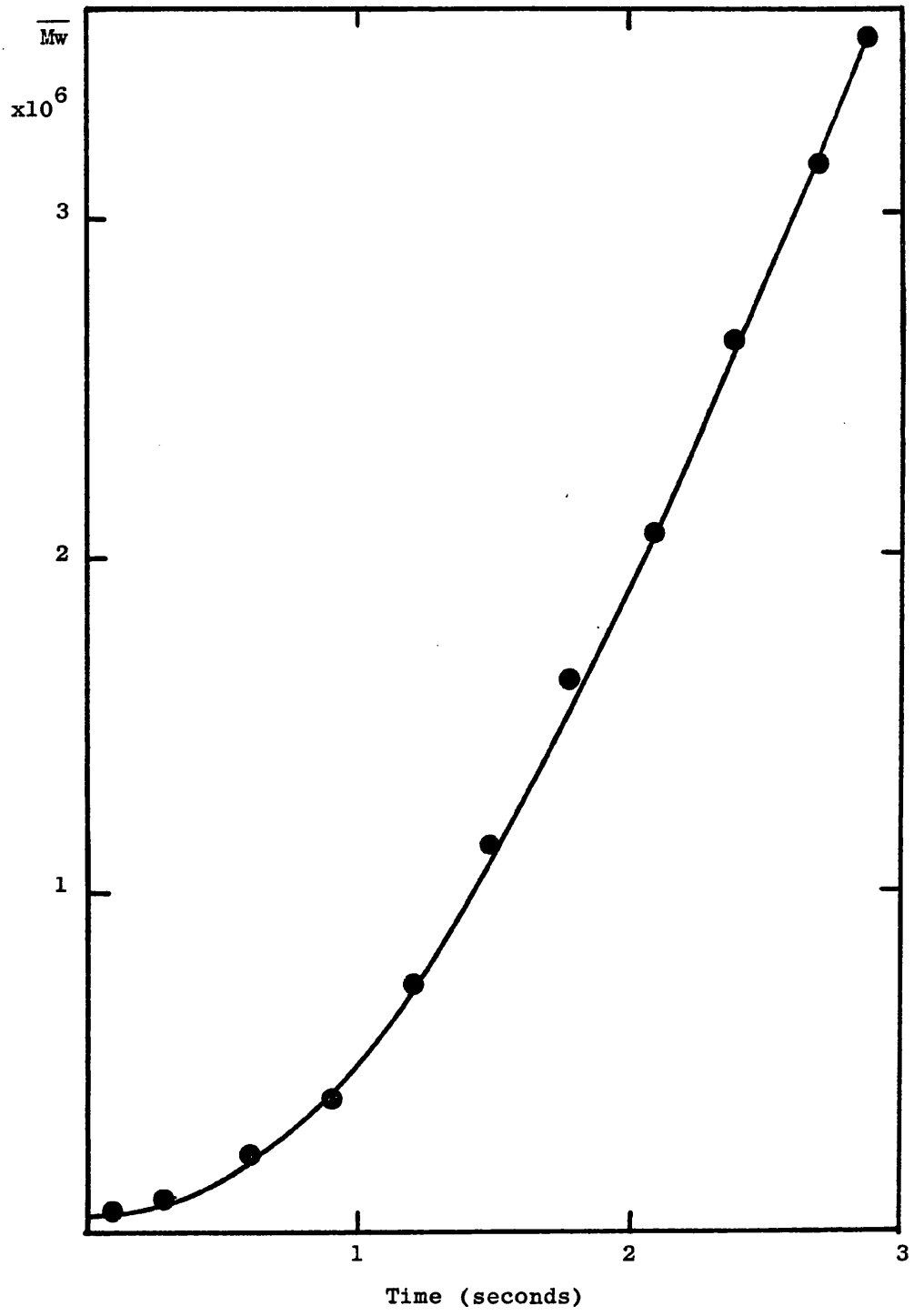

Fig. 4.9. Reaction profile for the aggregation of 1mg/ml α_{s1}-casein in the presence of 8.5mM Ca^{2+} at 23°C. ● represents experimental data points and the curve is calculated from the hypothetical mechanism.

to obtain best values for these six unknown quantities which were self compensating.

Although individually the rate constants exhibited no apparent trends related to reaction conditions, the first rate constant k_1 was always very much smaller than k_3 and k_5 by a factor of at least 10. This suggests that dimerization is the slowest step in the equilibrium in equation 4.22. Dimerization will require that the charge on each individual protein molecule has been reduced sufficiently for two molecules to associate, thereafter, the charge density is already sufficiently reduced to permit further aggregation.

The other forward rate constants k_3 and k_5 are large approaching the same order of magnitude as k_S. They are likely to be much less dependent on charge since the initial Ca^{2+} binding has already reduced the charge to permit dimerization and this is reflected in the lower values of b, the coefficient of Q^2 in the equilibrium constants K_2 and K_3.

Qualitatively, any reaction profile of α_{s1}-casein aggregation can be fitted by the theory proposed, i.e. an equilibrium which produces a precipitatable particle followed by aggregation according to a Smoluchowski type mechanism, and individual rate constants can be obtained which will reproduce the experimental curves very closely. Unfortunately the curve fit procedure has not produced rate constants which were consistent with changes in other parameters such as the calcium ion concentration etc. The mechanism proposed does however produce the correct overall shape of curve and successfully predicts the observed dependence of reaction rate on both Ca^{2+} and α_{s1}-casein concentration.

4.4.2 First stage of β-casein aggregation

The reaction profiles of β-casein aggregation show that the lag phase or first stage tends to be much shorter than the corresponding critical time for an α_{s1}-casein aggregation reaction. The weight average molecular weight is greater at a much earlier stage in the reaction (see Section 3.2).

The strong tendency for β-casein to undergo self association has been noted by several research groups (64-66). At 40°C micellar species formed from about 25 monomers seem to exist in 10 mg/ml solutions of β-casein (69). Although the maximum concentration of β-casein solutions used in this work was 2 mg/ml it does seem likely that monomer is not the predominant species in the β-casein solutions even before Ca^{2+} is added.

On this basis one might predict that a precipitable species is formed earlier in the course of the reaction. The precipitate fractions obtained for Ca^{2+}/β-casein combinations were much higher than for the equivalent α_{s1}-casein combinations. Apart from a few results at the lowest β-casein concentration, more than 75% of the β-casein generally precipitates.

Plots of the ln K_n versus Q^2, where n is the number of β-casein monomers in a precipitable unit and K_n is the equilibrium constant for formation of this precipitable oligomer (equation 4.7), could not be superimposed for any suitable value of n in contrast to the observations on α_{s1}-casein. This is a consequence of the high precipitate fractions obtained for the Ca^{2+}/β-casein combinations used. Only small differences in the precipitable $\left[\beta\text{-casein}\right]$ were obtained with different calcium concentrations (Section 3.6.3) which means that the precipitate concentration within a single β-casein concentration would appear to have little dependence upon charge, and is apparently

defined more by other factors.

Hence, the appropriate aggregating unit for β-casein could not be determined by the same method used for α_{s1}-casein although the reaction can be qualitatively explained in a similar manner to the α_{s1}-casein precipitation.

Since the second stage of β-casein aggregation could be fitted well to the von Smoluchowski theory of aggregation with an oligomer as the precipitable unit, the lag phase might well be an equilibrium in which this oligomer is formed. The exact number of β-casein monomers which constitute the required oligomeric state could once again be eight, but this cannot be established from the data available. If the precipitable β-casein unit is not in fact octamer but some other oligomeric state then the difference in the initial stages of β-casein compared to α_{s1}-casein could be explained. Alternatively, if β-casein is not monomeric at the initial point of kinetic measurement but rather the equilibrium has been shifted towards dimer or one of the other pre-precipitable oligomers, then the shorter first stage typical of β-casein reaction profiles would be predicted.

4.5.1 Temperature - Dependence of the α_{s1}-casein aggregation

The results shown in sections 3.3.1 and 3.3.3 indicate that the reaction rate, as measured by t_c and limiting slope, increases as the temperature of the reaction is increased. However, it was also shown that these two functions did not increase to the same extent. The critical time seems to be more temperature-dependent than is the limiting slope. The binding of Ca^{2+} to α_{s1}-casein is also known to be temperature-dependent (58). Thus, it is to be expected that the rate of equilibration and aggregation will not only change with changing temperature, but that this change will be enhanced by the effect of

temperature on Ca^{2+}-binding and hence Q^2, for the protein-Ca^{2+} complexes.

Accordingly, Q^2 for the α_{s1}-casein/Ca^{2+} combinations used as functions of temperature were calculated using the temperature-dependence of K^* and N, the binding parameters, given by Dalgleish and Parker (58), and the plot of the logarithm of the limiting slope against Q^2 was constructed (Fig. 4.10). The reaction rate appears to be almost linear with Q^2, and therefore it seems that, once again, the dominant factor in the temperature-dependence of the reaction rate is the charge carried by the casein/Ca^{2+} complex.

In section 4.3, it was established that the limiting slope, $\overline{dMw}/dt$, is defined by two factors, namely the concentration of precipitable protein and the rate constant for the Smoluchowski aggregation. Both of these factors are charge-dependent, as has been shown in sections 4.3.1 and 4.4.1. Thus, although the almost linear plot of ln (limiting slope) against Q^2 confirms the dependence of the overall reaction upon the charge of the complex, the two contributions to the limiting slope require to be defined.

To this end, data gathered from the results at 23°C was used to calculate the temperature dependence of the reaction. Since the form of the equilibrium constant K_8 is given by

$$\ln K_8 = \ln A - \frac{b\,Q^2}{T} \qquad (4.34)$$

it can be calculated from figure 4.4 that

$$\ln K_8 = 83.9 - 195.06\ Q^2/T \qquad (4.35)$$

Similarly from figure 4.7, it can be calculated that k_s has the form

$$k_s = 14.8 - 45.58\ Q^2/T \qquad (4.36)$$

For a reaction at a particular temperature, the protein concentration, the calcium concentration and the binding constants K^* and

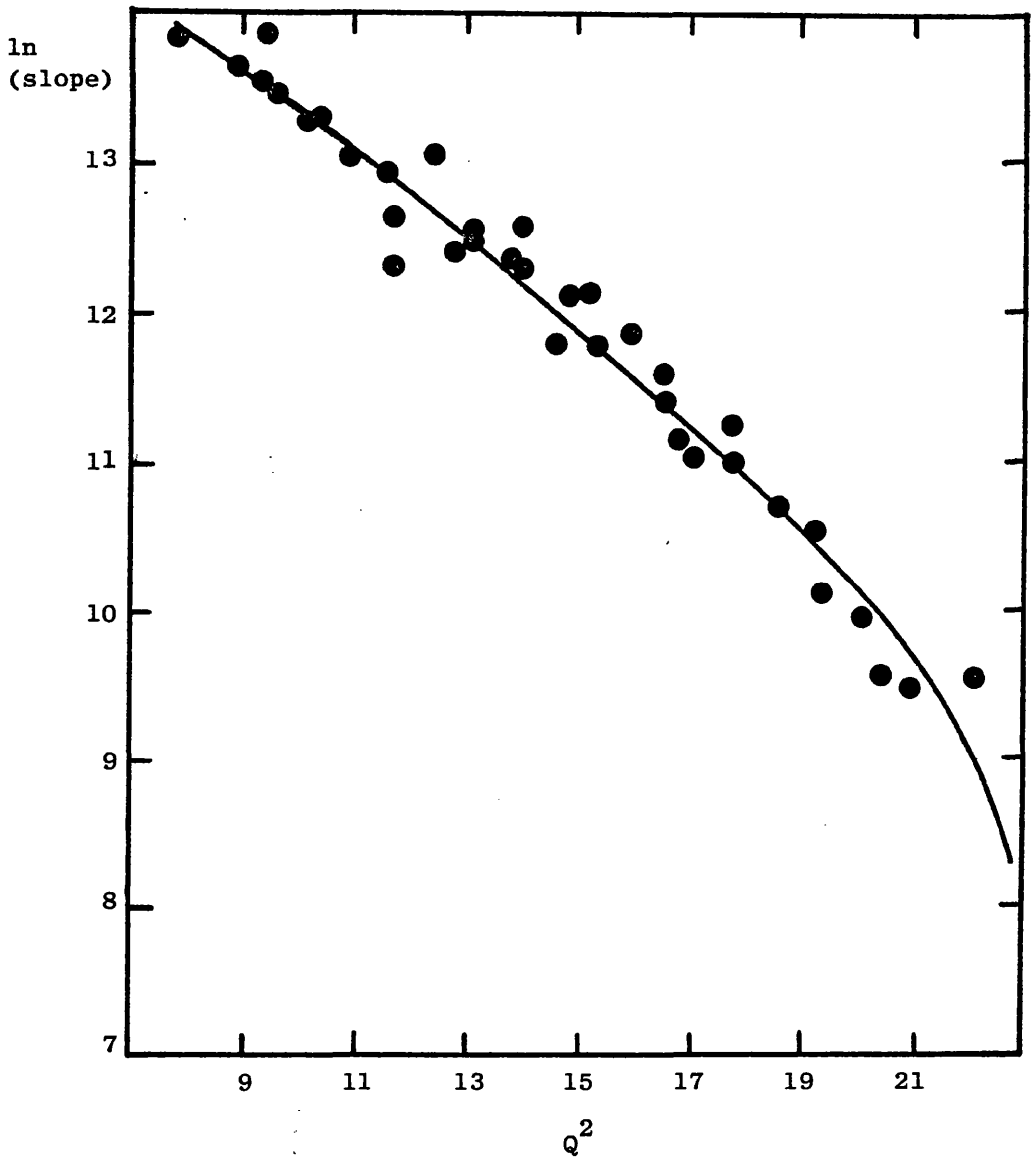

Fig. 4.10. Relationship between the rate of reaction as diagnosed by the limiting slope and the square of the average charge per α_{s1}-casein molecule (The charge differences are the result of changing the temperature). ($[Ca^{2+}]$ = 7mM and $[\alpha_{s1}\text{-casein}]$ = 1mg/ml).

N are known. From this information, $\bar{\nu}$ and Q^2 can be calculated and these in turn give values for K_8 and k_s using equations 4.35 and 4.36. The concentration of aggregating material, M_8 can then be found from K_8 and the protein concentration. (Since here a value of M_8 only is required, it makes no difference to the result if a single equilibrium constant or the multiple equilibrium constants K_1-K_3 are used, the results in calculating M_8 are the same).

At any particular temperature the values of M_8 and k_s calculated are inserted into equation 4.16 to give a value of the limiting slope. This calculation was repeated for all of the temperatures which were used in the experiments, thereby allowing a theoretical dependence of limiting slope upon temperature to be defined. To compare this with the experimental results, the logarithm of the observed limiting slope was plotted against reciprocal temperature as an Arrhenius plot (Fig. 4.11). It was pointed out earlier (Section 3.3.1) that this plot was not linear, as would be expected for a simple reaction, but showed a distinct curvature. The calculated temperature dependence of the limiting slope reproduces this curvature well, and gives a generally good fit to the experimental points, with the possible exception of the results at the lowest temperatures used.

The calculation of the theoretical curve involved no other assumption than that the barrier to aggregation between individual α_{s1}-casein-Ca^{2+} molecules or particles is generated by the charge on these molecules, so that the "activation energy" for the aggregation is defined only in these terms, and does not involve any other interactions. The close fit between the calculated curve and the experimental points can be taken as a good indication that this proposed mechanism is valid. This being so, the different temperature-dependence of the two stages of the reaction may be readily explained. The first-stage equilibrium is more dependent upon the

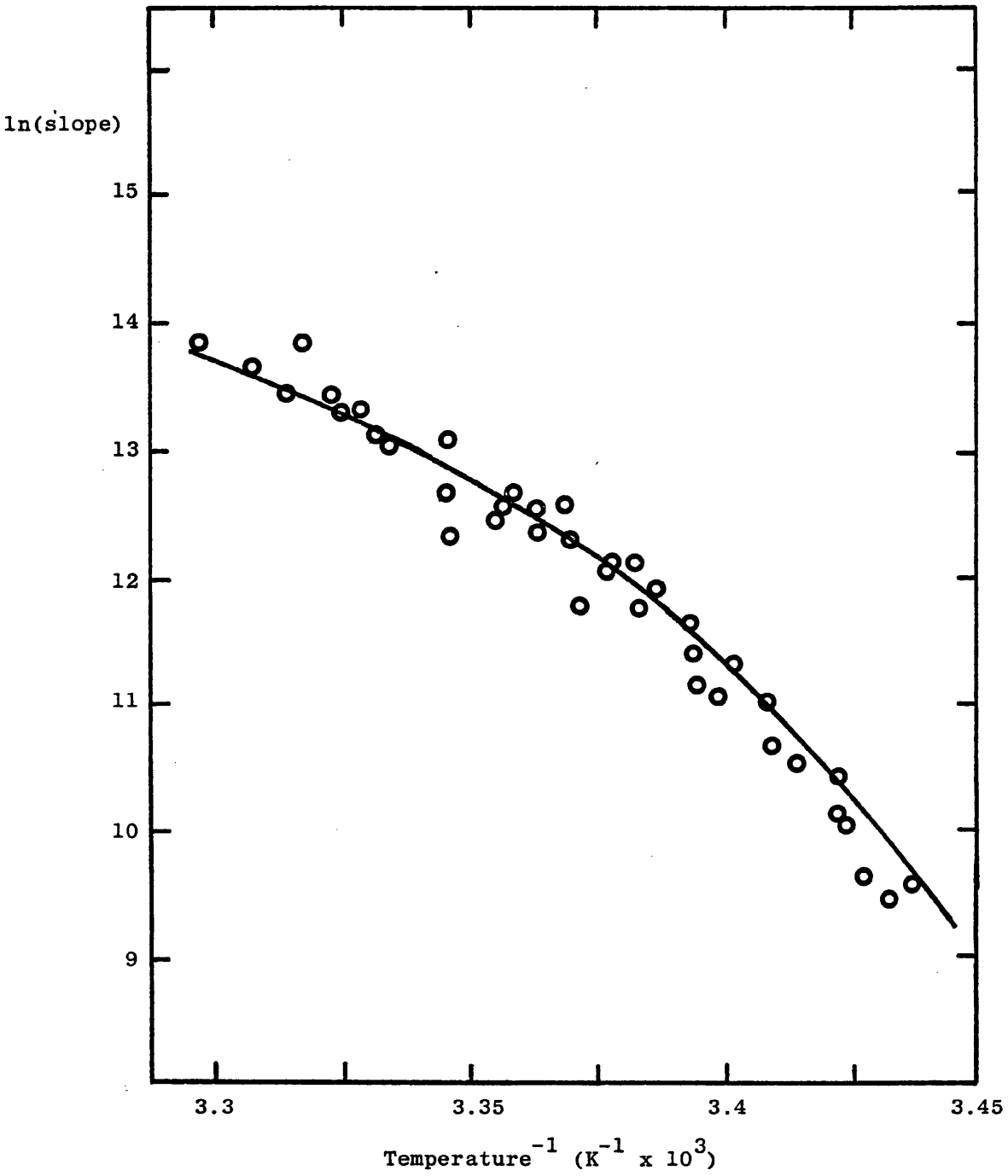

Fig. 4.11. Arrhenius plot of reaction rate as diagnosed by the limiting slope for 7mM Ca^{2+}/1mg/ml α_{s1}-casein.
O represents experimental results while the curve drawn is that calculated as described in Section 4.7.1.

protein charge than is the second stage, as shown by the coefficients of the Q^2 term in equations 4.35 and 4.36. As Q^2 changes with temperature, the greater effect will occur during the first stage of the reaction, as experiments demonstrated. (Notice that it will be the forward rate constant of the equilibrium which is the more charge-dependent, rather than the reverse rate constant. Thus the rate of equilibration, as well as the extent of precipitate formation, will be charge dependent to the extent shown in equation 4.35).

On the basis of the simple Arrhenius plot, the change of limiting slope with temperature gives apparent activation energies of more than 100 kJ/mole. This is a strangely large figure since the apparent activation energy has now been demonstrated to be dependent only on the change in the binding of Ca^{2+} to the protein. This is an equilibrium with a relatively low heat of reaction, namely 10 kJ/mole (58). Two factors are responsible for the apparently large activation energy. The first is the necessity to bind several ions of calcium to the individual protein molecules, which is an interactive process via the binding parameter N, thereby causing the apparent activation energy to be multiplied. The second is that at the extents of binding where rapid precipitation is observed ($\bar{\nu}$ = 8-10) a fairly small change in $\bar{\nu}$ can make a large change in Q^2, and hence in k_s and K_8. For example, if $\bar{\nu}$ increases from 9 to 9.5, Q^2 decreases from 25 to 16). Combining these two factors produces the high apparent activation energies which are found experimentally.

4.5.2. Temperature-Dependence of β-casein aggregation

It was shown in section 4.4 that the aggregation of β-casein appeared to be less charge dependent than was the case for α_{s1}-casein, certainly where the fraction of precipitable protein was concerned. The

limiting rate of aggregation was, however, strongly charge dependent (see Fig. 4.2). In the previous section the temperature-dependence of α_{s1}-casein/Ca^{2+} aggregation was successfully predicted by calculating the equilibrium constant for precipitate formation and the Smoluchowski constant from values obtained at 23°C. Such a calculation is not possible for β-casein mixtures because n, the size of oligomer particles taking part in the final aggregation step could not be defined. Therefore only a qualitative discussion of the temperature-dependence of the β-casein precipitation is possible.

Qualitatively, the temperature-dependence of β-casein is similar to that of α_{s1}-casein. The limiting slope, $d\bar{M}_w/dt$, for the reactions increases with temperature, and the values of t_c decrease with temperature, the decrease in t_c being greater than the increase in limiting slope, as for α_{s1}-casein (Fig. 3.14). The relative change of t_c and limiting slope is very marked for β-casein. Indeed, at the highest temperatures studied, the initial stage of the reaction seems to disappear altogether, and only a Smoluchowski-type aggregation is present. In α_{s1}-casein aggregation reactions the initial phase was definately present at all temperatures, and was never obscured by any change in reaction conditions. This implies that under some conditions, β-casein "pre-aggregated" into oligomeric micellar units. Such "pre-aggregated" units are formed by mainly hydrophobic interactions. Addition of Ca^{2+} then neutralizes the surface charge on these micellar units, allowing further aggregation. The extent of micellisation prior to Ca^{2+} addition depends upon the concentration of β-casein and temperature, as shown by Evans et al (69).

In contrast to α_{s1}-casein, the aggregation of β-casein can be envisaged as follows. Prior to the addition of Ca^{2+}, β-casein exists in a partially aggregated state, the degree of polymerization being dependent

upon concentration and temperature. When Ca^{2+} is added, the β-casein requires time to form units of precipitable material, if such units are not already present in the solution. These units then aggregate by the charge dependent Smoluchowski mechanism. The change in t_c with temperature therefore reflects not only the effect of change in calcium binding but also the change in initial aggregation state of the protein. From the results on the binding of Ca^{2+} to β-casein (74), the binding is more temperature-dependent than is the case for α_{s1}-casein (58). Furthermore, since the initial charge on β-casein is lower, small changes in $\bar{\nu}$ will affect β-casein more than α_{s1}-casein. The aggregation of β-casein in the absence of Ca^{2+} is also highly temperature dependent (69), so that the degree of oligomerization rises sharply with temperature.

All of these causes contribute to the high temperature-dependence of the observed aggregation mechanism. A full description, however, requires knowledge of the aggregation state of the β-casein under all of the experimental conditions used in this work. This must form part of a separate study.

4.6 General discussion

In the preceeding sections it has been shown that a mechanism based upon charge interaction can be used to completely describe the aggregation and precipitation of α_{s1}-casein in the presence of Ca^{2+}. This mechanism consists of two stages. During the first stage precipitable particles are formed via a monomer-octamer equilibrium, and these precipitable particles further aggregate in the second stage. This mechanism will predict that virtually no casein will precipitate until the protein charge has been sufficiently reduced. Although the charge on the protein is reduced by the binding of Ca^{2+}, there will be concentrations of Ca^{2+} below which precipitation will not be observed.

This is in accord with the experimental observations of this research group, and published work (54,56,58).

Even when the concentration of Ca^{2+} is considerably in excess of the critical concentration required to initiate precipitation, the first-stage equilibrium implies that not all of the α_{s1}-casein is precipitable. Although this has complicated the analysis of the kinetics of molecular weight growth, it is essential to consider this factor. The values obtained from the literature for the extent of precipitation of α_{s1}-casein at given concentrations of Ca^{2+} are not wholly self-consistent. However, it is true to say that results from this laboratory over a period of years, and not restricted to the work done for this thesis, confirm that the proportion of soluble casein diminishes, but never vanishes, even at high concentrations of Ca^{2+} (58,149).

A rather different interpretation of the kinetics of α_{s1}-casein-Ca^{2+} precipitation was applied in earlier work from this laboratory (149) than has been presented in this thesis. This previous interpretation was based on the concept of the α_{s1}-casein-Ca^{2+} monomer as a polyfunctional entity, and sought to use the principles of polymerization of such particles to explain the kinetics. However, this approach was abandoned for several reasons. First, only the precipitable fraction of material was considered in the kinetic interpretation, the non-precipitable material being ignored. Second, the nature of a "functionality" was obscure, and third, the way in which the theory had to be treated gave rise to a mechanism containing too many arbitrary constants to be satisfactory. Also, the true polyfunctional-type mechanism does not predict the linear second-stage growth of molecular weight in the reaction profile. It should perhaps be pointed out that the application of Avrami-type nucleation-growth kinetics has also been

studied in relation to the precipitation of the α_{s1}-casein-Ca^{2+} complex, and have been found not to apply. Generally, the failure of these theories of polymerization to explain the empirical observations can be ascribed to the certain following features of the reaction. The monomers are large and complex entities compared with the standard monomers in general polymerization reactions and many polymerizations occur in the bulk phase unlike the dilute solutions in which the casein aggregation kinetics were determined.

The charge-dependent model of the reaction has the virtue of simplicity, and is in accord with models of colloid flocculation (170, 171, 172, 152). The applicability of such models with reference to caseins has been discussed for many years, although few conclusions have been drawn until now. This has occurred largely because of a lack of appreciation and detailed study of the role of bound calcium ions. Published work on the binding isotherms was not extensive until the full study of temperature-dependence was made (58). Also, surprisingly few attempts were ever made to correlate precipitation of α_{s1}-casein with the binding of Ca^{2+}. Only qualitative studies of this interaction have been made. The work described in the preceeding chapters has attempted to make quantitative assessment of the effect of the binding of Ca^{2+} upon the charge on the protein, and hence the changes in precipitability and rate of precipitation of the protein. It appears from the results that a colloid model is perfectly adequate to explain the behaviour of α_{s1}-casein in all aspects of its precipitation, if full assessment of Ca^{2+} binding is made.

This does not appear to be true for β-casein, at least during the first stage of its aggregation. The different natures of the two proteins accounts for this diversity. Apart from short sections, the

two proteins are not homologous, and show different properties. It is in fact rather misleading that they should be named as if strong similarities existed. It appears that β-casein is considerably more amphiphilic in nature than α_{s1}-casein, and in particular it has a highly hydrophobic C-terminal region. The tendency of β-casein to form "micellar" aggregates even in the absence of Ca^{2+} is well established (64,69), in contrast to α_{s1}-casein, which aggregates only weakly in the absence of Ca^{2+} (40,44). The interpretation of observations on β-casein are complicated by this preaggregation. Whereas the first stage of the aggregation of α_{s1}-casein-Ca^{2+} represents the formation of precipitable particles from monomeric units, the first stage of β-casein-Ca^{2+} aggregation is probably extended growth of previously partly formed "micellar" units, the size of which appears to be variable, especially with temperature. Thereafter, the two proteins behave similarly, or relatively so. Thus the dominant factor controlling the pre-aggregation of β-casein is not the charge, but rather the tendency of the C-terminals of the proteins to interact via hydrophobic interactions.

Both proteins show a charge-dependent second-stage precipitation, and the difference between them is much less than in the first stage of the reaction. This can be reasonably explained by hypothesizing the structure of the aggregating particles. Once the precipitating units have been formed, both caseins will exist as particles carrying some surface charge, since the particles will form to minimize the number of hydrophobic residues in contact with solvent. Therefore even β-casein will now exist in a state where charge interactions will be dominant where surface to surface contact between aggregating particles is concerned. Thus alteration of this surface charge by the binding of Ca^{2+} will be of great importance.

This work has demonstrated the general validity of the charge-dependent model of casein interactions. As far as α_{s1}-casein is concerned this is the completed picture whereas considerable additional experimentation will be required before the complete details of the β-casein reaction and numerical values of the rate and equilibrium constants can be fully determined.

Appendix 1:- Weight average molecular weight for a Smoluchowski aggregation.

An aggregation reaction is considered where indefinite self-association can occur. If the initial condition is that there is a concentration ν_o of monomer, having molecular weight M_o, which is allowed to aggregate, the weight average molecular weight is given by:

$$\overline{Mw} = \frac{\Sigma M_x^2 n_x}{\Sigma M_x n_x} = \frac{\Sigma x^2 M_o \nu_x}{\Sigma x \nu_x}$$

where $M_x = xM_o$ and ν_x is the concentration term used instead of n_x which is the number fraction. From von Smoluchowski

$$\Sigma x \nu_x = \Sigma x \frac{\nu_o (k_s \nu_o t)^{x-1}}{(1 + k_s \nu_o t)^{x+1}}$$

Let $a = k_s \nu_o t$

$$\Sigma x \nu_x = \Sigma x \frac{\nu_o a^{x-1}}{(1 + a)^{x+1}} = \frac{\nu_o}{(1 + a)^2} \Sigma x \left(\frac{a}{1 + a}\right)^{x-1}$$

Using the summation $\Sigma x b^{x-1} = 1 + 2b + 3b^2 \ldots\ldots = \left(\frac{1}{1 - b}\right)^2$

and setting $b = a(1 + a)^{-1}$ gives

$$\Sigma x \nu_x = \frac{\nu_o}{(1 + a)^2} \left(\frac{1}{1 - b}\right)^2$$

Note that $(1 - b) = 1 - \frac{a}{1 + a} = \frac{1}{1 + a}$ therefore

$$\Sigma x \nu_x = \frac{\nu_o}{(1 + a)^2} \frac{1}{(1/1 + a)^2} = \nu_o$$

Similarly $\Sigma x^2 \nu_x = \nu_o \Sigma x^2 \frac{a^{x-1}}{(1 + a)^{x+1}}$

$$= \frac{\nu_o}{(1 + a)^2} \Sigma x^2 \left(\frac{a}{1 + a}\right)^{i-1}$$

Using the standard summation

$$\sum_{x=1}^{\infty} x^2 b^{x-1} = 1 + 4b + 9b^2 + 16b^3 \ldots\ldots = \frac{(1 + b)}{(1 - b)^3}$$

and the algebraic substitution of

$$1 + b = 1 + \frac{a}{(1 + a)} = \frac{1 + 2a}{1 + a}$$

then $$\Sigma x^2 \nu_x = \frac{\nu_o (1 + 2a) / (1 + a)}{(1 + a)^2 (1 - b)^3} = \nu_o (1 + 2a)$$

Thus $$\overline{Mw} = \frac{M_o \nu_o (1 + 2a)}{\nu_o} = M_o (1 + 2k_s \nu_o t)$$

TABLE 1: The reaction rates for several calcium and α_{s1}-casein concentration combinations at 23°C, as defined by the logarithms of limiting slope and critical time (t_c). The negative logarithm of the precipitate concentration of α_{s1}-casein is in terms of equivalent monomer concentration and the square of the average charge on the monomer (Q^2) is calculated by the method given in Section 2.4

Ca^{2+} (mM)	α_{s1}-casein (μM)	ln limiting slope	ln (t_c)	- ln ppt concn	Q^2
9.0	84.7	15.52	-1.46	9.51	5.88
8.5	84.7	14.98	-1.09	9.53	7.95
8.0	84.7	14.74	-0.90	9.57	10.49
7.5	84.7	14.11	-0.04	9.63	13.57
7.0	84.7	13.53	0.30	9.72	17.32
6.5	84.7	12.70	0.95	9.93	21.87
9.0	63.5	15.11	-0.96	9.87	5.20
8.5	63.5	14.53	-0.67	9.91	7.12
8.0	63.5	14.34	-0.59	9.93	9.49
7.5	63.5	13.73	0.14	10.05	12.40
7.0	63.5	12.78	0.75	10.21	15.94
6.5	63.5	11.57	2.14	10.55	20.24
9.0	42.4	14.19	-0.29	10.33	4.54
8.5	42.4	13.86	-0.04	10.39	6.32
8.0	42.4	13.41	0.17	10.40	8.53
7.5	42.4	12.81	0.95	10.54	11.25
7.0	42.4	11.84	1.91	10.63	14.57
6.5	42.4	10.83	2.92	10.95	18.63
9.0	31.8	13.56	0.34	10.69	4.22
8.5	31.8	13.31	0.49	10.72	5.93
8.0	31.8	13.03	0.54	10.82	8.06
7.5	31.8	12.00	1.81	10.94	10.68
7.0	31.8	11.20	2.55	11.17	13.90
9.0	21.2	12.85	1.22	11.18	3.91
8.5	21.2	12.34	1.37	11.25	5.55
8.0	21.2	11.74	1.90	11.38	7.59
7.5	21.2	10.93	2.82	11.54	10.13

TABLE 1 CONTINUED

Ca^{2+} (mM)	α_{s1}-casein (μM)	ln limiting slope	ln (t_c)	- ln ppt concn	Q^2
7.0	21.2	10.58	3.44	11.88	13.24
9.0	10.6	11.22	2.88	12.41	3.61
8.5	10.6	10.68	3.05	12.54	5.17
8.0	10.6	10.40	3.29	12.82	7.14

TABLE 2: The reaction rates for several calcium and β-casein concentration combinations at 40°C, as defined by the logarithms of limiting slope and critical time (t_c). The negative logarithm of the precipitate concentration of β-casein is in terms of equivalent monomer concentration and the square of the average charge on the monomer (Q^2) is calculated by the method given in Section 2.4

Ca^{2+} (mM)	β-casein (μM)	ln limiting slope	ln (t_c)	- ln ppt concn	Q^2
8.0	83.3	17.00	-3.20	9.46	3.00
7.5	83.3	16.22	-2.41	9.49	3.85
7.0	83.3	15.29	-1.48	9.50	4.89
6.5	83.3	14.10	-0.29	9.51	6.14
8.5	62.5	17.57	-3.77	9.75	2.15
8.0	62.5	16.90	-3.09	9.76	2.83
7.5	62.5	16.45	-2.64	9.80	3.66
7.0	62.5	15.30	-1.50	9.82	4.65
6.5	62.5	13.64	-0.16	9.82	5.86
9.0	41.7	17.61	-3.81	10.17	1.49
8.5	41.7	17.00	-3.20	10.19	2.02
8.0	41.7	16.57	-2.77	10.18	2.67
7.5	41.7	15.68	-1.87	10.26	3.46
7.0	41.7	14.78	-0.97	10.27	4.42
6.5	41.7	13.69	0.12	10.28	5.59
9.0	31.3	16.77	-3.41	10.48	1.43
8.5	31.3	16.52	-2.72	10.48	1.95
8.0	31.3	16.13	-2.33	10.53	2.59
7.5	31.3	15.40	-1.60	10.59	3.36
7.0	31.3	14.76	-0.96	10.61	4.31
6.5	31.3	13.22	-0.58	10.62	5.46
9.0	20.8	15.87	-2.96	10.91	1.37
8.5	20.8	15.45	-2.42	10.93	1.88
8.0	20.8	15.22	-1.42	10.93	2.50
7.5	20.8	14.61	-0.80	11.09	3.27
7.0	20.8	13.76	0.05	11.11	4.19
6.5	20.8	12.55	1.26	11.11	5.32

TABLE 2 CONTINUED

Ca^{2+} (mM)	β-casein (μM)	ln limiting slope	ln (t_c)	- ln ppt concn	Q^2
9.0	10.4	15.18	-1.37	11.76	1.32
8.5	10.4	14.77	-0.97	12.17	1.81
8.0	10.4	14.16	-0.35	12.19	2.42
7.5	10.4	13.58	0.23	12.22	3.17
7.0	10.4	12.97	0.84	12.33	4.08
6.5	10.4	12.24	1.88	12.40	5.19

TABLE 3: The measured reaction rates for the aggregation of α_{s1}-casein (1mg/ml) in the presence of Ca^{2+} (7mM) as defined by the logarithms by limiting slope and critical time (t_c), over the temperature range of 16°C to 30°C. The square of the average charge on the monomer (Q^2) was calculated from the known calcium binding at each temperature (58)

Temp °C	Temp^{-1} (K^{-1} x 10^3)	ln limiting slope	ln (t_c)	Q^2
16.28	3.455	1.99	>4.56	23.25
17.03	3.446	7.23	3.89	22.15
17.79	3.437	9.54	4.12	20.99
18.22	3.432	9.44	4.06	20.70
18.64	3.427	9.56	3.89	20.10
18.90	3.424	10.01	3.66	19.44
18.98	3.423	10.12	3.78	19.33
19.75	3.414	10.55	3.14	18.58
20.18	3.409	10.66	2.91	17.75
20.22	3.409	10.99	2.81	17.75
20.70	3.403	11.28	2.21	17.13
20.96	3.400	11.03	2.10	16.85
21.39	3.395	11.12	2.16	16.60
21.39	3.395	11.38	1.72	16.60
21.56	3.393	11.61	1.51	16.05
22.00	3.388	11.86	1.32	15.44
22.26	3.385	11.79	1.41	15.20
22.52	3.382	12.14	0.93	14.94
22.83	3.379	12.13	0.90	14.66
23.40	3.372	11.78	0.84	13.90
23.49	3.371	12.28	0.73	13.90
23.66	3.369	12.60	0.44	13.65
24.11	3.364	12.35	0.36	13.08
24.19	3.363	12.53	-0.12	13.08
24.55	3.359	12.56	0.18	12.85
24.81	3.356	12.42	0.16	12.37
25.62	3.347	13.09	-0.73	11.61
25.70	3.346	12.63	-0.24	11.61

TABLE 3 CONTINUED

Temp ^{o}C	Temp^{-1} ($K^{-1} \times 10^{3}$)	ln limiting slope	ln (t_c)	Q^2
25.70	3.346	12.29	0.32	11.61
26.15	3.341	12.98	-0.52	10.99
26.78	3.334	13.03	-1.08	10.39
27.23	3.329	13.32	-1.06	10.11
27.59	3.325	13.31	-1.05	9.65
27.68	3.324	13.47	-1.78	9.54
28.32	3.317	13.90	-1.97	9.33
28.50	3.315	13.47	-1.86	8.90
29.32	3.306	13.63	-1.91	8.24
30.15	3.297	13.87	-2.61	7.64

TABLE 4: The reaction rates of several Ca^{2+}/α_{s1}-casein combinations over a temperature range of 15°C to 27°C as defined by the logarithms of limiting slope and critical time (t_c)

Ca^{2+} (mM)	α_{s1}-casein (μM)	Temp (°C)	$Temp^{-1}$ ($K^{-1} \times 10^3$)	ln limiting slope	ln (t_c)
7.5	21.2	18.13	3.433	9.92	3.38
7.5	21.2	19.67	3.415	10.58	2.10
7.5	21.2	21.04	3.399	11.13	1.51
7.5	21.2	22.52	3.382	11.77	0.43
7.5	21.2	23.84	3.367	12.25	-0.18
7.5	21.2	25.44	3.349	12.87	-0.57
7.5	84.7	15.69	3.462	10.00	2.85
7.5	84.7	17.71	3.438	12.25	1.36
7.5	84.7	20.78	3.402	13.21	0.07
7.5	84.7	21.13	3.398	13.66	-0.19
7.5	84.7	22.17	3.386	14.05	-0.60
7.5	84.7	23.14	3.375	14.26	-1.09
7.5	63.5	15.94	3.459	10.78	2.86
7.5	63.5	16.86	3.448	11.26	2.56
7.5	63.5	19.84	3.413	12.62	0.87
7.5	63.5	20.61	3.404	12.74	0.40
7.5	63.5	21.65	3.392	13.39	0.25
7.5	63.5	23.14	3.375	13.81	-0.53
6.5	42.4	21.22	3.397	10.08	3.43
6.5	42.4	22.35	3.384	11.12	2.49
6.5	42.4	24.46	3.360	11.79	1.40
6.5	42.4	24.99	3.354	12.54	0.68
6.5	42.4	26.24	3.340	12.98	0.06
6.5	42.4	27.14	3.330	13.04	-0.48
8.5	42.4	16.76	3.450	11.59	4.04
8.5	42.4	17.88	3.436	12.79	3.05
8.5	42.4	19.41	3.418	13.42	2.39
8.5	42.4	20.44	3.406	13.85	1.62
9.0	42.4	16.53	3.452	12.46	2.67
9.0	42.4	18.56	3.428	13.20	1.77
9.0	42.4	19.67	3.415	13.76	1.00
9.0	42.4	21.30	3.396	14.34	0.44

TABLE 5: The reaction rates of several Ca^{2+}/β-casein combinations, over a temperature range of 32°C to 43°C, as defined by the logarithms of limiting slope and critical time (t_c)

Ca^{2+} (mM)	β-casein (μM)	Temp (°C)	$Temp^{-1}$ ($K^{-1} \times 10^3$)	ln limiting slope	ln (t_c)
9.0	83.3	32.37	3.273	12.24	3.15
9.0	83.3	33.49	3.261	14.28	1.50
9.0	83.3	34.53	3.250	15.16	-0.83
9.0	83.3	36.15	3.233	17.23	-3.92
9.0	83.3	37.11	3.223	17.54	-5.88
8.0	62.5	33.68	3.259	12.05	3.59
8.0	62.5	34.72	3.248	12.78	1.99
8.0	62.5	35.58	3.239	14.43	1.04
8.0	62.5	36.63	3.228	15.52	-1.02
8.0	62.5	37.79	3.216	16.05	-2.38
7.5	62.5	35.29	3.242	11.88	3.41
7.5	62.5	36.44	3.230	13.76	1.30
7.5	62.5	38.08	3.213	15.17	0.97
7.5	62.5	39.34	3.200	16.09	-3.06
7.5	62.5	40.42	3.189	16.72	-5.34
7.5	62.5	41.70	3.176	17.42	-
7.0	83.3	35.86	3.236	12.04	3.76
7.0	83.3	36.73	3.227	12.46	2.98
7.0	83.3	38.08	3.213	14.08	0.85
7.0	83.3	39.54	3.198	15.26	-3.03
7.0	83.3	40.22	3.191	15.56	-3.21
6.5	62.5	36.44	3.230	11.15	3.75
6.5	62.5	37.79	3.216	12.61	3.11
6.5	62.5	38.56	3.208	12.64	0.46
6.5	62.5	39.93	3.194	14.63	-0.62
6.5	62.5	41.01	3.183	15.82	-4.49
6.5	62.5	42.50	3.168	15.86	-5.10

References

1. James, A.T. and Webb, J. (1957). Biochem. J. 66, 515
2. Sebelien, J. (1885). Z. Physiol. Chem. 9, 445
3. Palmer, A.H. (1934). J. Biol. Chem. 104, 359
4. Sørensen, M. and Sørensen, S.P.L. (1939). C.R. Trav. Lab. Carlsberg, Ser. Chim. 23, 55
5. Davies, D.T. and White, J.C.D. (1960). J. Dairy Res. 27, 171
6. Braconnot, H. (1830). Ann. Chim. Phys. 43, 337
7. Osbourne, T.B. and Wakeman, A.J. (1918). J. Biol. Chem. 33, 243
8. Linderstrøm-Lang, K. (1929). C.R. Trav. Lab. Carlsberg, 17, 1
9. Mellander, O. (1939). Biochem. Z. 300, 240
10. Hipp, N.J., Groves, M.L., Custer, J.H. and McMeekin, T.L. (1952). J. Dairy Sci. 35, 272.
11. Waugh, D.F. and von Hippel, P.H. (1956). J. Am. Chem. Soc. 78, 4576
12. Thompson, M.P., Tarabbuk, N.P., Jenness, R., Lillevik, H.A., Ashworth, V.S. and Rose, D. (1965). J. Dairy Sci. 48, 159
13. Neelin, J.H. (1964). J. Dairy Sci. 47, 506
14. Schmidt, D.J. (1964). Biochim. Biophys. Acta 90, 411.
15. Woychik, J.H. (1964). Biochim. Biophys. Res. Commun. 16, 267
16. Swaisgood, H.E. (1973). C.R.C. Critical Reviews in Food Technology p. 375
17. Annan, W.D. and Manson, W. (1969). J. Dairy Res. 36, 259
18. Brignon, G., Ribadeau-Dumas, B., Mercier, J.C. and Pelissier, J.P. (1977). Febs Letters 76, 274
19. Mercier, J.C., Grosclaude, F. and Ribadeau-Dumas, B. (1973). Eur. J. Biochem. 40, 323
20. Grosclaude, F., Mahe, M.F. and Ribadeau-Dumas, B. (1973). Eur. J. Biochem. 40, 323

21. Hoagland, P.D., Thompson, M.P. and Kalan, E.B. (19). J. Dairy Sci. 54, 1103

22. Aschaffenburg, R. (1961). Nature (Lond.). 192, 431

23. Kiddy, C.A., Peterson, R.F. and Kopfler, K.C. (1966). J. Dairy Sci. 49, 742.

24. Thompson, M.P., Kiddy, C.A., Pepper, L. and Zittle, C.A. (1962). Nature (Lond.). 195, 1001

25. Grosclaude, F., Pujolle, J., Garnier, J. and Ribadeau-Dumas, B. (1966). Ann. Biol. Anim. Biochim. Biophys. 6, 215

26. Aschaffenburg, R. (1968). J. Dairy Res. 35, 447

27. Peterson, R.F., Nauman, Z.W. and Hamilton, D.F. (1966). J. Dairy Sci. 49, 601

28. Thompson, M.P. and Pepper, L. (1964). J. Dairy Sci. 47, 633

29. Mercier, J.C., Grosclaude, F. and Ribadeau-Dumas, B. (1972). Milchwissenschaft 27, 402

30. Hipp, N.J., Groves, M.L., Custer, J.H. and McMeekin, T.L. (1950). J. Amer. Chem. Soc. 72, 4928

31. Groves, M.L. and Kiddy, C.A. (1968). Arch. Biochem. Biophys. 126, 188

32. Gordon, W.G., Groves, M.L., Greenberg, R., Jones, S.B., Kalan, E.B., Peterson, R.F. and Townend, R.E. (1972). J. Dairy Sci. 55, 261

33. Groves, M.L., Gordon, W.G., Kalan, E.B. and Jones, S.B. (1972). J. Dairy Sci. 55, 1041

34. Groves, M.L., Gordon, W.G., Kalan, E.B. and Jones, S.B. (1973). J. Dairy Sci. 56, 558

35. Brignon, G., Ribadeau-Dumas, B., Grosclaude, F. and Mercier, J.C. (1970). Eur. J. Biochem. 22, 179

36. Whitney, R.McL., Brunner, J.R., Ebner, K.E., Farrell, H.M.Jr., Josephson, R.V., Morr, C.V. and Swaisgood, H.E. (1976). J. Dairy Sci. 59, 795

37. Manson, W., Carolan, T. and Annan, W.D. (1977). Eur. J. Biochem. 78, 411

38. Ho, C., Magnusson, J.A., Wilson, J.B., Magnusson, N.S. and Kurland, R.J. (1969). Biochemistry, Easton, 8, 2074

39. Bingham, E.W. (1979). J. Dairy Res. 46, 181

40. Schmidt, D.G. (1970). Biochim. Biophys. Acta 207, 130

41. Schmidt, D.G., Payens, T.A.J., van Markwijk, B.W. and Brinkhuis, J.A. (1967). Biochem. Biophys. Res. Commun. 27, 448

42. Herskovits, T.T. (1966). Biochemistry 5, 1018

43. Bigelow, C.C. (1967). J. Theor. Biol. 16, 187

44. Swaisgood, H.E. and Timasheff, S.N. (1968). Arch. Biochem. Biophys. 125, 344

45. Ho, C. and Waugh, D.F. (1965). J. Am. Chem. Soc. 87, 110

46. Scatchard, G. (1949). Ann. N.Y. Acad. Sci. 51, 660

47. Scatchard, G. and Black, E.S. (1949). J. Phys. Colloid Chem. 53, 88

48. Schmidt, D.G. (1970). Biochim. Biophys. Acta 221, 140

49. Ho, C. and Cohen, A.H. (1967). J. Biol. Chem. 242, 551

50. Payens, T.A.J. (1966). J. Dairy Sci. 49, 1317

51. Dickson, I.R. and Perkins, D.J. (1969). Biochem. J. 113, 7p

52. Ho, C. and Waugh, D.F. (1965). J. Am. Chem. Soc. 87, 889

53. Dickson, I.R. and Perkins, D.J. (1971). Biochem. J. 124, 235

54. Noble, R.W.Jr. and Waugh, D.F. (1965). J. Am. Chem. Soc. 87, 2236

55. Waugh, D.F., Slattery, C.W. and Creamer, L.K. (1971). Biochemistry 10, 817

56. Bingham, E.W., Farrell, H.M.Jr. and Carrol, R.J. (1972). Biochemistry 11, 2450

57. Slattery, C.W. (1975). Biophys. Chem. 3, 83

58. Dalgleish, D.G. and Parker, T.G. (1980). J. Dairy Res. 47, 113

59. Dalgleish, D.G. (1973). Eur. J. Biochem. 40, 375

60. Holt, C., Parker, T.G. and Dalgleish, D.G. (1975). Biochim. Biophys. Acta 379, 638

61. Ribadeau-Dumas, B., Brignon, G., Grosclaude, F. and Mercier, J.C. (1972). Eur. J. Biochem. 25, 505

62. Tanford, C. (1968). Advances in Protein Chem. 23, 147

63. Garnier, J. (1966). J. Mol. Biol. 19, 586

64. Payens, T.A.J. and van Markwijk, B.W. (1963). Biochim. Biophys. Acta 71, 517

65. von Hippel, P.H. and Waugh, D.F. (1955). J. Amer. Chem. Soc. 77, 4311

66. Sullivan, R.A., Fitzpatrick, M.M., Stanton, E.K., Anmino, R., Kissel, G. and Palmerite, F. (1955). Arch. Biochem. Biophys. 55, 455

67. Tanford, C. (1961). Physical Chemistry of Macromolecules, J. Wiley and Sons, New York

68. Thompson, M.P., Kalan, E.B. and Greenberg, R. (1967). J. Dairy Sci. 50, 767

69. Evans, M.T.A., Phillips, M.C. and Jones, M.N. (1979). Biopolymers 18, 1123

70. Hoagland, P.D. (1966). J. Dairy Sci. 49, 783

71. Pearce, K.N. (1975). Eur. J. Biochem. 58, 23

72. Thompson, M.P. (1971). In Milk Proteins: Chemistry and Molecular Biology. Ed. McKenzie, H.A., Ch. 11. Academic Press, New York

73. Creamer, L.K. (1972). Biochim. Biophys. Acta 271, 252

74. Parker, T.G. and Dalgleish, D.G. (1980). J. Dairy Res. (in press)

75. Slattery, C.W. and Waugh, D.F. (1973). Biophys. Chem. 1, 104

76. Waugh, D.F., Creamer, L.K., Slattery, C.W. and Dresdner, G.W. (1970). Biochemistry 9, 768

77. Mercier, J.C., Uro, J., Ribadeau-Dumas, B. and Grosclaude, F. (1972). Eur. J. Biochem. 27, 535

78. Tran, V.D. and Baker, B.E. (1970). J. Dairy Sci. 53, 1009

79. Wheelock, J.V. and Knight, D.J. (1969). J. Dairy Res. 36, 183

80. Swaisgood, H.E., Brunner, J.R. and Lillevik, H.A. (1964). Biochemistry 3, 1616

81. Hill, R.J. and Wake, R.G. (1969). Nature (Lond.). 221, 635

82. Herskovits, T.T. (1966). Biochemistry, 5 1018

83. Shimmin, P.D. and Hill, R.P. (1964). J. Dairy Res. 31, 121

84. Parry, R.M.Jr. and Carroll, R.J. (1969). Biochim. Biophys. Acta 194, 138

85. Rose, D. (1969). Dairy Sci. Abs. 31, 171

86. Garnier, J. and Ribadeau-Dumas, B. (1970). J. Dairy Res. 37, 493

87. Morr, C.V. (1967). J. Dairy Sci. 50, 1744

88. Waugh, D.F., Creamer, L.K., Slattery, C.W. and Dresdner, G.W. (1970). Biochemistry 9, 786

89. Carroll, R.J., Thompson, M.P. and Nutting, G.C. (1968). J. Dairy Sci. 51, 1903

90. Lin, S.H.C., Dewan, R.K., Bloomfield, V.A. and Morr, C.V. (1971). Biochemistry 10, 4788

91. Schmidt, D.G., Both, P., Markwijk, B.W., van and Buckheim, W. (1974). Biochim. Biophys. Acta 365, 72

92. Holt, C., Kimber, A.M., Brooker, B. and Prentice, J.H. (1978). J. Colloid and Interface Sci. 65, 555

93. Walstra, P. (1979). J. Dairy Res. 46, 317

94. Farrell, H.M.Jr. (1973). J. Dairy Sci. 56, 1195

95. Schmidt, D.G., Walstra, P. and Buckheim, W. (1973). Netherlands Milk and Dairy J. 27, 128

96. Dewan, R.K., Chudgar, A., Mead, R., Bloomfield, V.A. and Morr, C.V. (1974). Biochim. Biophys. Acta 342, 313

97. Schmidt, D.G. and Payens, T.A.J. (1976). Surface and Colloid Science 9, 165

98. Holt, C. (1975). Biochim. Biophys. Acta 400, 293

99. Sood, S.M., Gaind, D.K. and Dewan, R.K. (1979). New Zealand J. Dairy Sci. and Tech. 34, 32

100. Dewan, R.K., Bloomfield, V.A., Chudgar, A. and Morr, C.V. (1973). J. Dairy Sci. 56, 699

101. Sood, S.M., Sidlu, K.S. and Dewan, R.K. (1976). Milchwissenschaft 31, 470

102. Rose, D. (1968). J. Dairy Sci. 51, 1897

103. Niki, R. (1973). Netherlands Milk and Dairy J. 27, 249

104. Carroll, R.J., Thompson, M.P., Brunner, J.R. and Kolav, C. (1967). J. Dairy Sci. 50, 941

105. Downey, W.K. and Murphy, R.F. (1970). J. Dairy Res. 37, 361

106. Davies, D.T. and Law, A.J.R. (1980). J. Dairy Res. 47, 83

107. Payens, T.A.J. (1966). J. Dairy Sci. 49, 1317

108. Waugh, D.F. and Noble, R.W.Jr. (1965). J. Amer. Chem. Soc. 87, 2246

109. Creamer, L.K., Wheelock, J.V. and Samuel, D. (1973). Biochim. Biophys. Acta 317, 202

110. Almlöf, E., Larson-Raznikiewicz, M., Lindquist, I. and Munyua, J. (1977). Preparative Biochem. 7(1), 1

111. Kudo, S., Iwata, S. and Mada, M. (1979). J. Dairy Sci. 62, 916

112. Slattery, C.W. (1978). Biochemistry 17, 1100

113. Rose, D., Davies, D.T. and Yaguchi, M. (1969). J. Dairy Sci. 52, 8

114. Pyne, G.T. and McGann, T.C.A. (1960). J. Dairy Res. 27, 9

115. McGann, T.C.A. and Pyne, G.T. (1960). J. Dairy Res. 27, 403

116. Thompson, M.P. and Farrell, H.M.Jr. (1973). Netherlands Milk and Dairy J. 27, 220

117. Ashoor, S.H., Sair, R.A., Olson, N.F. and Richardson, T. (1971). Biochim. Biophys. Acta 229, 423

118. Garnier, J. and Ribadeau-Dumas, B. (1970). J. Dairy Res. 37, 269

119. Fuchs, N.Z. (1934). Phys. 89, 736.

120. Vreeman, H.J. (1979). J. Dairy Res. 46, 271

121. Slattery, C.W. and Evard, R. (1973). Biochim. Biophys. Acta 317, 529

122. Pepper, L. (1972). Biochim. Biophys. Acta 278, 147

123. Carroll, R.J., Farrell, H.M.Jr. and Thompson, M.P. (1971). J. Dairy Sci. 54, 752

124. Schmidt, D.G. and Buchheim, W. (1970). Milchwissenschaft 25, 596

125. Waugh, D.F. and Talbot, B. (1971). Biochemistry 10, 4153

126. Rose, D. and Colvin, J.R. (1966). J. Dairy Sci. 49, 1091

127. Slattery, C.W. (1977). Biophys. Chem. 6, 59

128. Schmidt, D.G., Both, P. and Koops, J. (1979). Neth. Milk Dairy J. 33, 40

129. Visser, J., Schaier, R.W. and van Gorkom, M. (1979). J. Dairy Res. 46, 333

130. Horst, M.G. (1963). Neth. Milk Dairy J. 17, 185

131. Knoop, A.M., Knoop, E. and Wiechen, A. (1979). J. Dairy Res. 46, 347

132. Lyster, R.L.J. (1979). J. Dairy Res. 46, 343

133. Holt, C. Personal communication.

134. Lin, S.H.C., Leong, S.L., Dewan, R.K., Bloomfield, V.A. and Morr, C.V. (1972). Biochem. 11, 1818

135. Manson, W. (1962). Int. Dairy Congr. 16th Copenhagen, B513

136. Boulet, M., Yang, A. and Riel, R.R. (1970). Can. J. Biochem. 48, 816

137. Davies, D.T. and White, J.C.D. (1960). J. Dairy Res. 25, 236

138. White, J.C.D. and Davies,D.T. (1958). J. Dairy Res. 25,

139. Bloomfield, V.A. (1979). J. Dairy Res. 46, 241

140. Steiner, R.F. (1952). Arch. Biochem. Biophys. 39, 333

141. Verwey, E. and Overbeek, J. (1948). Theory of the Stability of Lyophobic Sols, Elsevier Publishing Co., Amsterdam

142. Tang, L.H., Powell, D.R., Escott, B.M. and Adams, E.T.Jr. (1977). Biophys. Chem. 7, 121

143. Coggeshall, N.D. and Saier, E.L. (1951). J. Am. Chem. Soc. 73, 5414

144. Pekar, A.H. and Frank, B.H. (1972). Biochem. 11, 4013

145. Lewis, M.S. and Adams, E.T.Jr. (1968). Biochem. 7, 1044

146. Koren, R. and Hammes, G.G. (1976). Biochem. 15, 1165

147. Amdur, I. and Hammes, G.G. (1966). in Chemical Kinetics, Principles and Selected Topics, N.Y., McGraw-Hill, p.61

148. Smoluchowski, M. Von (1917). Z. Phys. Chem. 92, 129

149. Parker, T.G. and Dalgleish, D.G. (1977). Biopolymers 16, 2533

150. McKenzie, H.A. (1971). in Milk Proteins: Chemistry and Molecular Biology, Acad. Press, N.Y., London, Chap. 10.

151. Bloomfield, V.A. and Morr, C.V. (1973). Netherlands Milk and Dairy J. 27, 103

152. Mysels, K.J. (1959). in Introduction to Colloid Chemistry, Interscience Pub., N.Y., London. p.323

153. Payens, T.A.J. (1979). J. Dairy Res. 46, 291

154. Overbeek, J.Th.G. (1952). in Colloid Science, Vol. 1. (Ed. H.R. Kruyt) Amsterdam: Elsevier

155. Derjaguin, B. (1940). Trans. Faraday Soc, 36, 203

156. Horne, D.S. and Dalgleish, D.G. (1980). Int. J. Biol. Macromol. 2, 154

157. Cowie, J.M.G. (1973). in Polymers: Chemistry and Physics of Modern Materials, Billing & Sons Ltd., Guilford and London. Chap. 2.

158. Parker, T.G. and Dalgleish, D.G. (1977). J. Dairy Res. 44, 79

159. Gordon, M. (1962). Proc. Royal Soc. A268, 240

160. Zittle, C.A. and Custer, J.H. (1963). J. Dairy Sci. 46, 1183

161. Zittle, C.A. (1961). J. Dairy Sci. 44, 2101

162. Manson, W. (1965). Biochem. J. 94, 452

163. Thompson, M.P. and Kiddy, C.A. (1964). J. Dairy Sci. 47, 626

164. Stacey, K.A. (1956). in Light Scattering in Physical Chemistry, Butterworths, London

165. Debye, P. (1947). J. Phys. Chem. 51, 18

166. Rayleigh, Lord (1899). Phil. Mag. 47, 375

167. Zimm, B.H. (1948). J. Chem. Phys. 16, 1099

168. Elias, H.G. (1972). In Light Scattering from Polymer Solutions. Ed. Huglin, M.B. Academic Press, London and N.Y.

169. Horne, D.S. (1979). J. Dairy Res. 46, 265

170. Dalgleish, D.G. (1980). J. Dairy Res. 47, 231

171. Payens, T.A.J., Wiersma, A.K. and Brinkhuis, J. (1977). Biophys. Chem. 6, 253

172. Payens, T.A.J. (1977). Biophys. Chem. 6, 263